AN INVESTIGATION INTO THE USE OF ELECTRODE MASS MEASUREMENT TO OPTIMISE AN ELECTROSTATIC PRECIPITATOR UNIT.

By

Sathish Kumar Pershad, NHD(Mech Eng)

Dissertation submitted in compliance with the requirements for the Masters Degree in Technology in the School of Mechanical Engineering at the Port Elizabeth Technikon.

Date of Submission

2001

Promoters :

Dr DG Hattingh

Mr M Newby

AN INVESTIGATION INTO THE USE OF ELECTRODE MASS MEASUREMENT TO OPTIMISE AN ELECTROSTATIC PRECIPITATOR UNIT.

By

Sathish Kumar Pershad, NHD(Mech Eng)

Dissertation submitted in compliance with the requirements for the Masters Degree in Technology in the School of Mechanical Engineering at the Port Elizabeth Technikon.

Date of Submission

2001

Promoters :

Dr DG Hattingh

Mr M Newby

ABSTRACT

Author : **Sathish Kumar Pershad**

Title : **An Investigation Into The Use Of Electrode Mass Measurement To Optimise An Electrostatic Precipitator Unit.**

Electrostatic precipitators (ESP's) can be simply described as particle collection devices and service a wide variety of industries. This particle collection can either be classed as a cleansing or product recovery (or both) process. They can be found in fossil fueled power generation plant (municipal incinerators, iron and steel industries (sinter plants, coke ovens), non ferrous industries, rock products (cement, lime), chemical and petrochemical (detarrers, de-oilers)

They have been around for approximately 70 years and their fundamental principle of operation has not changed much during this time. What has changed is the demand on their operating efficiency. Environmental pressure as well as the loss of product has forced ESP's to perform even better than before. This performance enhancement is two-fold : an increase in collection efficiency and a reduction in maintenance and wear costs.

This project researches the use of mass measurement techniques to optimise the operation of ESP's from both the above mentioned perspectives.

CONTENTS

Chapter 1 : Research Proposal **Page**

Chapter 2 : Experimentation at Eskom's Hendrina Power Station

Chapter 3 : Experimentation at Eskom Lethabo Power Station

Chapter 4 : Conclusion

Chapter 5 : References

Chapter 6 : Appendices

LIST OF FIGURES

LIST OF TABLES

LIST OF PLATES

GLOSSARY OF TERMS

Figure A, below, illustrates the different parts of an ESP unit and helps understand their positioning. The various manufacturers do have slight differences in design, but the three field Lurgi design shown has fairly common characteristics.

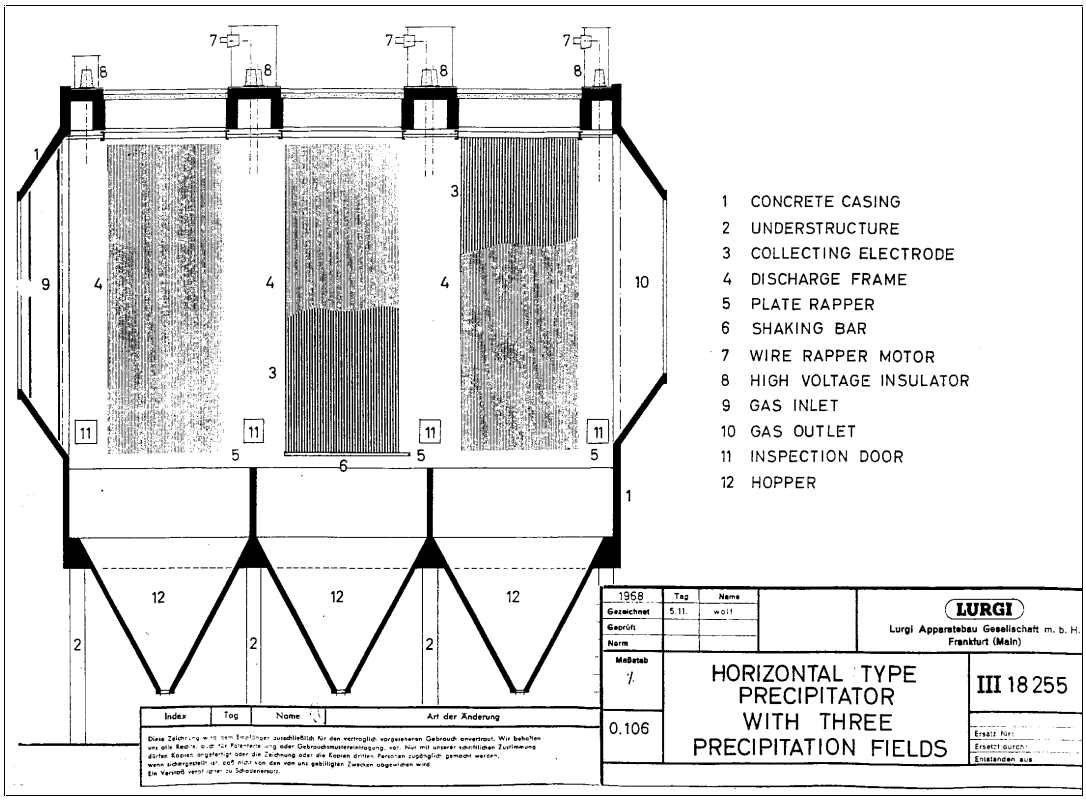

Figure A : Lurgi 3 Field ESP Schematic

90:7:3 – Eskom's Generation plant operation philosophy. The numbers refers to a breakdown of the plants status as a percentage of a total time period. This period is usually defined as a particular year.

90%: Plant is generating electricity or available for generation.

7%: Time allowable for planned outages and maintenance.

3%: Time allowable for forced/unplanned outages.

ANVILS – Rapper striking plates which transmit the rapping forces to both collecting and discharge electrodes.

ASPECT RATIO – A dimensionless ratio of the length of the precipitator casing divided by its height.

BACK CORONA/IONISATION – Discharge originating from the CE with a polarity opposite to that of the CE. It is caused when the potential gradient through the CE dust layer exceeds the breakdown strength of the gas.

CARRIER BEAM – Mechanical bar used to attach each collector plate and is attached to the roof beams by bolts or clamps.

CASING - An air-tight box-like structure constructed from either steel, or concrete or a combination thereof. A collection of fields usually arranged in series is contained within a casing.

CAPCO - Chief Air Pollution Control Officer of the Department of Environmental Affairs and Tourism (DEAT). South African governmental body legislating and controlling pollution issues.

COHPAC – Compact Hybrid Particulate Collector. Bagfilter plant located after an ESP to act as a polishing device.

COLLECTING ELECTRODE (CE). The electrode upon which charged dust is deposited in an ESP. Manufactured from sheet metal in various shapes to enhance stiffening and prevent buckling. Usually connected to ESP metal structure and is thus earth or ground. Typical dimensions are 14 m height, 4 m width, and 1,2 mm thick.

CONTROL EQUIPMENT – Also known as “electrical controller” – electrical components used to regulate the DC potential supplied to the discharge electrode system.

CORONA – A “crown” of electrical discharge from the places on the surface of a conductor (enhanced by sharp edges) at which there is an electric field high enough to ionise surrounding gas/dust.

CV – Calorific value of fuel measured in megajoules per kilogram (MJ/kg).

DEAD/POWER OFF or REDUCED POWER RAPPING - Rapping of fields with the energisation voltage either reduced or completely turned off. Performed with difficult, “sticky “ ashes with the aim of reducing the holding forces that keep them on the CE and DE.

DUCT – Pathway that channels/transports gas from boiler to ESP and then to the smoke stacks.

DE - DISCHARGE ELECTRODE. Frame consisting of either barbed metal strips or spiral square spring steel. Isolated from ESP structure and energised via the T/R sets. Barbs or spiral shapes exist as a method of enhancing corona formation towards DE.

ENERGISATION VOLTAGE - dc voltage supplied by T/R sets to DE’s.

FIELD - A collection of CE’s and DE’s. A field is generally as long as the length of the CE’s/DE’s. Two and three field ESP’s were common in the 1960’s and 1970’s, but as higher efficiencies were required, five to eight field ESP’s have become common.

HOPPER – Vessel located at the bottom of the precipitator fields into which dust is collected after being rapped from the electrodes.

HAMMER - mechanical device used to rap electrodes. Can weigh between 2 kg to 12 kg.

ID FAN – induced draught fan drawing air through the boiler. Usually located downstream of the ESP unit.

LOADCELL – mechanical load measuring device, usually with strain gauges applied, the purpose of which is to accurately determine applied loads to the device. Typical accuracies range from 0.01% to 0.5%.

LOAD LOSS – the boiler/turbine has to decrease generated load and operate at a lower load than capable of. Usually due to malfunctioning equipment causing a decrease in critical input or output parameters.

MCR – boiler maximum continuous rating (power),

EMISSION or OPACITY MONITOR - instrument that transmits a light beam and measures extinction by determining the obscuration of the light source. These instruments are installed in either the ESP outlet ducts or in smoke stacks, and when correlated with isokinetic sampling, provides a widely accepted method of monitoring particulate emissions.

P/S – Power Station

PARTICULATE EMISSIONS – Usually measured as mass per flowrate. Commonly measured as milligrams per standard cubic meter of flow (mg/Sm^3). The "standard" cubic meter allows for the correction of "Actual" boiler conditions (mg/Am^3).

RAPPING – The process of exciting either the CE or DE with the purpose of dislodging collected material. Achieved in a variety of ways – most common is by rotary hammers. Other methods include electromagnetic hammers, electrode lift & drop systems, sonic horns.

RE-ENTRAINMENT – The introduction of already collected dust into the gas flow.

SCA – Specific Collecting Area – The area of CE that an ESP has per unit volume flow-rate of gas. Units used are seconds per meter ($^s/_m$)

SKEW FLOW – Gas carrying dust burden has velocity gradients across one or both dimensions of the flow.

TSI – Technology Services International. A division of Eskom Enterprises under which the author is currently employed.

T/R SETS - transformer/rectifier sets. Electrical devices that covert the supply ac voltage to dc voltages for application to the DE's. Typical modern DE voltages are 45 kV and 800 mA.

UNIFORM FLOW – Gas carrying dust burden has equal or close to equal velocities across both dimensions.

ACKNOWLEDGMENTS

The successful completion of this project would have been impossible without the support, advice, assistance and encouragement of others. I should like to record my sincere thanks and appreciation to the following :

Eskom, in its overall global state, for providing me opportunity to be employed in this research project's related fields of expertise, for financial resources, access to personnel, training and plant without which this project would not have been possible.

Eskom Resources & Strategy – for making available the entire, rather substantial funding required to complete this project.

Eskom – Hendrina and Lethabo Power Stations. For making available their plant and for the support of the relevant site personnel, especially their system engineers.

Mr M Newby, Eskom TSI, Promoter, friend, mentor and manager for guidance, direction, encouragement and more encouragement in all phases of the project.

Dr D Hattingh, Promoter, Head of Department – Mechanical Engineering - Port Elizabeth Technikon for the opportunity and encouragement to complete this project.

TSI – Stress and vibration team, Eskom and industry specialists, Mr R S Hansen, Dr H Brandt, Mr W Schmitz, Mr D Gibson, Dr S Higgins, Mr F J Bosch, Mr P Pretorius for insight by sharing their experience and wisdom.

Sincere thanks to the following companies for use of material

Lurgi SA	Figure A
Ultra Systems, Australia	Figure 1.2
Hamon Rothemühle Cottrell GmbH	Figures 1.3, 1.4, 3.1,

-

AUTHORS DECLARATION

At no time during the registration for the degree of Masters of Technology has the author been registered for any other university degree.

This project was funded completely by Eskom and intellectual property rights to the research are held by Eskom.

Presentations and Conferences Attended

- An Introduction to United States of America ESP Rebuild Technology, South Africa, 1998
- Strain Society of South Africa (SSSA) Annual Event, 2000.
- Paper accepted for ICESP VIII, Alabama USA, May 2001

Signed ……..

Date ……

Chapter 1 : Research Proposal

1.1 INTRODUCTION

Electrostatic precipitators (ESP's) can be simply described as particle collection devices. This particulate collection occurs for two basic reasons, either pollution control or product recovery or both. In the power industry, it is used primarily as a pollution control device. Other industries using them are municipal incinerators, air conditioning systems, pulp and paper plants, rock products (cement, lime, gypsum), chemical and petroleum industries (detarrers, deoilers, acids), iron and steel plants (coke ovens, blast furnaces, sinter plants), and non-ferrous metal plants (aluminium, copper, gold).

ESP's have been around for approximately 70 years and their fundamental principle of operation has not changed much during this time. What has changed is the demand on their operating efficiency. Environmental pressure in the form of stricter reductions in emission levels as well as the need for increased product recovery has necessitated optimal ESP performance. ESP's can be large devices with many costly, high maintenance components. ESP downtime usually critically affects the overall plant process. In power generation plant, a defective ESP resulting in higher than licensed emission levels can cause the enforcement of a generation load loss to bring emission levels down. Alternate devices to ESP's have been cyclones in the past, and fabric filters currently.

In power generation plant, the ESP is usually located after the airheaters and before the induced draft fans and smoke stacks. Flue gases exiting the boiler, via the airheaters are cleaned by the ESP before being released into the atmosphere via

the stacks. Figure 1.2, shows a schematic of where the ESP is typically located in power plant.

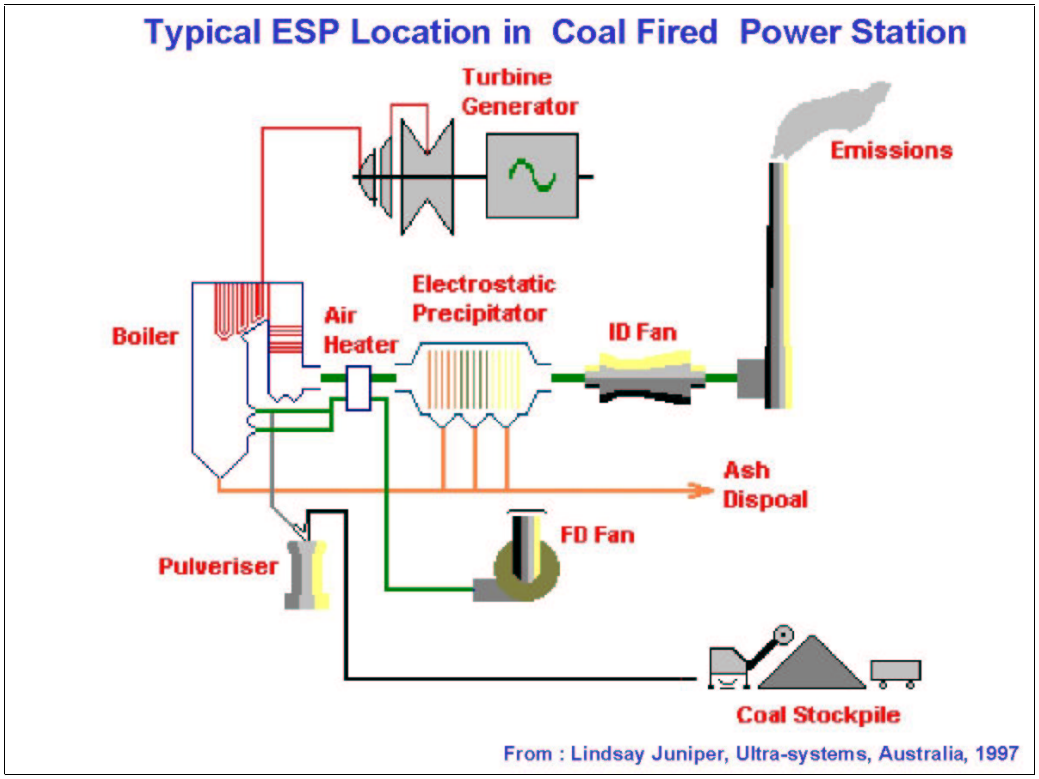

Figure 1.2 : ESP Location in Power Generation Plant

Figures 1.3 and 1.4, below, show an arrangement of collecting electrodes (CE's) and discharge electrodes (DE's). CE's are constructed from plate steel (typically 1.2 to 1.8 mm thick) and shaped so as resist buckling. DE's are constructed from strips of metal (various shapes and sizes) suspended between a rigid frame.

Dust laden gases flow through a system of parallel passages of DE's and CE's as shown in Figure 1.3 and 1.4 below. CE's are grounded whilst a negative voltage (typically 30-50 kV and 400-1000 mA) is applied to the DE's. A corona is then generated from the DE to the CE. The dust flowing within the passage is electrostatically charged and migrates towards the CE (relatively positive). Dust/ash

collects on the CE until it is dislodged by rapping (impacted upon), where it then falls into a hopper and is carried away by some type of ash handling plant.

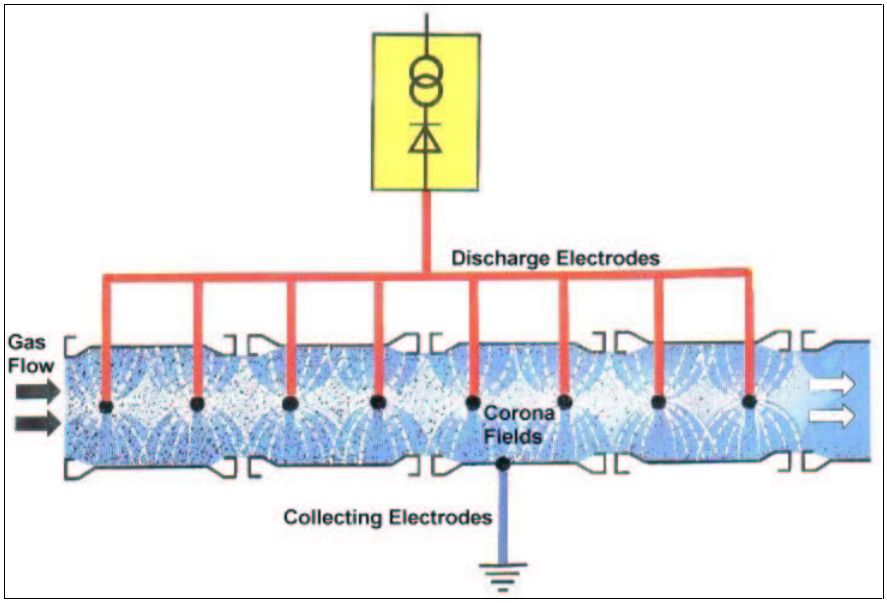

Figure 1.3 : Basic ESP operation principle

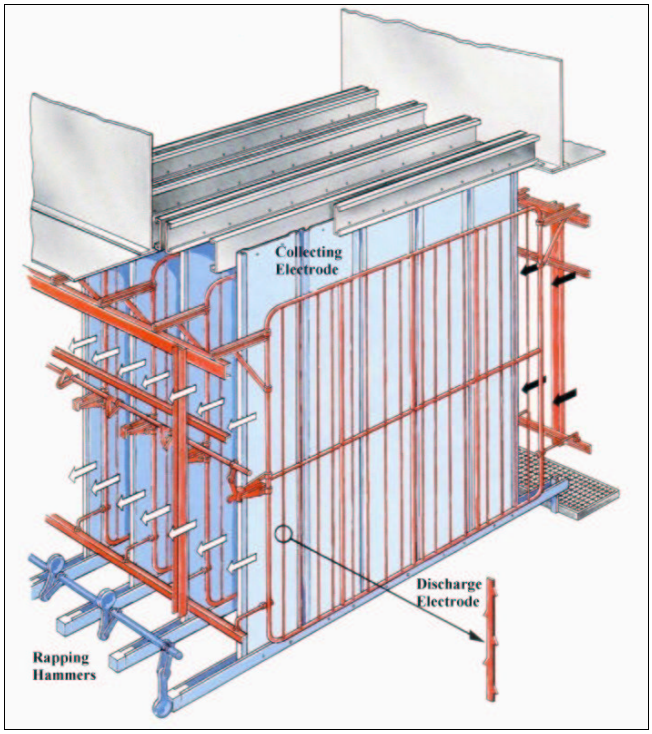

Figure 1.4 : Three dimensional view of a single field.

Eskom is currently South Africa's largest power utility. Total generation capacity is in the order of 38150 MW and is composed of, coal-fired (33878 MW or 88,8 %) , nuclear (1930 MW or 5,1 %, hydro/pumped storage schemes (2000 MW or 5,2 %) , and gas turbines (342 MW or 0,9 %).

Coal fired power plants require gas cleaning apparatus installed to remove flyash from the flue gas exiting the boiler before being released into the air. Looking closer at the coal fired stations, we find that 25918 MW or 76,5 % are being serviced by electrostatic precipitators (ESP's), with the remaining 7960 MW or 23,5 % being serviced by bagfilter plants.

Eskom, in line with its goals of becoming the lowest cost producer of electricity for growth and development in the world, burns low-grade coal. Considering that Eskom coals could easily have ash contents as high as 33 %, the role performed by gas cleaning equipment and more specifically ESP's takes on immense importance.

From the above figures, the need for high efficiency ESP's becomes apparent in the challenge to reduce particulate emissions. Techniques are constantly being sought, developed and retrofitted to improve the operation of electrostatic precipitators. These include flow modifications of the flue gases, flue gas conditioning, new rapping methods and better controllers of the electrical apparatus of the ESP. These techniques are being researched by the relevant specialists in Eskom.

One technique that has been experimented upon, although only once and not in Eskom, is the use of collecting electrode mass measurement to optimise the operation of ESP's. The studies were conducted by the Electric Power Research Institute (EPRI) in the USA approximately twenty years ago. Those tests concluded that the research showed potential and further testing was required to gauge its full effect.

The advent of very sophisticated control systems in the subsequent years now suggests that a combination with CE mass measurement now promises great potential. ESP operation factors not able to be optimised to their full extent can now be addressed. The move to intelligent, automated plant management and control systems in industry in general means that an operational collecting electrode mass measurement system can provide a major step in ESP operation and design.

1.2 THE PROBLEM STATEMENT AND RESEARCH QUESTIONS

This project proposes to investigate and develop the use electrode mass measurement in optimising ESP performance.

The research questions to be answered are :-

- What methodology should be used to measure CE ash loading.
- Once measured, how must the data be analysed and interpreted.
- Does the data provide meaningful insight into the operation of the ESP unit and if so, what characteristics/phenomena are displayed.
- What corrective actions can be implemented to effect a positive change in ESP collection rates.
- What, if any other, ESP efficiency factors, though not investigated here, could benefit from the data measured and/or corrective steps thereafter.

1.3 THE SUBPROBLEMS

1.3.1 Choice of experimental unit.

1.3.2 Study of ESP geometry to determine CE mass measurement method.

1.3.3 Study of conditions to determine relevant instrumentation.

1.3.4 Installation of all equipment and commissioning of system.

1.3.5 Measurement of ash collection patterns.

1.3.6 Analysis of data

1.3.7 Conclusions

1.3.1 Choice Of Experimental Unit.

Eskom has 9 power stations currently being serviced wholly, or partly by ESP based gas cleaning systems. Any one of these power stations could benefit if the technique proves successful. However, considering the costs and time of this research, the experimental unit will have to be carefully chosen. The major criteria will be the need to better ESP performance as soon as possible. Some ESP units operate at relatively good efficiencies due to a variety of reasons. These include being relatively new and thus in good mechanical condition and/or the retro-fitment of other enhancement methods. Coal quality is another major factor that causes ESP's to operate at different efficiencies. In choosing the experimental unit these as well as accessibility based on outage schedules, boiler unit load size will be considered.

1.3.2 Study Of ESP Geometry To Determine CE Mass Measurement Method.

The chosen ESP unit will then be studied to determine the most suitable manner of determining CE mass measurement. Specific areas will be CE suspension, space available to work in and accessibility. Loadcells will then be designed to suit the ESP structure.

1.3.3 Study Of Conditions To Determine Relevant Instrumentation.

The loadcell chosen has to endure severe operating conditions. It has to operate, without deviations in accuracy over a temperature range of 0 to 140°C usually encountered inside ESP's. Penetration by ash is another hazard.

The loadcells will have to be powered by appropriate amplifiers and power supplies. The energisation voltage of approximately 50 kV on the DE, in close proximity (± 150 mm) to the CE means that electrical noise could easily corrupt the loadcell signals. The amplifier system must thus possess noise reduction/elimination capabilities. The amplifier should also provide an output that is compatible with the stations PLC system if it is going to be used in future as a control device by the power station. A datalogger will be required to record the loadcell outputs. The datalogger must also be accessible via modem or Eskoms LAN system to enable remote contact and data downloading. This will be essential to save time, effort and costs.

The above amplifiers, datalogger and other electronic equipment represents a substantial cost and will have to be protected against electrical overloads. Lightning and supply voltage power surges constitutes a severe risk to the system. The ESP energisation voltage is another risk to be borne in mind. Suitable electrical surge protection will have to be researched and installed to protect equipment.

1.3.4 Installation Of All Equipment And Commissioning Of System.

Once a measurement system has been designed to suit the chosen ESP unit, the equipment will be purchased and or constructed. The equipment, and loadcells in

particular will have to be designed and installed so as not to interfere with the operation of the ESP unit. The ESP unit is critical for the operation of the boiler unit and Eskom will not tolerate load losses due to faulty experimental equipment. Therefore, care must be taken to ensure that no load losses are suffered by Eskom due to the equipment chosen, or installation procedures.

It is proposed that collection trends of two CE's per field be monitored. The two CE's selected for each field should be adjacent to each other and would serve as a verification of the integrity of their individual operation. The unit chosen will not have skewed flow installed and hence the flow distribution will be assumed to be uniform across the width of the ESP casing. Total collection will be calculated by multiplying the ash collected by the number of electrodes per field.

1.3.5 Measurement Of Ash Collection Patterns.

Present rapping conditions will be documented. This will enable, these conditions to be returned to after any adjustments have been made to determine the before and after conditions for the efficiency test. The collection patterns, for present rapping conditions and as determined from loadcell readings will be recorded. This will then be used as a basis to compare the benefits of any rapping adjustment procedures.

1.3.6 Analysis Of Data.

The collection trends will then be studied to reveal particular characteristics and based on them, recommendations will then be made to improve the operation of the ESP.

A final report will be compiled detailing the entire course of the project. An evaluation of the use of loadcells as an optimisation technique will be done. The benefits of this technique in conjunction with other ESP technologies/activities will be discussed. Future use or research will be recommended.

1.3.7 Conclusion

The conclusion will address the hypothesis, that is, is CE mass measurement a suitable method of optimising an ESP.

1.4 THE LITERATURE REVIEW

1.4.1 General

Research by Tassicker[1], has concluded that the measurement of ash collection rates has great potential in the optimisation of ESP operations. Loadcells are used to determine collecting electrode ash loads, and the information is a real time, in situ reflection of the ESP's operation.

The results obtained were very positive and when further instrumentation was installed greater success was expected. No further information was found on the proposed future research. The technique involves the suspension of the electrodes from loadcells. The loadcells are connected to amplifiers situated outside the gas stream and the output signals from the amplifiers are then connected to suitable display and storage units. The results showed that "after two months in the field, there was no indication of deterioration in performance."

At present we cannot quantify the field collection rate of each individual field. This project will quantify the amount of ash collected by each field. This information

would prove to be immensely valuable as a research tool as it could show us where to concentrate our other optimisation efforts. The knowledge of each field's collection rate provides excellent correlation of other work such as CFD, plant mechanical modifications, electrical modifications and apparatus.

The knowledge of each field's performance could provide us with indications to where enhancement opportunities exist or need to be implemented.

Presently, we have the ability to quantify vibration of electrodes due to the rapping process. However, we do not have the ability to say what amount of vibration is sufficient to dislodge the collected ash. This quantity of vibration is dependant on a number of factors. These include ash resistivity, effects of gas flow, distribution of vibration throughout the electrode. These factors are usually unique for each power station or ESP type at a power station. Laboratory experimentation has been done by other researchers but the correlation to site conditions has not been definite.

The fact that the loadcells provide an indication of the dislodgement of collected ash means that an opportunity exists to correlate vibration intensity to ash dislodged. Opportunities also exist to modify the rapping system of one ESP unit, or one field and then gauge its influence on the collection and dislodgement of ash.

Re-entrainment refers to the phenomena when dust or ash that has already been collected on the collecting electrode comes off and is introduced back into the gas/dust stream. Some of the reasons for this include rapping, electric factor, gas flow and ionic wind. Rapping is responsible for the greatest re-entrainment quantity.

The project aims to optimise rapping so as to reduce the effects of re-entrainment. Re-entrainment losses will be attempted to be measured.

The timing of rapping can be very important for effective ash collection and dislodgement into the hopper. Rapping at too frequent intervals can result in re-entrainment problems as well as undue wear and tear of the plant.

Research by Harold Bowman and Richard Roberts [2], has produced some very interesting results. The generally accepted concept that CE's should be as clean as possible during ESP operation was shown to not be the best for ESP performance. Contrary to this popular idea, their research, which is based on in-situ tests on an actual ESP unit, has shown that a thick ash layer on the CE reduces sodium depletion and enhances ESP efficiency. The rapping cycles were rescheduled such that the CE was rapped less frequently and a thicker ash layer was maintained. A secondary benefit of this is the reduction in wear and tear of the plant.

This project will test the ESP performance under different rapping schedules in an effort to obtain the best rapping schedule. The information derived from the loadcells will be an ideal gauge of the effectiveness of changes to the rapping schedules and will be used as a measure to fine tune the sequence and timing of rapping.

The "power-off" or "reduced power" rapping technique basically requires the energising power to a particular area of the ESP unit to be turned off totally or reduced and the electrodes in that area rapped. The purpose of turning the power off is to remove the corona current and the force holding the dust layer to the electrode thus making its dislodgement via rapping easier.

It has to be borne in mind that the section of ESP that is not fully energised during rapping will not be collecting ash and hence stack puffs could occur. The power-off

technique was quite common in earlier designed ESP's and is not commonly used in modern installations due to rapping puffs. It's use is not recommended but the reasons for this are not very clear.

Since Eskom is the world's largest single operator of ESP units, it is felt that the technique should be evaluated at our power stations. Eskoms larger, "six pack" (six generating units) power stations have multiple field ESP units (Matimba Power Station - 8 fields) and stack puffs could not prove to be a problem if one field is de-energised.

The ESP unit chosen has three fields and stack puffs could become a problem. This technique will thus have to be carefully evaluated.

As a result of the loadcells providing a real time, on-line indication of the ESP's collection rates and patterns, it yields an excellent opportunity of correlating the effects of associated plant equipment and operating conditions on ESP performance. Previous research[1] found that boiler sootblowing has a distinct effect on ash dislodgement. When sootblowing occurred, a large percentage of the ash layer on the CE was dislodged. The exact implications of this will have to be determined. The effect of unit load, operating temperatures, sootblowing can be trended against ESP collection performance and a rapping schedule defined accordingly.

After defining a rapping schedule for different ESP conditions, the loadcells could be linked to an ESP controller device that would automatically vary the rapping to appropriate ESP conditions. This would prove to be of major benefit to the power station as they would have a closed loop control system to operate the ESP unit. The viability of this aspect will only be scanned with further research in the future.

Flue gas conditioning has become a popular method of improving ESP performance. Hendrina P/S Unit 5 has a flue gas conditioning system installed. Presently, the injection of SO_3 is controlled against boiler load. The information obtained from the loadcells could be used to control the amount of SO_2 injected versus ESP operating conditions. This intelligent use of the correct amount of additives in relation to specific ESP operating conditions at a specific time could lead to cost savings. This aspect will have to be researched.

The paper " Studies of Rapping Re-entrainment from Electrostatic Precipitators [3]" by Yamamoto et al describes a laboratory scale set-up to view re-entrainment using the laser light sheet technique. This technique uses a He-Ne laser light source and the light sheet is formed from a half cylindrical rens. Particle trajectories can then be viewed when this light source is introduced into the ESP scale model. One conclusion is that primary particles re-entrained by rapping into the gas stream can be reduced if the dust layer cake is highly packed on the CE.

"An Experimental Study Of Electrostatic Precipitator Plate Rapping And Re-Entrainment[4]" by Lee et al, represents work in the understanding of ash collection, rapping and re-entrainment. Again a laboratory scale experimental set-up is proposed. This enables hopper ash collection to be measured. At present this is not measured in our Lethabo test set-up. According to their work, collection and rapping efficiencies can be defined as:

$$\text{Collection efficiency} = \frac{\text{Ash collected in hopper}}{\text{Ash input to field}}$$

$$\text{Rapping efficiency} = \frac{\text{Rapped ash collected in hopper}}{\text{Ash precipitated in field}}$$

Predictably, an increase in precipitation time produced an increase in ash layer thickness. However, above 4,2 mm (and 120 minutes), this trend reversed. In our experience on the first field at Lethabo Power Station (data captured during a failed rapper timer (3.8.7 and Figure 3.1.7)), the CE saturated at a load of 480 kg. Assuming an CE ash density of 500 kg/m^3, and a uniform ash layer thickness on the CE, this translates to an thickness of 6,2 mm. This value is higher than that in the laboratory scale experimental studies. In their tests, the reversal of collection efficiency was attributed to back corona as well as gravity induced ash breakaway of the ash layer. In our tests, gravity, surprisingly (high ash resistivity = less holding forces) does not cause ash breakaway.

Also, collection efficiency for ash layer thicknesses of 1,3 mm and 4,2 mm were measured at 96,2 % and 71,7 % respectively. Collection efficiency decreased with an increasing ash layer and was attributed to a reduction in the fly ash electrical mobility. Interestingly, this rate was fairly linear up to 4,2 mm as was not the case in our full scale studies. Our optimised rapping times for field 1(see 6.3.2) had collection for 13 minutes. This at a rate of 3 kg/minute potentially leads to an ash load of 39 kg. Using assumptions as above, this translates to an ash thickness of 0,5 mm. If the ash thickness is 1,3 mm (for highest collection efficiency) as in the experimental scale study are considered optimum, then the collection time period must be increased to 33 minutes for an ash load of 100 kg.

Rapping efficiency was, predictably found to increase proportionately with rapping acceleration levels. It was concluded that the optimum ash layer thickness to be rapped was 3,5 mm considering rapping and collection efficiencies.

1.4.2 Present Day Rapping Systems

No significantly new rapping trends have been noted during the course of this research project. However, one area of rapping systems that is receiving increasing attention is in the rebuild and refurbishment of ESP's. Considering that Eskom has approached the stage where ESP upgrades are required, it will be important to note the experiences of other rebuilds.

Although not totally new, the use of rigid discharge electrodes (RDE's) and magnetic impulse - gravity impact (MIGI) rapping systems has become the preferred choice when upgrading ESP's. The advantages of RDE's and MIGI rapping are briefly mentioned below.

1.4.2.1 Rigid Discharge Electrode ESP's

Figure 1.5 shows a typical rigid frame (RF) ESP design system while Figure 1.6 shows a typical RDE design. The advantages of RDE's can be summarised as follows:

Its design makes use of less steel and hence lesser load is exerted on the support members. The supporting structure does not have to be strongly designed as for rigid frame (RF) electrodes.

The space between the trailing plate edges of one field and the leading plate edges of the next field (also used as inspection walkways) can be reduced from the usual 1,2m to 2,1m (in RF designs) to between 0,46m and 0,61m. This means that in a retrofit scenario, the specific collection area (SCA) can be increased significantly by about 35%.

Smaller electrical sections and hence greater sectionalisation promotes control of the ESP and hence enhances performance.

Design is sturdier than RF and the common problem of broken discharge wires is greatly minimised. Hence ESP downtime is minimised and performance maintained.

Enhanced electrical performance due to better corona discharge.

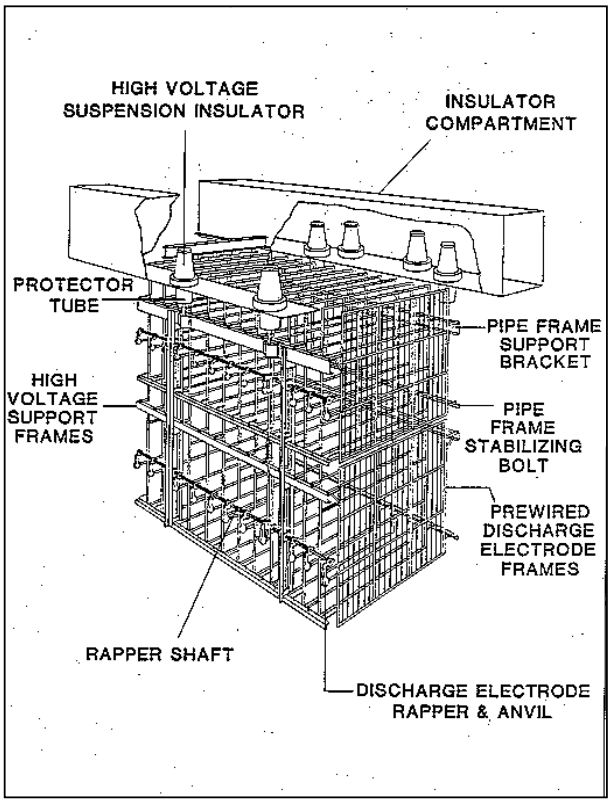

Figure 1.5 : Typical Rigid Frame (RF) system

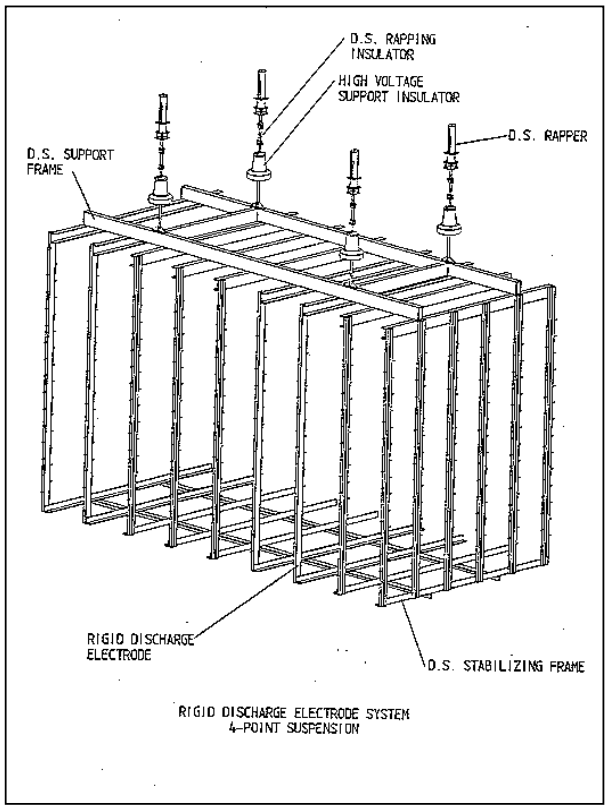

Figure 1.6 : Typical Rigid Discharge Electrode (RDE) system

1.4.2.2 Magnetic Impact-Gravity Impulse(MIGI) Rapping System

The magnetic impulse-gravity impact (MIGI) rapping system has gained popularity over the recent years and in conjunction with RDE's, has become an almost automatic choice in the ESP upgrade trade, especially in the USA.

Figure 1.7, shows the typical components of a MIGI rapping system and Figure 14 shows the system installed in an ESP. The system consists primarily of an electrically energised coil and a metal slug, weighing between 4,5 and 9 kg, depending on application. The coil is energised and this causes the slug to be drawn into (in this case, lifted) the coil. When a rap is required, the coil is de-

energised and gravity causes the slug to fall, and via appropriate linkages, the electrode support frame is impacted.

The above operation means that by controlling the coil energisation levels, slug lift height can be controlled. This results in an online, variable rapping intensity adjustment system.

The advantages of MIGI systems can be summarised as follows:

- Variable rapping intensity by virtue of design. Rapping intensity can be varied on almost an instantaneous basis. Promotes rapping optimisation for varying conditions (e.g. boiler load changes). Rapping becomes a more controllable process and can be integrated with the electrical controller. In tumbling hammer systems, this in only possible by changing hammers with those of different masses. This can be very expensive, time consuming and no online adjustment is possible.

The options of integration of the MIGI and loadcell systems will lead to a very efficient and effective rapping system.

These rappers are installed directly above the ESP field and two positives arise from this. Firstly no space is “wasted” in between fields and SCA’s are increased. Secondly, the installation position ensures easy accessibility (even with ESP on load) and this promotes quick, on-line maintenance

There are no moving parts located in the gas burden. Hence frictional wear and tear usually associated with tumbling hammer systems are reduced. The number of hammers used is also much less (vibration transferred via curtain carrying beams

and then to electrodes as opposed to individual hammers per electrode). Maintenance costs are thus reduced.

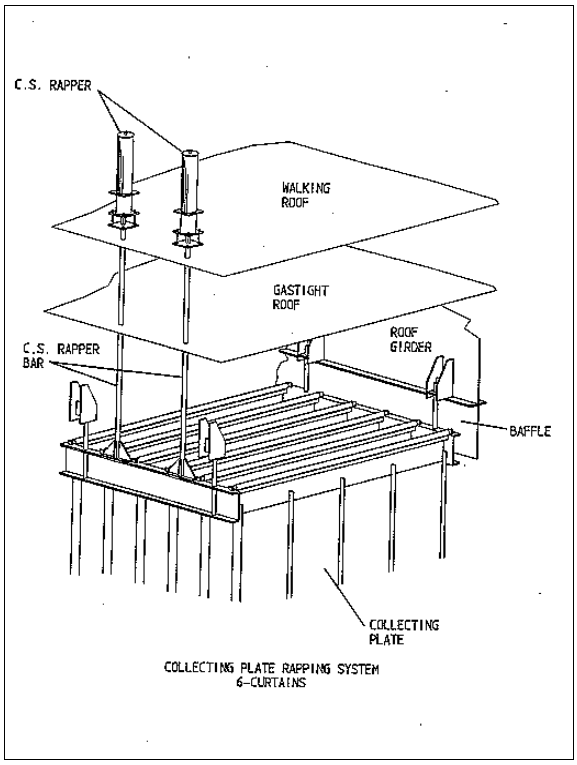

Figure 1.7 : Typical MIGI rapping system.

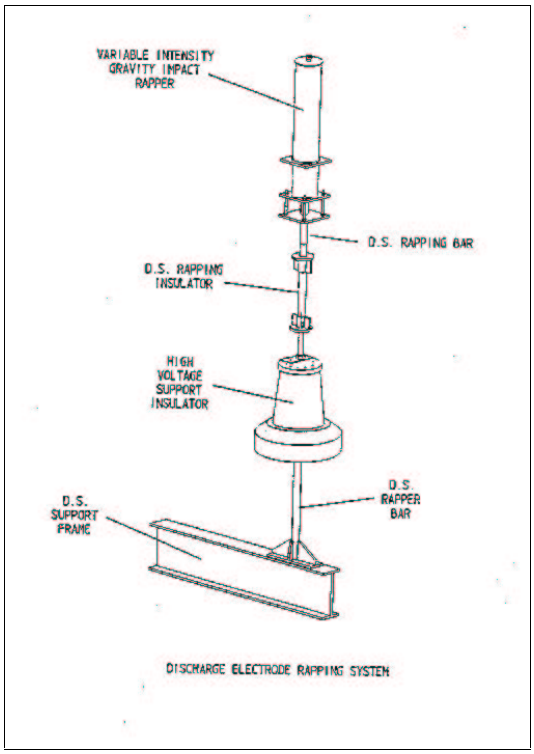

Figure 1.8 : Example of MIGI Rapping in service.

1.4.2.3 Applicability Of This Research

Loadcells can be used just as, if not more effectively in MIGI based rapping systems as they are in tumbling hammer systems. Since MIGI based systems often have the ability to vary rapping intensity and frequency, they provide the ideal result to a an ESP control system having loadcell “sensors” installed. The plant control system then has the ability to, based on ESP operations (from loadcells), to optimise itself.

1.5 HYPOTHESIS

ESP electrode mass measurement is a suitable method of optimising ESP performance.

1.6 DELIMITATIONS OF THE RESEARCH

Only CE's will be considered in this research. DE's whose collection patterns could also have an influence on ESP performance will not be considered.

Rapping parameters to be considered/experimented will be the timing of cycles. Power off/reduced power, which could benefit immensely from this project will not be tested. However, the interaction of this research with all other rapping related will be discussed.

The research will be conducted only on a full scale, operational ESP unit. Scale models, and rapping simulation techniques will not form part of this project.

The research will be limited to one ESP unit casing per power station.

1.7 OUTPUT

Development and evaluation of the use of CE mass measurement to optimise an ESP unit.

1.8 SIGNIFICANCE OF THE RESEARCH

Eskom has instituted an environmental policy that clearly defines and measures its operations impact on the environment. A significant area of its environmental policy is its goal of reducing particulate emissions. Many Eskom coal fired power stations were planned and built 15 to 30 years ago. ESP's at these power stations were designed to operate at specific efficiencies for certain emission levels as laid down in the CAPCO licenses. These licenses have through the years become stricter and

penalties (e.g. load losses to bring particulate emission levels within license specifications) are enforced. Some original licenses ranged for particulate emissions of approximately 200 mg/Sm^3 when these levels were considered to be adequate and acceptable. Present day acceptable levels are considered to be 50 mg/Sm^3 or less and original licenses are constantly being reviewed. Also, the age and subsequent physical degradation of many ESP's does not help the overall situation.

The much newer bagfilter system gas cleaning system, by virtue of its design (mechanical filtration) operates at high efficiencies. However considering various factors it is unlikely than many, if any, further bagfilter plants will be built in the future. Therefore, new and improved ESP upgrade technologies will have to be implemented/retrofitted to meet regulations. Other upgrade/improvement technologies that form part of Eskom's holistic approach to ESP improvement are skew flow, flue gas conditioning, COHPAC (bagfilter plant at end of ESP), new rapping systems etc. With the exception of skew flow, the other technologies represent a large capital and/or maintenance outlay. These costs can be as large as 50 fold the cost of rapping optimisation using electrode mass measurement, providing that sufficient improvement gains can be obtained. Skew flow can be complemented by this research and combined, and can provide a very cost effective alternative to other upgrade options.

In the light of the above, this projects overall benefits would be to:

- Reducing Eskoms particulate emission levels and impact on the environment.
- Ensuring Eskoms capability to supply electricity to South Africa by reducing/eliminating ESP plant downtimes.
- Provide cost savings by:-

- Avoiding penalties such as load losses.
- Reducing wear and tear on ESP plant due to possible shortened “rapping on” times thus minimising fatigue failures.
- Prolonging or negating the need for more expensive ESP rebuilds/refurbishments and/or new technologies.
- The generation of income for Eskom through the marketing and sale of this technology, to relevant ESP parties both local and worldwide..

1.9 THE ASSUMPTIONS

Uniform flow across the ESP field will be assumed, and thus the measurements of two CE’s per field will be assumed to be representative of the whole fields performance.

1.10 A METHODOLOGICAL JUSTIFICATION

This change in mass is due to the precipitated flyash and the loadcells provide information on dust layer thickness, stage collection efficiencies, rapping re-entrainment and efficiency of rapping. The advantage of this technique is that it provides real time, on-line information of the instrumented precipitator. Thus by changing some of the operating parameters and monitoring the resulting changes via the loadcells, the optimum operating conditions can be obtained.

1.11 RESOURCES AND BUDGET

The project budget total was R1 500 000 and funded in total by Eskom. All intellectual property rights are held by Eskom. Permission must first be obtained from Eskom to use any information contained herein.

1.12 RESEARCHERS QUALIFICATIONS

National Higher Diploma – Mechanical Engineering

Chapter 2 : Experimentation at Eskom's Hendrina P/S

2.1 INTRODUCTION

Hendrina Power Station is located in the Mpumalanga province of RSA, approximately 40 km from Middelburg. Hendrina P/S has ten boiler units, each with a nominal generating capacity of 200 MW providing a total station generation capacity of 2000 MW. All ten units were commissioned between 1970 and 1976. Presently, Hendrina P/S is Eskom's oldest generating station. Hendrina P/S was commissioned with ESP units cleaning the exhaust boiler flue gases on all units. Unit 1 is of the Brandt/Rothemühle type, Units 2 to 5 are three field ESP's of the Lurgi type as shown in the general schematic in Figure 1.1. In later years, these units had flue gas conditioning systems installed to assist in mimimising emissions. Units 6 to 10 were originally two field ESP's but these were later upgraded to fabric filter gas cleaning systems as particulate emission levels became stricter.

2.2 CHOICE OF HENDRINA P/S FOR EXPERIMENTATION.

The ESP unit identified for experimentation is Hendrina Power Station, Unit 5, right hand casing. This decision was based on a variety of reasons. The most important reason, however, is that the emission levels at Hendrina Power Station are relatively high and there is a need for improvement of ESP performance. Hendrina Power Station is a ten boiler unit station. Each boiler unit has an ESP unit consisting of two casings (left and right hand). Units 1 to 5 have six field (three per casing) Lurgi ESP units while Units 6 to 10 have four field (two per casing) Rothemühle (Brandt) ESP units. ESP units 6 to 10 have been converted to bagfilter ash collection units and hence their performance has been improved.

Methods are needed to improve the efficiency of ESP units 1 to 5. These units already have flue gas conditioning and skew flow has already been implemented in Unit 5 left-hand casing.

The installation of the loadcells would require the ESP unit to be on outage. The outage schedule of Units 1 to 5 was reviewed and it was found that Unit 5 would be on outage from the 14/05/96 to the 7/06/96. This time period, although at relatively short notice would suffice for the installation of the loadcells. The Unit would then return to service and the rest of the measurement system (external to ESP unit) would then be installed. An outage for Unit 5 had been planned for approximately February 1996 and at this time, repairs or modifications could then be done. It should be remembered that this technique has not been experimented/implemented in Eskom and thus unseen problems could surface. If these problems are with the system within the ESP unit, then our repairs, etc. are limited to unit outage schedules.

Most of the tests done thus far (for Hendrina Units 1 to 5) have been done on Unit 5. This serves as further motivation to use this unit for experimentation as we will have a fair knowledge of its operational characteristics.

2.3 HENDRINA ESP GEOMETRY AND OPERATING SPECIFICATIONS.

Figure 1.1, shows a casing layout of Hendrina Power Station's ESP Units. Each boiler unit is serviced by two, parallel ESP casings. Table 1.1, shows the relevant specifications of these casings.

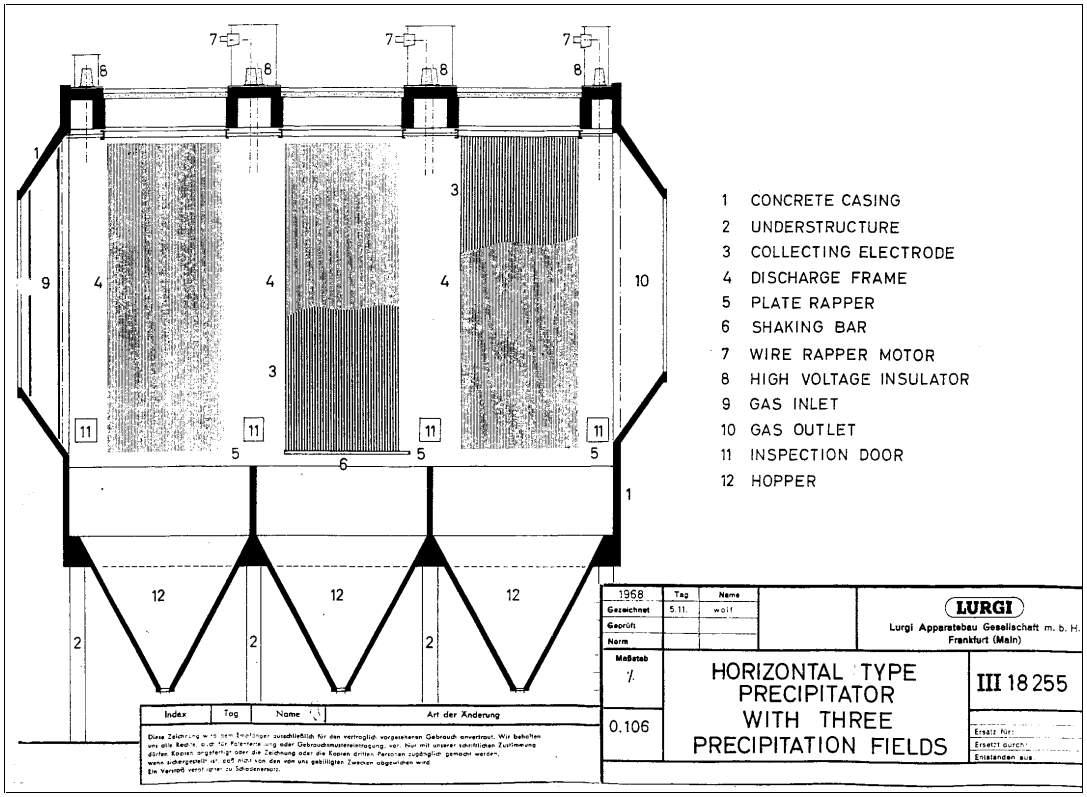

Figure 1.1 : Lurgi 3 Field ESP Schematic

Table 1.1 : Hendrina P/S ESP Specifications

Design Data	
Boiler rating (at 97% MCR)	200 MWe
Efficiency (at 97% MCR) for all fields in service	98 %
Parallel Casings	2
Plate (CE) Height	10,5 m
Plate (CE) Length	3,84 m
Lanes per filter casing	60
Pitch between lanes	250 mm
Fields in series per pass	3
Plate (CE) area total	29030 m^2
Flow area (total)	315 m^2
Specific collecting area (SCA)	75,6 s/m
Aspect Ratio	1,1
Casing Construction	Concrete
Operating Data	
Gas volume flow rate	384 m^3/s
Gas temperature	138 °C
Dust Burden	30,9 g/m^3
Treatment time	9,5 s
Migration velocity (Deutsch)	51,7 mm/s
Gas velocity at electrodes	1,2 m/s
Coal Specification	
Ash content	26,2 %
Sulphur content	0.8 %
Net C.V	24.7 MJ/kg

2.4 DESIGN OF LOADCELL AND SUPPORT STRUCTURE.

Since the CE mass measurement technique has not been done by Eskom before, the collection trends of two CE's per field would be monitored. Thus for the three field unit the mass variations of six CE's would be monitored. The two CE's selected for each field would be adjacent to each other. This would serve as a

verification of the integrity of their individual operation. The flow distribution will be assumed to be uniform across the width of the ESP casing and thus the information derived for the instrumented CE's should apply to all CE's of that field. The mass of six CE's, two per field, would be monitored. These are indicated in Figure 2.3.

A site inspection was done to determine a method of suspending CE's from loadcells. The general work area, was also inspected. The inspection revealed that very little work-space existed at the CE suspension points. The top of the CE's and DE's were not accessible due to the ESP design. The ESP is encased in a concrete casing with no manholes on the roof. Access to the top of the electrodes from within the ESP unit is not possible due to the position of the roof beams and protection plates. The only access in is via manholes and ladders located at the bottom of each field. When loadcells are installed, the total CE load has to be transferred from the suspension clamp to the loadcell to obtain a mass measurement and change thereof as ash is collected and dislodged. The transfer of load requires the entire CE to be lifted some distance. The space limitations mean that this was going to be a very difficult task.

Considering the CE loading configuration, and the space available to work in, it was decided that two loadcells would simply support each end of the CE suspension beam. Each of these loadcells would thus have to be connected in parallel to provide the total CE load. The market was scanned for an appropriate loadcell type. For this loading configuration, the most suitable loadcell would be of the shear beam type. A local company, LOADTECH (Pty Ltd) was found to supply shear beam loadcells. These however would not withstand the temperatures required. After discussions, it was decided that their LT 300 - 1K type loadcell could be customised to suit our application.

Figure 2.1, shows the area of interest for determination of the mass of the CE. From the accessibility limitations, the only area available for installation of a loadcell is highlighted in Figure 2.2

The loadcell installation has been developed so as not to interfere with the operation of the ESP unit. The CE's being monitored will be lifted a height of 10 mm from their present suspension brackets to enable their mass to be transferred to the loadcells. The CE's with lateral motion will still be restricted by their original design. Therefore, the possibility of lateral motion and a shorting of the CE and DE is not incurred. The loadcells have a factor of safety of approximately 8, before they break. However, in the unlikely event of loadcell mechanical failure, then the relevant CE will fall a distance of 10mm onto its original suspension bracket. This should not incur any risks.

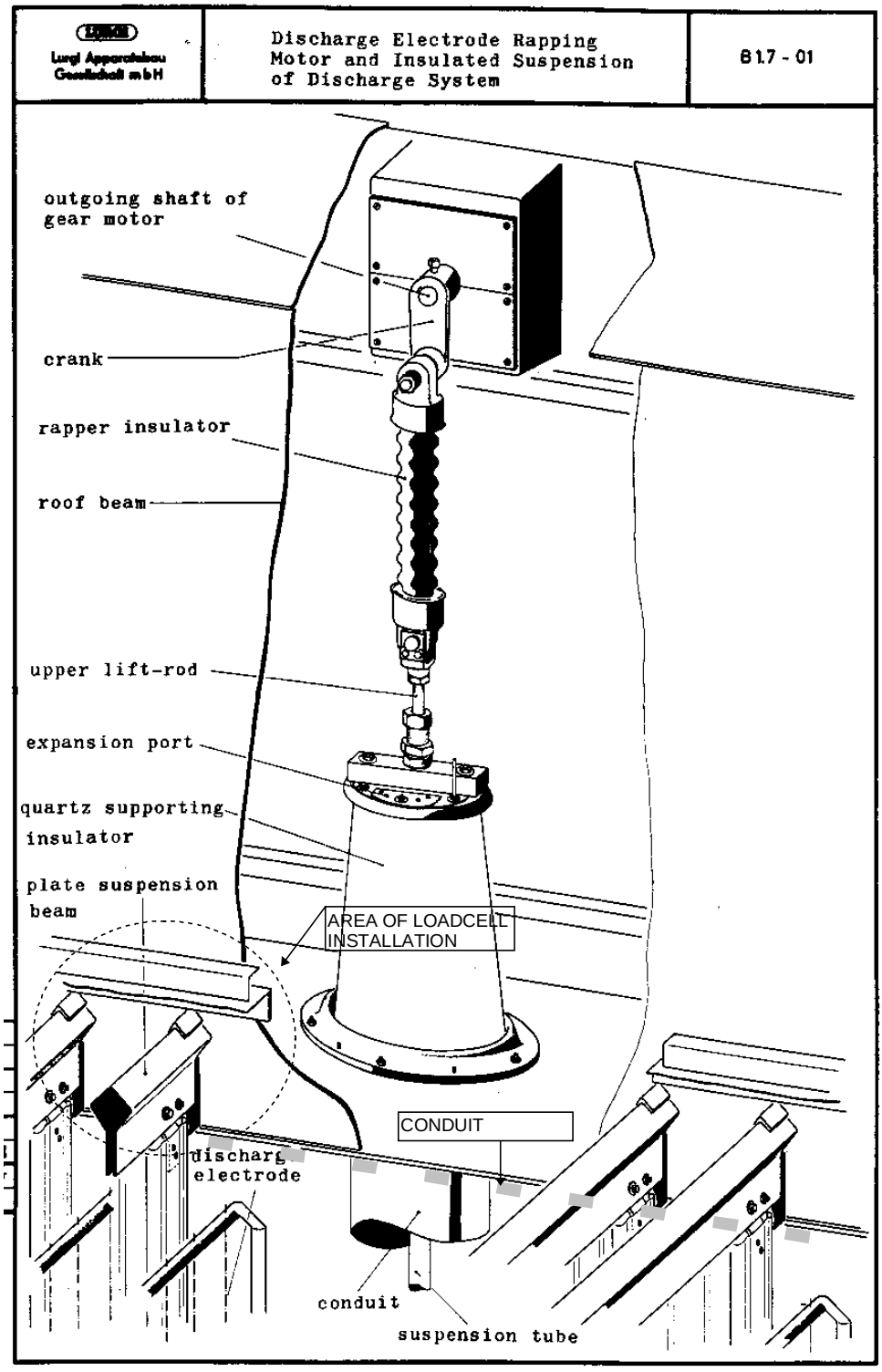

Figure 2.1 : Hendrina P/S ESP CE and DE Suspension Design

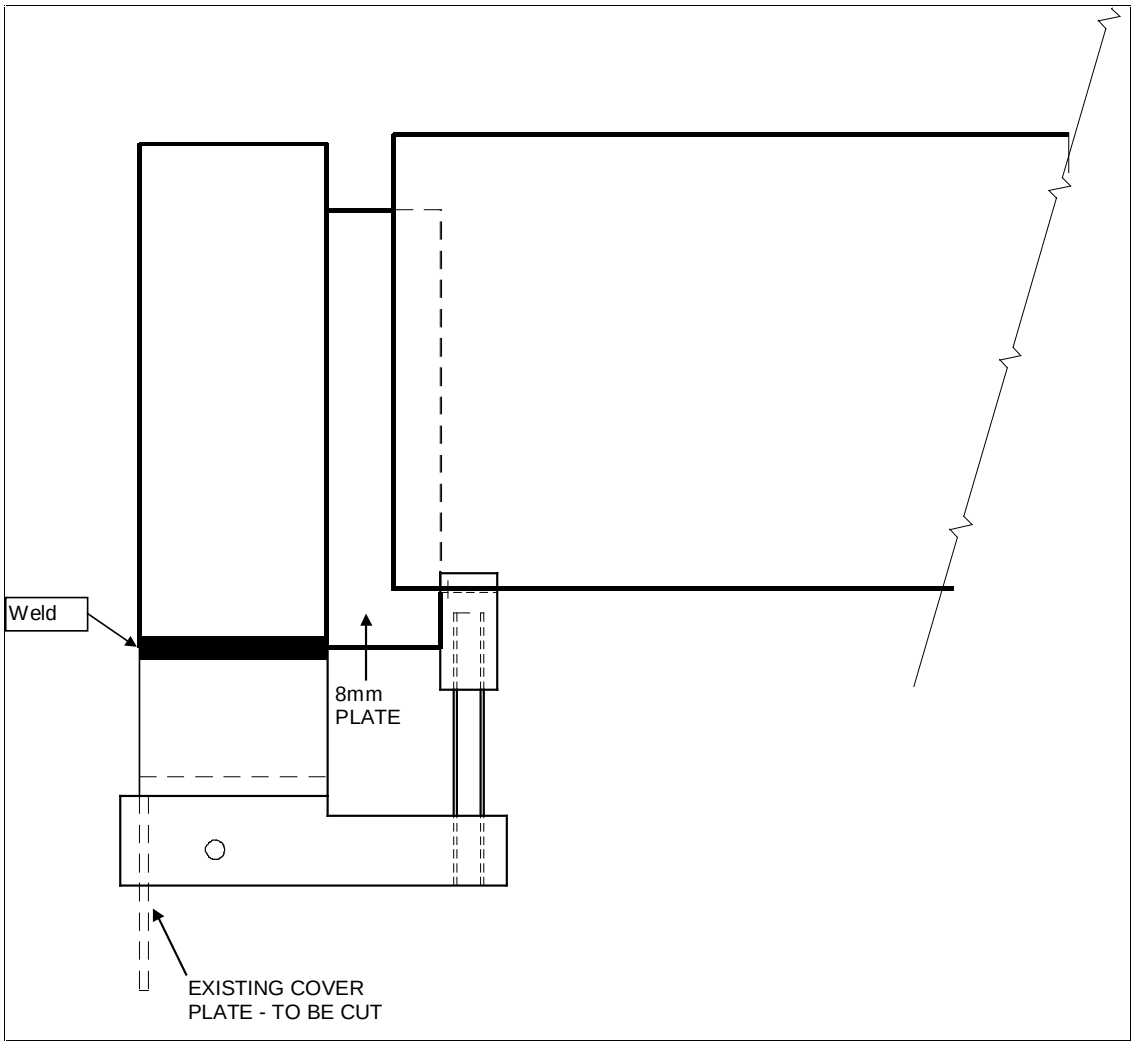

Figure 2.2 : Loadcell and CE carrier beam suspension design.

Plates 2.1 and 2.2, below shows front and side views of the loadcell and attachment bracket. This assemble would be welded onto the CE carrier beam as shown in Figure 2.2. The weld strength calculations are shown in Appendix A.

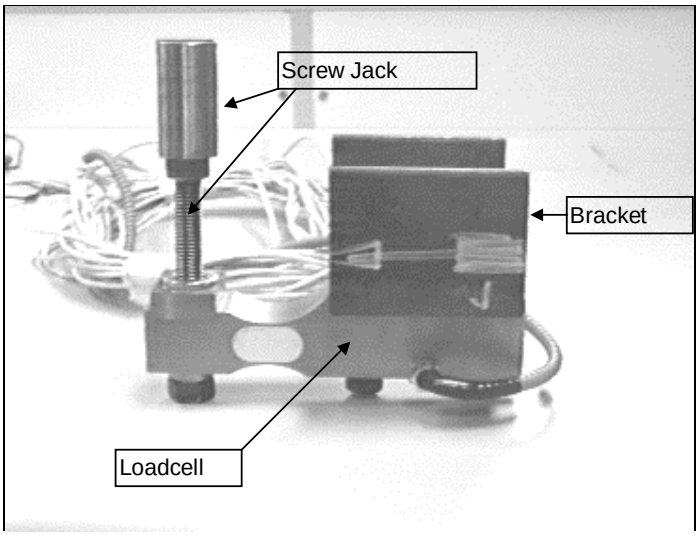

Plate 2.1 : Side view of loadcell, bracket and screw jack.

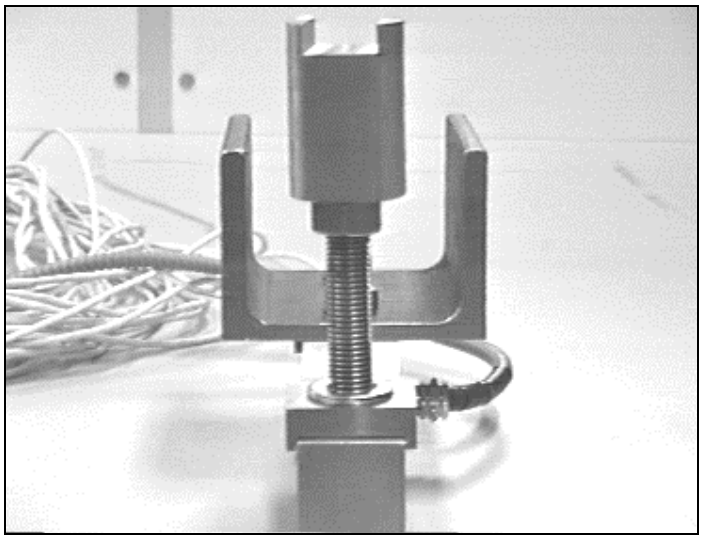

Plate 2.2 : Front view of loadcell, bracket and screw jack.

The mass of a clean collecting electrode was calculated to be approximately 695 kg. Assuming an ash layer of 3 mm on both sides of the collecting electrode, a bulk density of flyash of 1210 kg/m^3, then the total mass of plate and ash would be 1183 kg.

The loadcell chosen has to endure severe operating conditions. It has to operate, without deviations in accuracy over a temperature range of 0 to 140 degrees centigrade and it has to withstand penetration by ash. The cable used within the ESP casing also has to endure the 0 to 140 degree's centigrade temperature range. The loadcells also had to be available and installed in a very short time period to coincide with Unit 5's outage schedule. The above operating conditions meant that standard commercially available loadcells could not be used.

The specifications of the LT 300 -1K customised loadcell are:

Rated Output [RO]	=	2 mV/V , ± 0.1%
Accuracy Class	=	0.1%
Non Linearity	=	0.02% RO
Compensated Temp. Range	=	0 to 140°C
Safe Overload	=	1500 kg
Breaking Load	=	4000 kg
Construction	=	EN24 Steel

2.5 LOADCELL INSTRUMENTATION AND DATA RECORDING SYSTEM

As mentioned above, the loadcell used has to be carefully chosen so as to endure the harsh conditions within the ESP casing. Similarly, the equipment chosen to power and amplify the loadcell signal has to be thoughtfully chosen.

Figure 2.3 shows a top view of the ESP roof and the location of the loadcells and the cable paths. Figure 2.4 shows a corresponding side view of the casing and the loadcell cable path to the transformer room, where all the amplifiers and datalogging equipment will be located.

The amplifiers chosen have to be able to power the long cable length (90m) without signal corruption. They also have to have excellent noise resistance capabilities due to the close location (200mm) of the loadcells to the high voltage DE's.

The datalogger used should have the necessary accuracy as well as a fast enough sampling capability. It must also have sufficient and secure storage facilities to ensure also measured data is captured.

All the above equipment needs to be protected against current and voltage surges. Part of the solution is proper earthing of equipment, but more importantly suitable surge arrestors must be installed. This was required to protect the amplifiers and datalogger from both internal ESP spark-overs as well as lightning strikes.

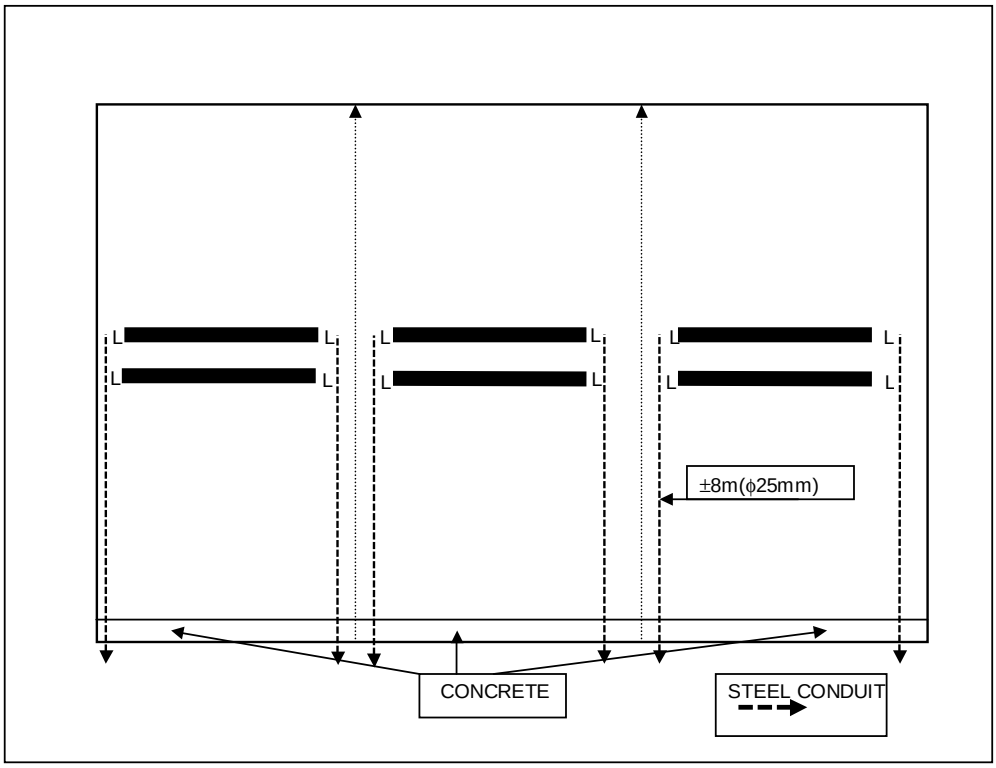

Figure 2.3 : Top view of ESP casing and loadcell location

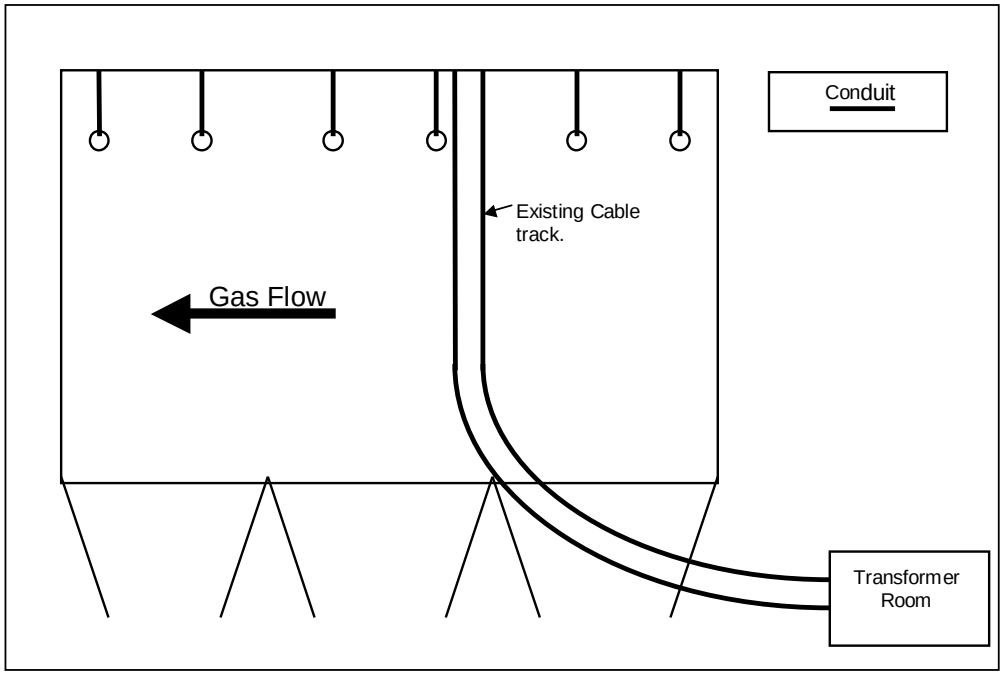

Figure 2.4 : Side view of ESP casing and transformer room

2.6 INSTALLATION OF ALL EQUIPMENT AND COMMISSIONING OF SYSTEM

Plates 2.3 to 2.6, below show different views of the actual installation configurations. Plate 2.3, below shows an end view of the two adjacent CE's and the installed loadcells.

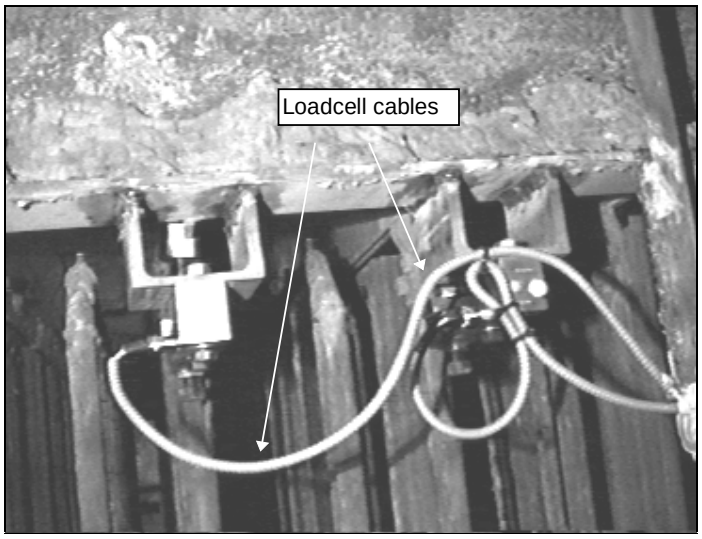

Plate 2.3 : End view of loadcells installed in-situ.

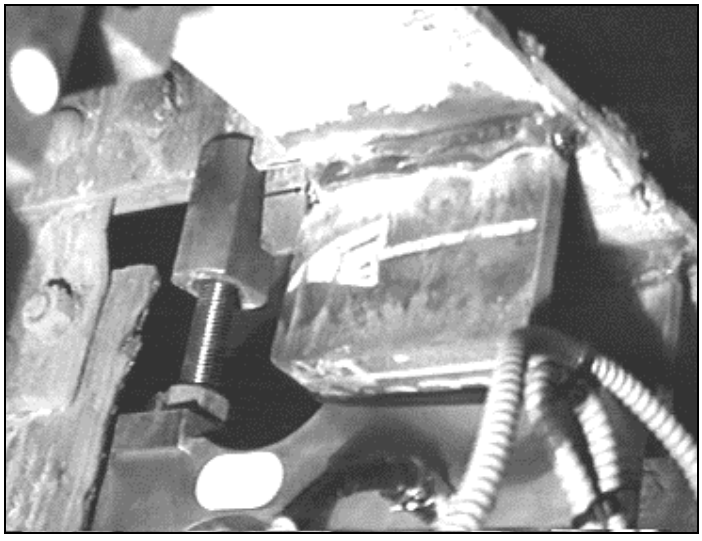

Plate 2.4 : Side view of an in-situ installed loadcell.

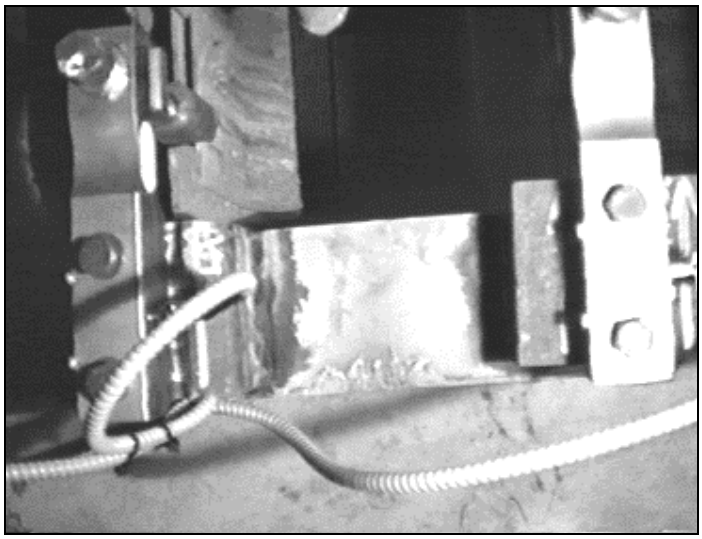

Plate 2.5 : Bottom view of installed loadcell.

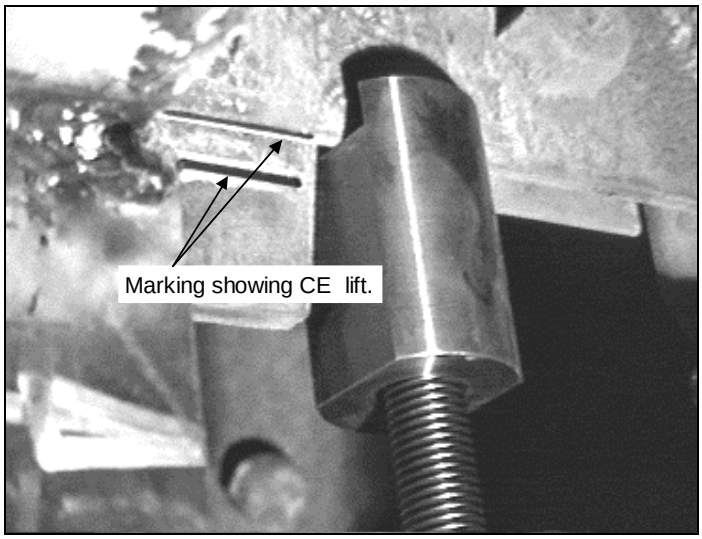

Plate 2.6 : CE lifted by approximately10 mm.

Recording Equipment used were :

HBM AE301 Clip Amplifiers	:	6 off
HBM DA101 Display Units	:	2 off
Surgetek Surge Arrestors	:	6 off
Datataker DT600 datalogger	:	1 off

Since each CE is suspended at each end by a loadcell, these two loadcells are connected in parallel.

The “clean” CE mass was noted after the ESP was washed. It is noticed that these masses range between 435 kg and 570 kg. This may seem like large variations between CE’s that are supposed to be identical. However, two possible explanations exist. Firstly the CE’s are approximately 20 years old and during that period wear and tear occurred. Each CE therefore had different wear characteristics. Secondly, the washing process does not remove all the ash from the CE. It was noticed during the loadcell installation that huge amounts of ash still remained on the CE’s. These differences in mass, are however not a problem as only the dynamic change of the CE’s collection pattern is required. This will become evident later.

The outlet duct on the test casing has an opacity monitor installed. It is of the SICK RM41 type and its output (converted to voltage) is also recorded in the DT600 recorder. This signal is only used for trend indications when rapping adjustments are made.

Each loadcell is rated to 2 $^{mV}/_{V}$ = 4000$\mu\varepsilon$ (microstrain) = 1000 kg.
For two loadcells connected in parallel, 2 $^{mV}/_{V}$ = 4000$\mu\varepsilon$ (microstrain) = 2000 kg = 3V output from HBM Clip AE301 Amplifier. The manipulation accounting for the parallel connection is done in the spreadsheet program.

The channels have offset values comprising the deadweight of the CE as well as system variations. These are quantified when the unit is off load and the CE’s have been rapped clean and are then manipulated via the spreadsheet.

The datalogger is controlled via it's proprietary software, DELOGGER PRO V3. This was used to program the DT600 for all the test sessions. The data downloaded from the DT600 is in "*.csv" format and as such can be directly viewed/manipulated by Microsoft Excel. The datalogger inputs were wired in as differential voltages. Scanning intervals ranged between five and thirty seconds, depending on requirements.

2.7 MEASUREMENT OF ASH COLLECTION TRENDS

Figure 2.5 shows the start-up collection patterns for the 25/03/97. The graph shows a 24 hour cycle. Data was logged every 5 seconds to provide adequate resolution. The large variations in overall CE load is noted. This occurs due to the loadcell offset values being intentionally left unbalanced as it is easier to distinguish the different measurements on each figure. Ash dislodged due to rapping is not very visible from this view, but zooming in at a later stage will clarify this. Of particular note is the logical behaviour of Field 1a and Field 2a. When Field 1a shows an increase in collection, Field 2a shows a corresponding decrease. Since these two CE's are in line with each other in fields 1 and 2, this trend illustrates the systems sensitivity to changing collection patterns. From this data, no distinct changes can be seen in ESP performance between night and day. This can be expected as Hendrina is a base load station and unit 5 generally operates at a nominal full load of 190 MW.

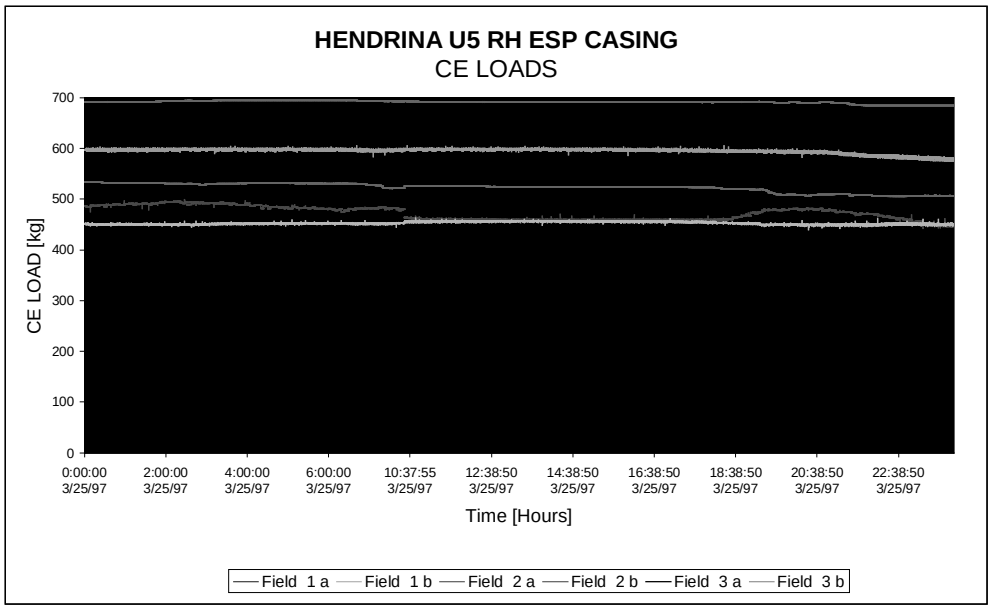

Figure 2.5 : Start-up collection patterns for 25 March 1997

Figure 2.6, below, shows collection patterns for the 28/03/97. It was decided to allow the ESP unit some time to "settle in" to operating conditions. This resulted from two reasons : firstly the unit has been on outage for approximately three weeks but secondly, and more importantly, the ESP unit had been washed during the outage. The washing has removed the base ash coating on the CE's resulting in an "abnormal" start. Therefore 3 days were allowed for the unit to "settle in". From Figure 2.6, though not too clearly, the effects of rapping on the CE ash load become evident. The data when measured during the subsequent months without temperature and electrical noise problems showed consistency and therefore, data from the 3/10/97 was used for analysis.

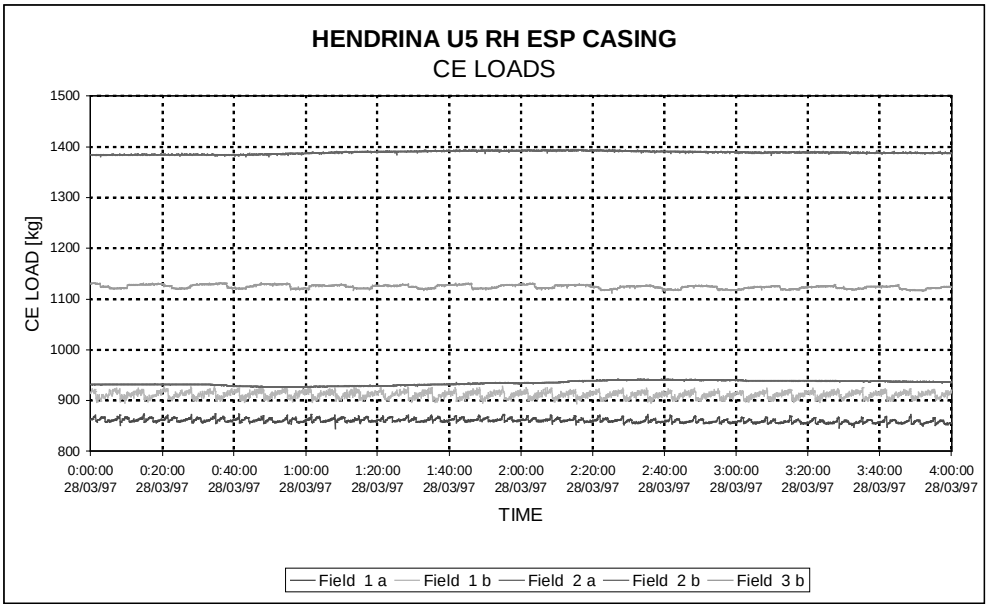

Figure 2.6: Collection patterns for 28 March 1997 - 0:00:00 to 04:00:00.

Figure 2.7, below, shows data for a 24 hour period on the 3/10/97 after the interim loadcell operation solution was implemented. Figures 2.8 to 2.13 show shorter appropriate time periods of collection patterns.

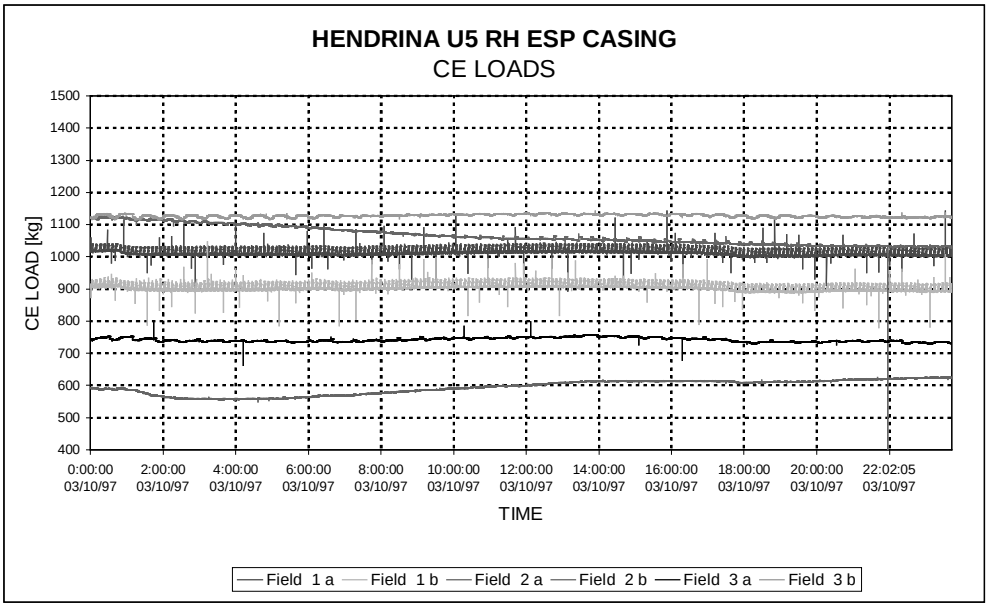

Figure 2.7 : Collection patterns for 10 October 1997 – 0:00:00 to 24:00:00.

The data from Figures 2.8 to 2.13, below depicting the amount of ash collected have been summarised in Table 2.1**.** It is assumed at this stage that re-entrainment is zero, since an efficiency test has not been conducted to determine the inlet dust burden. We know that this is however not the case, but for the purposes of this discussion, as well the first round of optimisation action re-entrainment will not be considered. Considering that each field has 60 CE's, the collection rates are then calculated in Table 2.2.

Table 2.1 : Summary of Collection Trend Analysis

Measurement Position	**PER CE**	
	Ash Discharge [kg/rap]	**No. of raps/hr**
Field 1 a	21	9
Field 1 b	24	9
Field 2 a	6	3
Field 2 b	6	3
Field 3 a	8	2
Field 3 b	10	2

Table 2.2 : Summary of Collection Rates

Measurement Position		**Collection Rate [kg/min]**	**Average Collection Rate [kg/min]**
FIELD 1	Field 1 a	189	3.38
	Field 1 b	216	
FIELD 2	Field 2 a	18	0.3
	Field 2 b	18	
FIELD 3	Field 3 a	16	0.3
	Field 3 b	20	

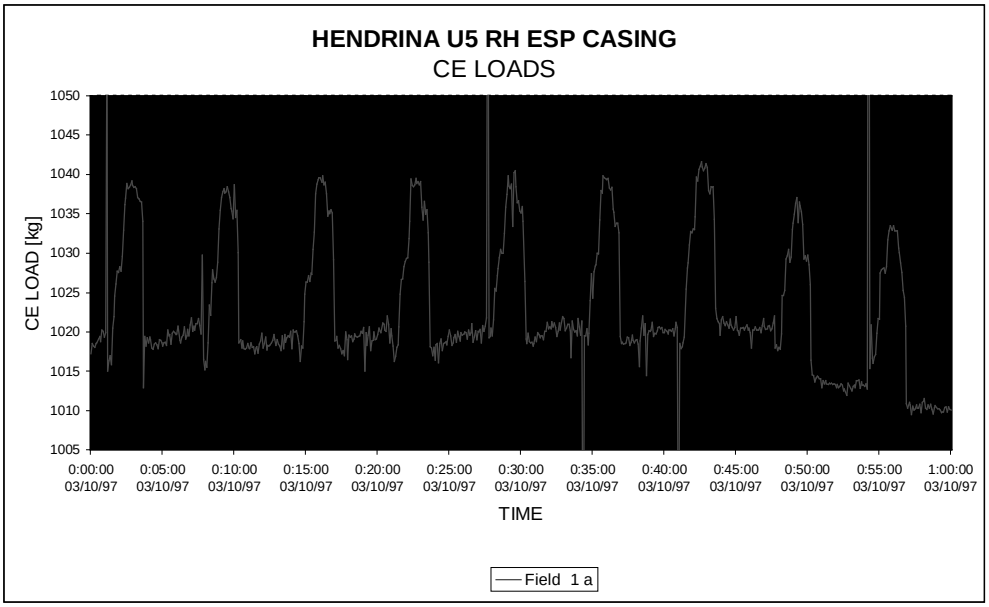

Figure 2.8 : Field 1 a collection trend between 00:00:00 and 01:00:00

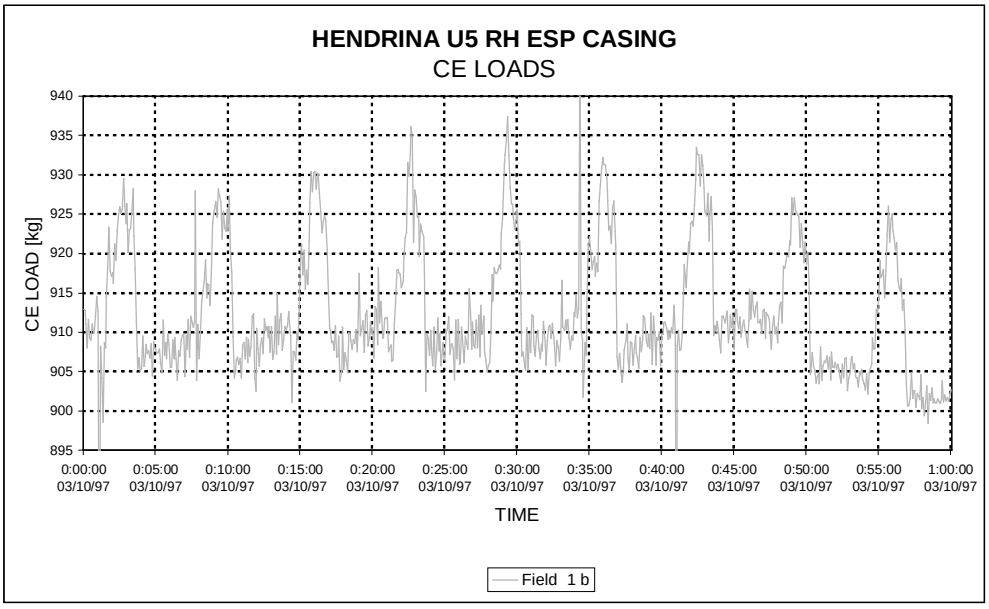

Figure 2.9 : Field 1 b collection trend between 00:00:00 and 01:00:00

From Table 2.1, 150 tons/hr or 85% of total ash collected is collected by Field 1. This is a fairly general result, as the first field in an ESP is subjected to the total dust burden and thus its efficiency is usually the highest in the casing. From Figures 3 and 4, the quantity of ash dislodged during a rap, correlate well with each other. Also from these figures, we can see that the shape is fairly similar.

Field 1 is on a rapping cycle of 20 seconds on, and 20 seconds off. Using a motor speed 0,33 rpm (1rev/3 minutes), the amount of raps calculates to 10 per hour. From Figures 2.8 & 2.9, we see 9 raps per hour. The one less rap per hour cannot be explained with certainty at this stage. The motor speeds used in calculations have been design ones. These could have changed with new gearbox ratios (after repairs), or their could be a delay between the controller's commands and the motors switch-gear.

Of particular significance from Figures 2.8 and 2.9, is the behaviour of the CE in collecting ash after a rap. There is approximately five minutes of inactivity from the CE. Over an hour this translates to about 45 minutes of wasted time indicating the field is being used for only 15 minutes. When the CE does begin collecting, we find it is saturated in about a minute.

It is recommended that, as a once off, the rapping be completely turned off for a period of one hour in Field 1. The purpose here is to determine the threshold for the amount of ash that can be collected, before rapping disturbs/dislodges the ash layer. Once this quantity, and more importantly, the time it takes to reach its threshold is determined, we will have the optimum time before rapping is required.

This will provide a basis from which to adjust the rapping cycles and/or electrical energisation in an effort to reduce the inactivity time, and thus have more collection peaks and raps in an hour.

The loadcell technique has clearly shown where and why Field 1 is performing poorly or not as well as it could perform. The data obtained from the figures could not be obtained previously, and it is doubtful what other existing methods would reveal the information gathered.

From Table 2.1, 1.08 tons/hr or 7,5% of total ash collected is collected by Field 2. Figures 2.10 and 2.11, below also exhibit different characteristics to Field 1. Here we can see that longer rapping-off times lead to wasted time once the CE has collected as much as it can collect. After about 2 minutes, the CE has already reached its maximum load. However, it then, due to the rapping-off times, remains at this load for about 15 minutes. Therefore, in an hour we have about 45 minutes of inactivity time.

Field 2 has shown poor performance in relation to Fields 1 and 3. It's collection rate should be higher than field 3 but is not. The data recorded over the past 8 months indicate this to be the general case. Figures 2.10 & 2.11 show the ash collection and dislodgement peaks, but these are not as distinct as those of fields 1 or 3.

The first of two possible reasons are electrical problems. This can and will be checked out as soon as possible as it does not require an outage.

The second likely reason is a misalignment of the CE rapping hammer shaft. If it is misaligned by a small degree, even as little as 5 mm, then the imparted acceleration intensities could be much less than designed. This would lead to the relatively lower amount of ash dislodged from the CE each time it is rapped. During the next outage, the alignment of rapping gear must be examined and vibration intensities needs to be quantified and compared to other fields. Considering the very poor state of Hendrina P/S's ESP internals, this is the most likely reason.

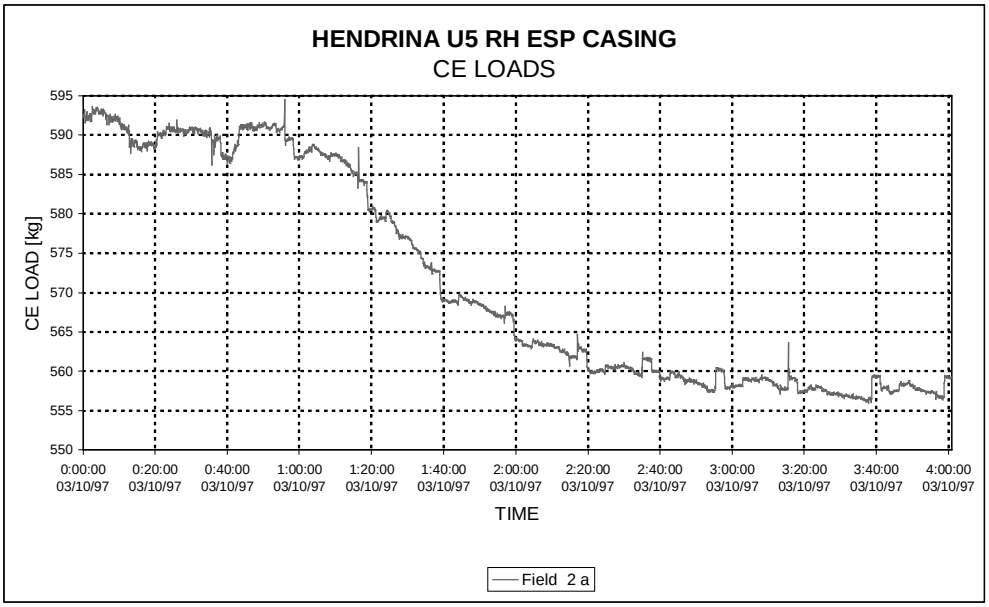

Figure 2.10 : Field 2 a collection trend between 00:00:00 and 04:00:00

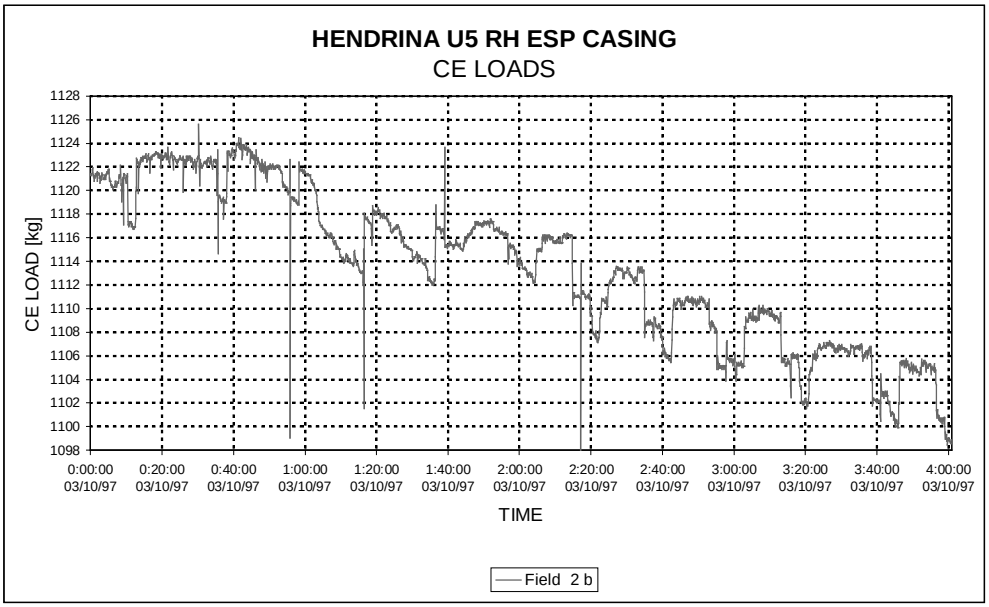

Figure 2.11 : Field 2 b collection trend between 00:00:00 and 04:00:00

Generally, a more conservative rapping regime is practiced in the last field of an ESP casing. This is done to minimise rapping puffs. However, rapping puffs are only visible at the stack for levels below approximately 80 mg/Sm^3 (milligrams per standard cubic

meter) and become more significant as this level drops. However, in Hendrina's case, the lowest emission levels on unit 5 are about 140 mg/Sm^3 (per casing) and generally much higher. Therefore, rapping puffs would not be visible compared to the general stack emissions. (5 units, 2 casings each).

From Table 2.1, 1,08 tons/hr or 7,5% of total ash collected, is collected by Field 3. From figures 7 and 8, we see the effects of a conservative rapping regime. There are just seven points of ash collection and dislodgement in a four-hour period. A closer look at these two figures reveals, as in field 2 that the dislodgement and collection times are fairly short. Five minutes is required for a CE to be emptied of its dust burden. Five minutes is also required for the CE to collect as much as it can collect. The time in between ash dislodgement and collection is fairly short as opposed to Field 1, which is advantageous This is a good situation. However, the long wasted times, as in Field 2, that the CE spends when it has reached its maximum collection mass, is a cause of concern. Approximately twenty minutes passes, before the CE is emptied, and this results in a period of between thirty and forty minutes of time in every hour when the field is inactive.

The ash collection rates do not correlate to the last efficiency tests done at Hendrina. This is most likely due to the center CE's of Hendrina collecting much more ash than the outer CE's. Since a uniform flow had been assumed across the width of the casing, loadcells were only installed in the center electrodes. The amount of ash collected by center electrodes are higher, and when multiplied by the total number of electrodes, gives erroneous values. This is however not a major problem, as the timing of rapping is the major factor. Also the CE loads provide a relative reference from which improvements can be seen.

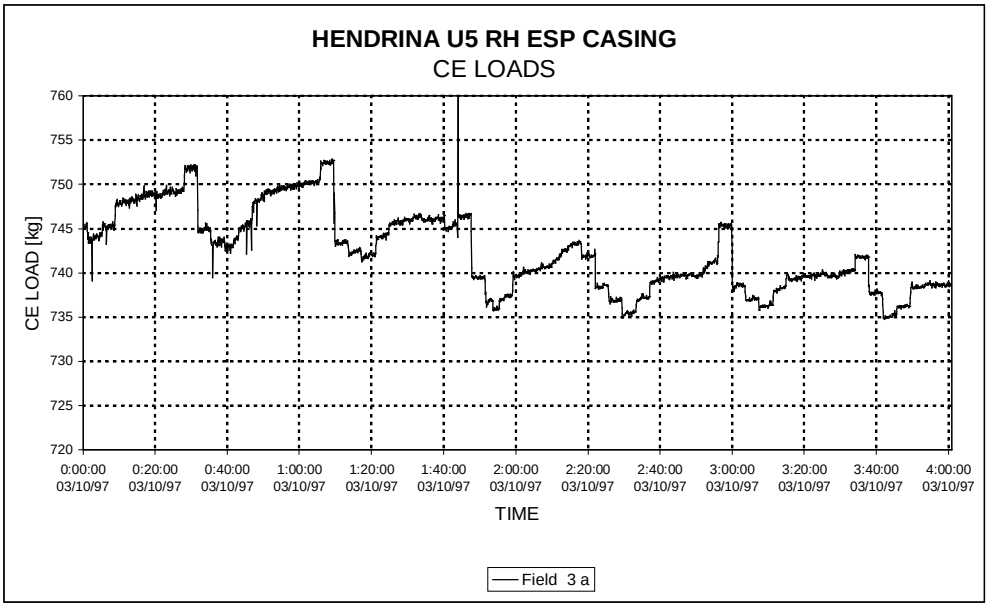

Figure 2.12 : Field 3 a collection trend between 00:00:00 and 04:00:00

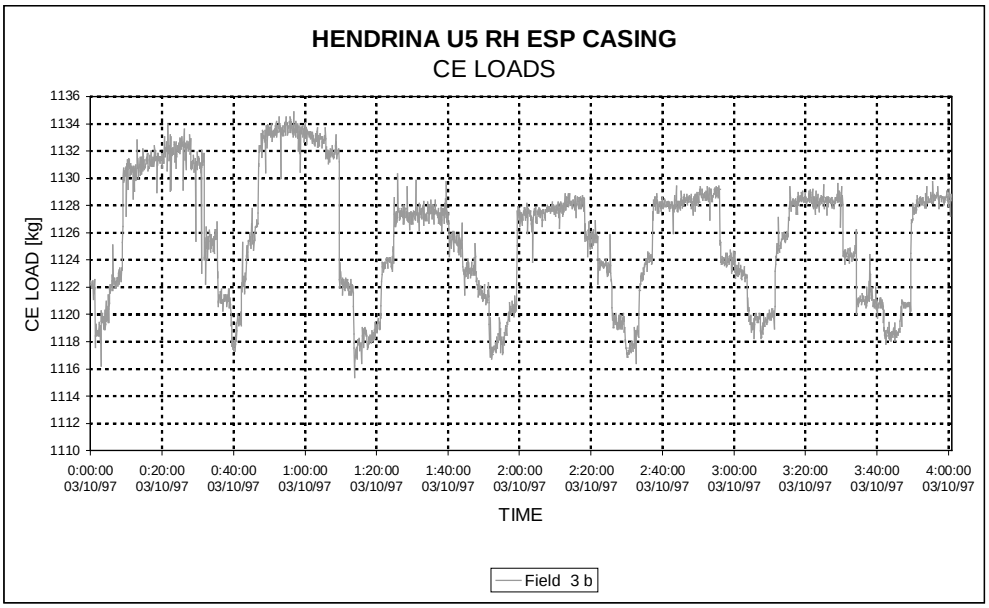

Figure 2.13 : Field 3 b collection trend between 00:00:00 and 04:00:00

2.8 ELECTRICAL CONTROLLER INVESTIGATIONS

Based on the rapping-off tests, as well as the peculiar measurements recorded from field 2, it was decided to conduct voltage/current (VI) curve tests to determine if the fields were operating within acceptable electrical specifications.

The controller card installed in the test unit is an analogue GEECOMATIC one. There is no plant management system (PMS) installed on the ESP and hence the combination of the above equipment means that VI curves have to be taken manually. The presence of suitably capable personnel to perform this work in the past has been a problem. The results obtained are shown in Figure 2.14.

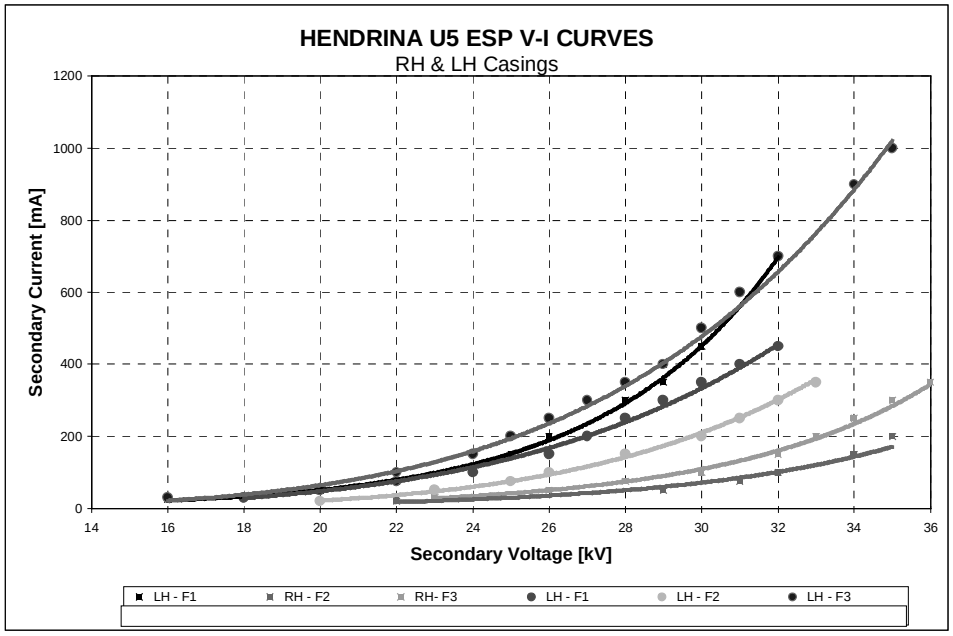

Figure 2.14 : Hendrina Unit 5 ESP V-I Curves

- The electrical tests indicate that there is no back-ionisation present in the casings measured. This can be expected due to the presence of FGC at this unit.
- All the curves were drawn to the point at which arcing and sparking became constant, and the controller continually de-loaded the transformer at these points.

- The first fields of both casings seem to be getting an acceptable power input. The LH casing's first field power input could be higher when compared to the RH casings energisation.
- The reason for RH - field 2's poor and peculiar collection pattern as documented from loadcell data can be clearly seen in Figure 2.14. Field 2, cannot be properly energised, with a maximum power input of 200 mA before continuous arcing and sparking occurs. This results in the controller starting up and shutting down continuously causing poor power input. This behaviour causes the transformer to operate at extremes as it loads and de-loads and can be distinctly heard when standing in the transformer room. One possible reason for the low power input is dirty, clogged discharge electrodes. This will be investigated during the next outage.
- Both casings field 3's display similar energisation characteristics with power input being on the slightly lower side.

2.9 PROBLEMS EXPERIENCED

The problems experienced during the research at Hendrina Power Station have been relatively few and were limited to damage of the loadcells, which were located inside the ESP casing.

In the first problem, an air heater fire occurred, upstream of the ESP. This is a totally random event, but they do occur occasionally in power plant operation. During this, ESP temperatures can rise to about the 250º C level. This causes total failure of the loadcells and they have to be refurbished.

In the second problem, the loadcells experienced gradual failure over a period of 4 months. Due to accessibility limitations to visually inspect the loadcells, diagnosing failure was difficult. When the opportunity finally presented itself to remove the loadcells

and inspect, it was found that the silicon sealant used to seal critical strain gauged areas in the loadcell body had perished. In most cases, originally sealed areas were completely open to the gas flow. Subsequent investigations revealed that the use of silicon inside ESP's is not recommended. While silicon has the ability to withstand high temperatures, its resistance to the constituents of boiler flue gas, particularly sulphur and its compounds is very weak. Now considering that Hendrina Power Station also has FGC, where SO_3 is injected into the ESP, the loadcell failures are very well explained.

2.10 DISCUSSION

The peculiar, under-performing behaviour of RH field 2 can be attributed to low power input. It is recommended that this be investigated at the next outage. The controller technology at Hendrina is not as technologically advanced as it could be. Hence the options available to optimise the ESP are restrictive and emission reductions are minimised.

The electrical tests (VI curves) are a useful and essential tool to understand and hence optimise ESP's. Problem areas can be also be detected from the tests.

Despite the above, results obtained thus far show that the concept of using loadcells to optimise ESP performance is a sound one with immense potential. Ash collection patterns were, for the first time, successfully monitored on an operational, full scale ESP unit.

The data obtained firstly provides an indication of the performance of each field in itself and then in relation to the other fields. The timing of rapping, as discussed previously, is critical. If the rapping is not adjusted in relation to the specific fields behaviour, then performance declines. The data obtained, simplistically reveals when and where rapping

should occur. In Hendrina P/S's case, if the inactivity times are minimised, then emissions can be conservatively estimated to reduce by 30 to 60 %.

Accessibility to the internals of the ESP at Hendrina has proved to be a major stumbling block to the projects time scales. Failures and problems are difficult to diagnose and correct considering Hendrina base load status as well as Eskom- Generation's 90:7:3 goals.

2.10.1 Internal and External Loadcell Installations

For the purpose of this project, an external loadcell installation can be defined as one where the loadcell is located away from the gas stream, thereby not coming into contact with the flue gases. An internal loadcell installation can be defined as one where the loadcell is installed within the ESP casing and hence comes into contact with the flue gases.

At Hendrina P/S, an internal loadcell installation was initially used. This was primarily due to the concrete casing construction (difficult and expensive to cut into) as well as the limited space available at the CE suspension beam support locations. The loadcell chosen was thought to suit the conditions perfectly. This has however, not been the case. While the loadcell was able to operate perfectly within the hot, high voltage environment, it was affected by acidic attack of its critical sealant area.

Possible solutions to the above are:

- Use of ESP environment resistant sealants. An investigation into this is currently being conducted by Eskom, but is considered outside the scope of this project.

- Use of hermetically sealed loadcells. These would have to be custom built to suit the high temperature environment and can presently be considered to be expensive.

- Design of airtight cooling chambers in which the loadcells are located. The ESP's suction capabilities can then be used to draw clean, cool (ambient), "purge" air over the loadcell while keeping out the flue gases.

- The use of the loadcells constructed from high temperature (capacitive) strain gauges. These can be rated to temperatures around 600°C. However, these are fairly new, and hence popular loadcell configurations are not available. Sensitivities are also not as good as foil strain gauges and the driving of long cable lengths will be problematic.

Internal loadcell installations have the advantages of :

- Being generally cheaper than an external loadcell installation. This originates from the reduced supporting structure required, associated labour costs and shorter plant downtimes.
- Being easier to install, especially in concrete casings.

Their disadvantages are :

- Prone to failure from being exposed to the harsh internal ESP environment. Also, they are exposed to high temperatures possible during boiler start-ups and air heater trips.
- Access to inspect, remove and repair being restricted to planned or forced boiler outages. These can be as long as three years.

- One set of loadcells cannot be used across many ESP units easily due to access limitations.

An external loadcell installation will be considered for the next experimentation phase of this project. This new testing phase is discussed further in the next chapter.

The advantages of an external loadcell installation are :

- The design enables access to the loadcell even with the unit on load. A further bonus is that the loadcell can also be removed with the unit on load. These factors promote, if necessary, repairs of the loadcell while the unit is on-line. As part of a continous measurement and control system, this is a necessity.
- One set of loadcells can be used across many ESP units as they can easily removed and refitted, even with the units on load.
- Not being in contact with the flue gas ensures loadcell safety from usual harsh ESP environmental conditions.
- Common, commercially available, ambient temperature rated loadcells can be used.

The disadvantages of external loadcells are:

- More expensive than internal loadcell installation.
- Loadcells are installed outside the ESP casing and connecting rods penetration positions have to be gas tight sealed. This gas tight seal can cause a friction problem with connecting members and measurement errors can occur.
- Not easily installed in units with concrete casings.

2.10.2 Further Experimentation

The premature failure of the loadcells at Hendrina P/S has resulted in the projects objectives not being fulfilled. The causes of loadcell failures have, nevertheless been determined and it is recommended that further experimentation occur. For a variety or reasons, detailed below, it is recommended that this further experimentation occur at Eskom's Lethabo P/S.

The casings at Lethabo are of steel, and not concrete. This makes installation and wiring less difficult if an external loadcell installation is chosen.. But, more importantly, it easily enables cooling of the loadcells by external means.

Each unit has four casings as opposed to the conventional two. This allows for a casing to be isolated with a minimum load loss. Therefore if any changes need to be made to the loadcells, then the problem of accessibility, which has hindered us at Hendrina would not be a problem.

Each casing at Lethabo P/S has seven fields as opposed to the three at Hendrina P/S. This provides greater opportunity and flexibility for optimising the rapping system and hence, ESP efficiency.

As a possible future venture, one set of loadcells can be used across all units at Lethabo Power Station. Only the necessary supporting structure needs to be installed on each unit and the loadcells, by virtue of the accessibility and mobility, can be moved across units for optimisation purposes.

Lethabo P/S ESP's are newer, and hence it's internals are is a sounder mechanical condition as compared to that at Hendrina P/S.

Lastly Lethabo's ESP performance has started to show a gradual decline. The loadcell technique, in conjunction with the multiple ESP fields and two sided CE rapping provides a potentially good basis for substantial improvements.

If the loadcell technique is implemented at Lethabo, then new hammer designs can be tested when required. The advantage of using the loadcell technique, is that the entire field does not need it's hammers to be changed. Hammers are changed on a few (one CE's), and two CE's have the existing hammers installed. These four CE's are then suspended from loadcells and the new hammer designs are evaluated against existing hammers and the improvements in ash dislodgement can then be quantified and compared to the existing hammers. This methodology is logical, as improvements are quantified, but it is also cost-effective as whole fields do not need new hammers. The accessibility advantage at Lethabo P/S, means that many new designs can be tested relatively quickly without unit load losses or outages.

2.11 SUMMARY

The concept of using loadcells to measure the collection of ash within an ESP has been shown to be a viable one. The loadcell measurements at Hendrina P/S has demonstrated that it is indeed possible to measure the collection patterns of the CE's. However, the premature loadcell failures have prevented the complete optimisation of the ESP unit. As such, we cannot measure the effectiveness of using loadcells to optimise an ESP. Apart from the loadcell failures, the instrumentation methodology and data measurement systems have been successful.

The cause of premature loadcell failures has been determined and will be eliminated in future installations.

Continued testing and optimisation at Hendrina Power Station is not viable. Further testing and optimisation will have to conducted at another power station and Lethabo P/S has been chosen for continuation of the research.

Chapter 3 : Experimentation at Eskom's - Lethabo P/S

3.1 INTRODUCTION

Lethabo Power Station, as shown in Plate 3.1, is located in the town of Vereeniging, Free State province, South Africa. It is a six unit, coal fired power station, each unit capable of generating a nominal 620 MW. The station was built between the years of 1980 and 1990. Up until 1996, Lethabo was the only station in the world that burns coal with a low calorific value of between 15 and 16 MJ/Kg and and ash content as high as 42%.

Plate 3.1 : Eskom's Lethabo Power Station

For reasons detailed previously in 2.11, the research project will now conduct tests at Lethabo Power Station.

3.2 LETHABO ESP GEOMETRY AND OPERATING SPECIFICATIONS.

The ESP units at Lethabo Power Station are of the Rothemúhle/Brandt type. Each boiler unit is serviced by four, parallel ESP casings as opposed to the conventional two. Figure 3.1 shows a detailed view of the Lethabo ESP type. These casings have seven fields, each field being approximately 5 m long and 15 m high, giving an aspect ratio of 2.4. The ESP's at Lethabo Power Station are amongst the largest built in the world, primarily due to the high ash content of the coal burned. Plate 3.2 shows a side view of the ESP casing. Each field is one hopper wide, when viewed square-on.

Plate 3.2 : Side view of Lethabo ESP Unit Casings

Plate 3.3, is an aerial view of the ESP casings. Note the four ESP casings per boiler unit, including the ducting from casing outlet to smoke stacks.

Plate 3.3 : Top view of Lethabo ESP Unit Casings

Figure 3.1 shows a cut-away section of the ESP type at Lethabo P/S. Two casings are shown. This Figure depicts a four-field casing whereas Lethabo P/S has seven fields. The other components are however, very similar

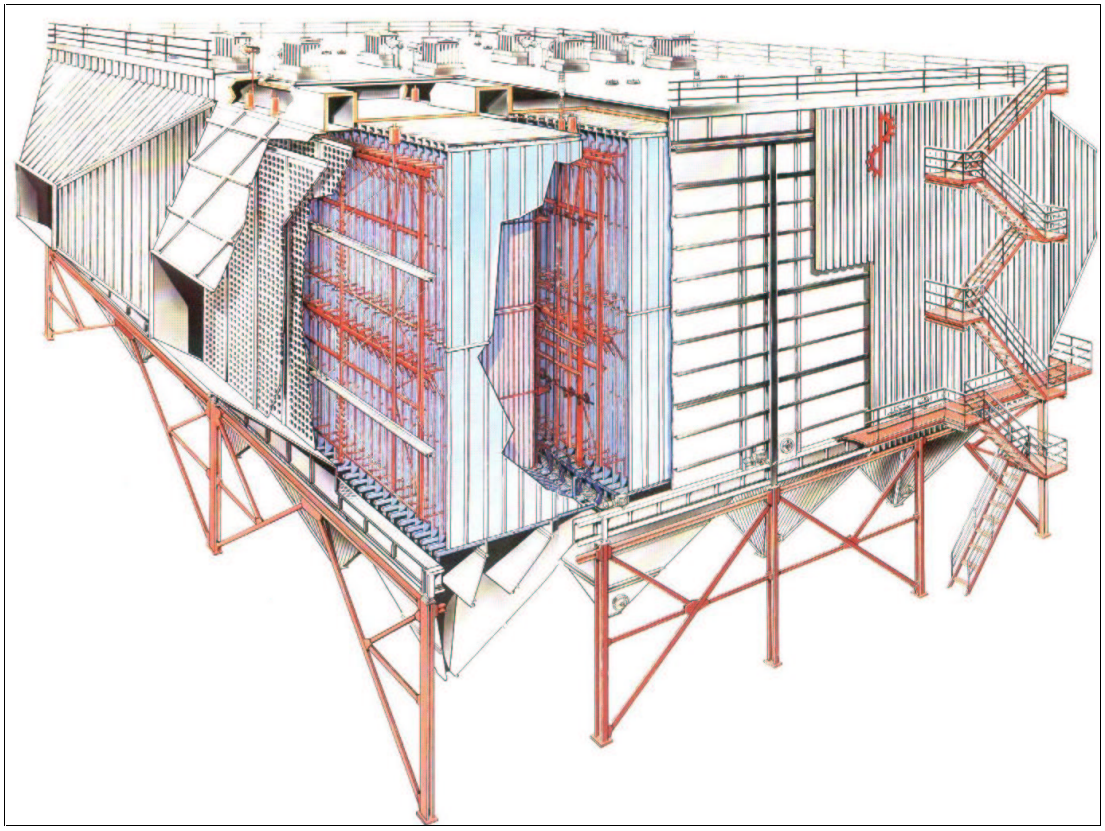

Figure 3.1 : Cutaway section of Lethabo P/S ESP unit

Table 3.1, below indicates more specifications of the Lethabo ESP unit's.

Table 3.1 : Lethabo Power Station – ESP Specifications

Design Data	
Boiler rating (at 97% MCR)	600 MW
Efficiency (at 97% MCR) for all fields in service	99.88
Parallel Casings	4
Plate (CE) Height	15 m
Plate (CE) Length	5.1 m
Lanes per filter casing	46
Pitch between lanes	300 mm
Fields in series per pass	7
Plate (CE) area total	190 000 m^2
Flow area (total)	817 m^2
Specific collecting area (SCA)	191.6 s/m
Aspect Ratio	2.4
Casing Construction	Steel
Operating Data	
Gas volume flow rate	997 m^3/s
Gas temperature	130 °C
Dust Burden	50 g/Sm^3
Treatment time	28.7 s
Migration velocity (Deutsch)	35.1 mm/s
Gas velocity at electrodes	1.2 m/s
Design Coal Specification	
Ash content	35 %
Sulphur	1 %
Net C.V	16.8 MJ/kg

Table 3.2, below shows the present coal specification at Lethabo P/S. The qualities of coal that effects ESP performance are shown. These qualities have deteriorated to their present levels and this has caused a decrease in ESP efficiencies. These coal qualities lead to the description of “difficult” or low-grade coal from an ESP operation perspective.

Table 3.2 Current Lethabo P/S Coal Quality

Current Coal Specification	
Volatile Matter	18.7 %
Ash	42 %
Sulphur	0.58 %
CV	15 MJ/Kg

3.3 DESIGN OF LOADCELL INSTALLATION AND SUPPORT STRUCTURE.

The installation method of loadcells at Lethabo Power Station could either be of the internal or external types. However, in the light of previous loadcell failures and after several site inspections it was decided to use the external loadcell method. This decision was aided by the construction geometry.

A similar approach as to the number of loadcells per CE and the number of CE's per field at Hendrina P/S was adopted at Lethabo P/S. Each field has 2 CE's instrumented with loadcells to provide the measurements. The only major difference was that Lethabo ESP units have seven fields in series as opposed to Hendrina P/S's three. Hence, a total of 28 loadcells (2 CE's per field x 2 loadcells per CE x 7 fields) would have to be installed.

An external loadcell system was designed and this is shown in Appendices B and C. Calculations were performed to determine the loading on the supporting members and an installation methodology that combined minimum plant modifications and costs was determined.

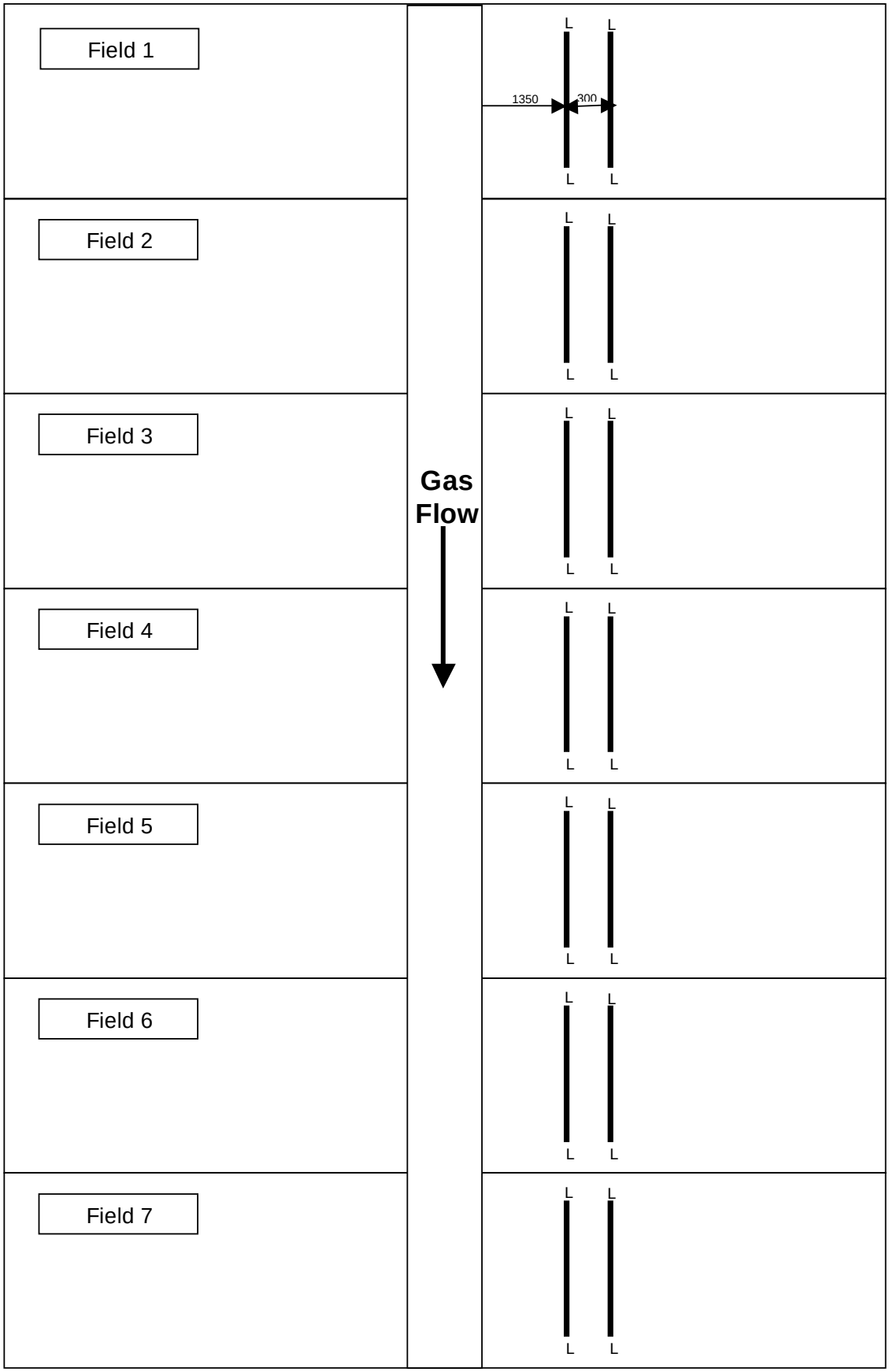

Figure 3.2 : Schematic Top View of Loadcell Location

3.4 LOADCELL INSTRUMENTATION AND DATA RECORDING SYSTEM

The equipment used at Hendrina Power Station was moved to Lethabo P/S, and an additional eight channels of amplifiers and displays were purchased. A total of fourteen loadcell channels (14 CE's, two loadcells connected in parallel) were installed at Lethabo Power Station. Since the datalogger, a DT600 unit can accommodate either ten differential or thirty single ended voltage inputs, single ended inputs had to be used.

The outlet duct on the test casing has an opacity monitor installed. It is of the SICK RM41 type and its output (converted to voltage) is also recorded in the DT600 recorder. This signal is only used for trend indications when rapping adjustments are made.

Each loadcell is rated to 1,5 $^{Mv}/_{V}$ = 3000με (microstrain) = 3000 kg.

For two loadcells connected in parallel, 1,5 $^{Mv}/_{V}$ = 3000με(microstrain) = 6000 kg = 3V. The manipulation accounting for the parallel connection is done in the spreadsheet program.

The channels have offset values comprising the deadweight of the CE as well as system variations. These are quantified when the unit is off load and the CE's have been rapped clean and are then manipulated via the spreadsheet.

The data retrieval format used previously at Hendrina P/S was used here.

3.5 INSTALLATION OF ALL EQUIPMENT AND COMMISSIONING OF SYSTEM

The loadcell installation had to correspond with the next planned outage and commenced on the 5/09/98 and was completed on the 14/09/98. A contractor, JJ's

Construction, under the supervision of TRI was used to perform the installation work. The work was performed according to the sequence of events described in Appendix 2.

It should be noted that since this installation was not budgeted in the 1998 project (1997 research budget closed before it become evident that another installation was required), finances were a problem area. Due to this, the installation could not be totally completed in 1998. The loadcells and all supporting structure were installed. However, instrumentation (some of which will be moved from Hendrina Unit 5) will have to purchased and installed during the 1999 year. This however does not require an outage for completion.

Plates 3.4 to 3.7 show various views of the loadcell installation.

Plate 3.4 shows the penthouse hot roof section cut open and the two test CE's. These CE's are 5,1m in length and have 300mm spacing between them.

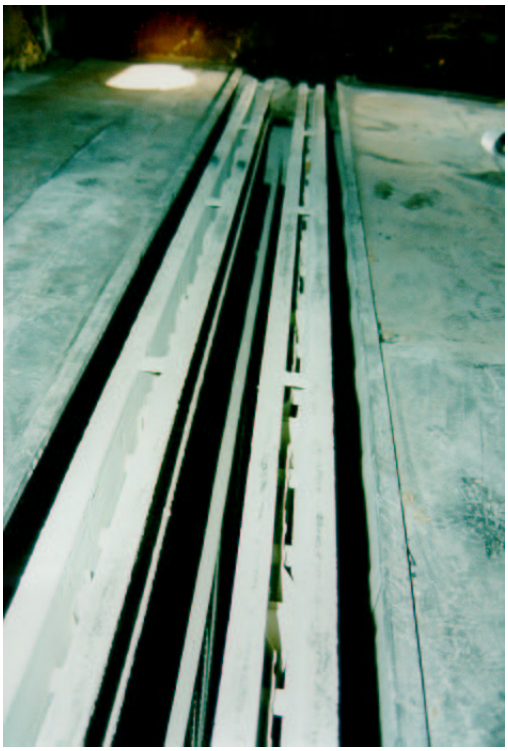

Plate 3.4 : Cut-open hot roof section

Plate 3.5, below. shows the completed installation view of each CE end. Each CE end h one channel section installed. It is bolted onto the main roof beam. These channels and rods which penetrate the hot roof are visible in Plate 3.5. This penetration point is sealed with a bellow-like, gas tight seal. This seal must not exert any load on the rod as this could give inaccurate measurements. This seal, due to cost constraints, was made from high temperature, fabric filter material, specially treated to minimise porosity. Commercially available viton seals are recommended for future applications.

Plate 3.5 : Penthouse section installation view.

Plate 3.6 shows the view of the loadcell installed within the supporting channel section, as viewed from the cold or walking roof. Its accessibility and removal features can be seen.

Plate 3.7, below, shows the loadcells sections closed with steel box-like covers, as viewed from the walking roof.

Plate 3.6 : Loadcell & support member as viewed from the ESP roof.

Plate 3.7 : Closed loadcells and supports.

3.5.1 Measurement System Fluctuation With Temperature

During the commissioning tests as well as later on, it was discovered that all the loadcell channels fluctuated in a sinusoidal manner. These variations were very surprising considering that identical equipment was used for previous tests at Hendrina P/S.

Investigations showed that these cycles were very consistent and peaked at around midday and dipped in the morning, usually just before sunrise. After further investigations, it was found that the fluctuations corresponded to temperature – midday or thereabouts being the hottest with the morning being the coldest.

The system consists of various components – these being the CE and supporting structure, loadcell, cable length (120m), surge-arrestor, amplifier, display and datalogger. In situ-tests were then conducted on each of the associated components using known reference standards and through the process of elimination the problem area was narrowed down. It was found that all components operated within specification, however, the combination of the long cable length in-between amplifier/recording equipment and loadcell caused the fluctuations.

The amplifier type was essentially chosen to power long cable lengths(up to 500m) as well as adjust for cable voltage losses. Suprisingly, these amplifiers worked perfectly with similar cable lengths previously at Hendrina P/S. Investigations are still ongoing, but at the time of writing this, all evidence points to some sort of “thermocouple” effect being induced into the system. If this is the case, efforts will be made to eliminate it at it’s source. If this is unsuccessful, then the automatic control planned for future work must be designed so as to adjust displayed results according to measured deviations.

These variations were quantified on three occasions when the unit was off load and hence measurements can be adjusted, when required. Tests most affected are those that span six continuous hours or more and commence in the morning. Hence tests were not conducted in this "non-ideal" period. Rapping-off/field optimisation tests have much shorter time periods, typically 1 hour or so and are not affected. Also when studying the amounts of ash discharged from the CE due to rapping, the measurements are relative to each other for the instantaneous impact and thus minimally affected by system drift.

3.6 MEASUREMENT OF ESP "AS FOUND" EMISSION LEVELS

3.6.1 Introduction

In order to assess the effectiveness of the rapping optimisation process, it was decided to measure the outlet emissions before any optimisation was conducted. This state will be refered to as the ESP units "As Found" state. After optimisation, these tests will again be carried out and this will be refered to as the "Post Optimisation/Efficiency" tests.

3.6.2 Instrumentation and Methodology

In determining the efficiency of an ESP unit, measurement of the inlet and outlet dust concentrations must be made. These measurements are commonly referred to as isokinetic sampling tests. This test consists of positioning a sharp edged nozzle in the duct and extracting a flow sample of the gas, isokinetically. These samples are taken at pre-selected positions, in a suitable cross-section of the duct to provide a representative average of the gas flow in the whole duct. The particulate matter in the collected sample is separated from the gas via a mechanical filter medium. For isokinetic sampling, the gas velocity at the sampling point in the duct has to be measured, and the corresponding

sample gas flow has to be calculated and adjusted. After sampling, the collected particulate matter is completely recovered, dried and weighed. The particulate concentration is then determined by measuring the sample's gas flow and dividing it into the measured particulate mass

The equipment used is :

- A sampling probe tube with entry nozzle;
- A particle separator
- A gas metering system, in-stack or external;
- A suction system

During these isokinetic tests, it is essential that stable boiler conditions are maintained. To prevent spurious events, a temporary operating instruction is issued to the boiler operator. Certain boiler parameters are forced to remain constant so that these do not cause erroneous emission measurements. For the test period, these are:

- Constant boiler load. (MW)
- No mill changes.
- No sootblowing.
- No overfull ash hoppers.
- No frequency biasing on boiler/turbine unit.

3.6.3 Results and Discussion

It was necessary to determine the ESP's "as found" condition and efficiency prior to optimisation efforts. Isokinetic sampling tests, according to prescribed methods and standards was conducted by T-S-I's emissions measurement team on the 16th and 17th April 1999. Table 3.3 shows the rapping times used by Lethabo Power Station prior to

the start of this project. During the efficiency test sessions, the loadcells were monitored to characterise collection patterns. The opportunity to correlate the duct opacity monitor(SICK RM41) was also taken. The isokinetic test results are shown in Table 3.4.

Table 3.2 records the rapping on-off times being used by Lethabo Power Station prior to the loadcell optimisation tests. An isokinetic sampling test was conducted to determine the ESP casings "as found" baseline performance as well as to correlate the opacity meter on the outlet duct.

Table 3.3 : Rapping times used for "As found" Efficiency Tests

LETHABO UNIT 5 RH INNER ESP CASING				
	FRONT HAMMER SHAFT		**REAR HAMMER SHAFT**	
FIELD	**Pause/Off**	**Run/On**	**Pause/Off**	**Run/On**
1	no front/leading edge shaft		3 sec	6 hrs
2	3 sec	30 sec	3 sec	40 sec
3	5 sec	20 sec	5 sec	30 sec
4	1,5 hrs	20 sec	1,5 hrs	30 sec
5	4 hrs	20 sec	4 hrs	30 sec
6	5 hrs	20 sec	5 hrs	30 sec
7	1 hr	4 sec	1 hr	6 sec

It should be noted that, with the exception of the first field, each field has two CE rapper shafts. These shafts are located at the bottom of the fields and rap the leading and trailing CE edges. All rapper motors at Lethabo P/S has a continuous speed of 180 s per revolution.

Table 3.4: Isokinetic Efficiency Test Results - Lethabo Unit 5, Right Hand, Inner Casing

TEST		1	2	3	4	5	6
DATE		16/04/99	16/04/99	16/04/99	17/04/99	17/04/99	17/04/99
BOILER LOAD	MW	620	620	620	620	450	450
POSITION	**RH INNER INLET**						
START TIME		9H30	13H13	16H20	9H12	12H20	14H48
END TIME		11H00	15H10	18H25	11H25	13H40	15H40
Barometric Pressure	mbar	850.6	849.0	849.0	867.9	859.0	851.9
Static Pressure	mbar	-22.28	-21.99	-21.90	-21.74	-16.20	-15.78
Total Pressure	mbar	-21.65	-21.46	-21.09	-20.86	-15.90	-15.48
Gas Temperature	DEG C	142	143	131	147	142	140
Gas Velocity	m/s	13.3	11.7	15.2	15.6	8.9	9.0
Gas Flow/ sec	m^3/s (ATP)	211.11	185.03	239.52	247.24	141.00	143.53
Gas Flow/ sec	m^3/s (STP)	113.65	99.06	125.86	134.21	77.12	78.19
Dust Concentration	g/m^3 (ATP)	44.38	46.20	42.92	46.48	48.31	41.26
Dust Concentration	g/m^3 (STP)	82.44	86.29	81.68	85.62	78.95	75.72
TEST		1	2	3	4	5	6
DATE		16/04/99	16/04/99	16/04/99	17/04/99	17/04/99	17/04/99
POSITION	**RH INNER OUTLET**						
START TIME		9H25	13H31	16H10	9H05	12H13	14H33
END TIME		11H00	15H00	17H30	10H46	13H45	16H00
Barometric Pressure	mbar	850.6	849.0	849.0	867.9	859.0	859.0
Static Pressure	mbar	-24.84	-25.47	-25.98	-25.44	-18.28	-17.99
Total Pressure	mbar	-23.56	-24.24	-24.79	-24.19	-17.46	-17.23
Gas Temperature	DEG C	137	140	141	138	136	135
Gas Velocity	m/s	18.8	18.6	18.2	18.4	14.8	14.3
Gas Flow/ sec	m^3/s (ATP)	265.60	270.56	265.74	266.34	213.29	207.48
Gas Flow/ sec	m^3/s (STP)	144.28	145.25	142.45	147.16	118.09	115.10
Dust Concentration	mg/m^3 (ATP)	89.6	96.6	101.1	77.2	85.7	94.0
Dust Concentration	mg/m^3 (STP)	165.0	180.0	188.6	139.7	154.8	155.0
ESP EFF	%	99.80	99.79	99.77	99.84	99.80	99.80
STACK MONITOR OUTPUT	%	38.55	42.48	45.62	32.82	28.98	28.91
OUTLET DUCT MONITOR OUTPUT	mA	9.29	12.06	12.53	8.21	7.42	6.84

Table 3.4, above shows the results of the emission measurements. Six tests were conducted, four at the nominal full operating load of 620 MW and two at 450 MW. From an emission perspective, the four full load tests are most significant as these are the maximum levels to be experienced. Also, this boiler spends the most of its generating time at full load. The two 450 MW tests were done to provide more data points to

correlate the emission monitor. The emission monitors output is of the analogue current state (2-20 mA range) and this is shown in Table 3.4. It can be seen that at full load, the outlet emission ranges between 139 and 188 mg/Sm^3. From the above results, it can be seen that, the inlet dust burden to the ESP casing is extremely high at between 81 and 86 g/Sm^3 for boiler full load conditions. While a high inlet duct burden was expected, these higher than expected levels were surprising, though not unbelievable considering the coal type burned. These ash inlet levels are amongst the highest experienced by ESP's in general. At full load, the casing operated at efficiencies between 99,77% and 99,84%, which is remarkably good. These measurements will be discussed later, in comparison to the "post" optimisation measurements.

3.6.4 Correlation of Emission (Opacity) Monitor

An emission (opacity) monitor (type, SICK RM41) was installed on the outlet duct of the test casing. This was used as a trend indicator for subsequent experimentation as it is not possible to continuously conduct isokinetic measurements.

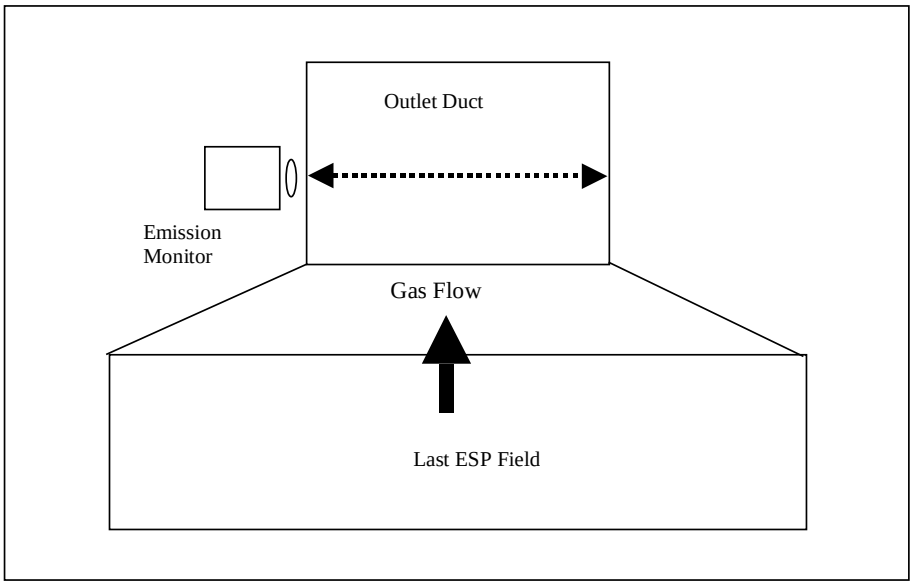

Figure 3.3 : Location of Emission Monitor in ESP Unit

Figure 3.3, above shows a top view schematic of the location of an emission monitor in an outlet ESP duct. The monitor transmits it laser beam across the gas flow, thereby measuring extinction by determining the obscuration of its reference light source by ash particles flowing through.

The emission monitor's electrical output is recorded on the existing datalogger. Figure 3.4, below shows its correlation. Its equation is shown in the Figure.

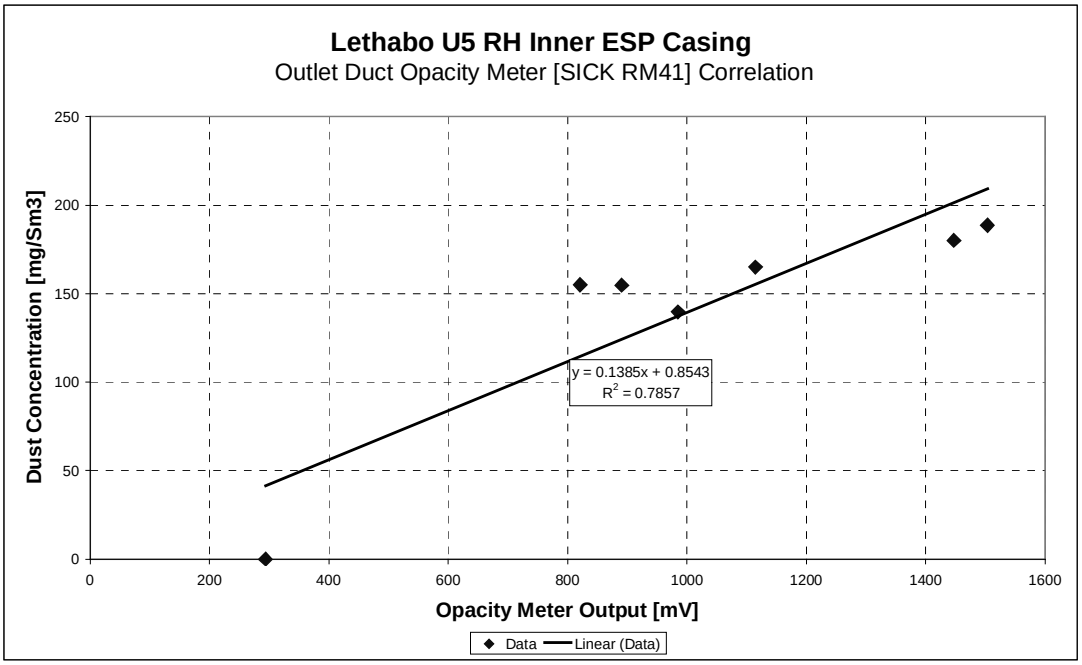

Figure 3.4 : SICK RM41 Emission Monitor Correlation

3.7 MEASUREMENT OF ESP "AS FOUND" COLLECTION CHARACTERISTICS

3.7.1 Introduction

During the isokinetic tests of section 3.6, the loadcell signals of all the CE's were recorded so as to provide insight into the ESP casings existing performance patterns, on a field by field basis. These are now shown below.

3.7.2 Results

Figures 3.6 to 3.10 show the loadcell measurements for tests conducted on 16th April 1999.

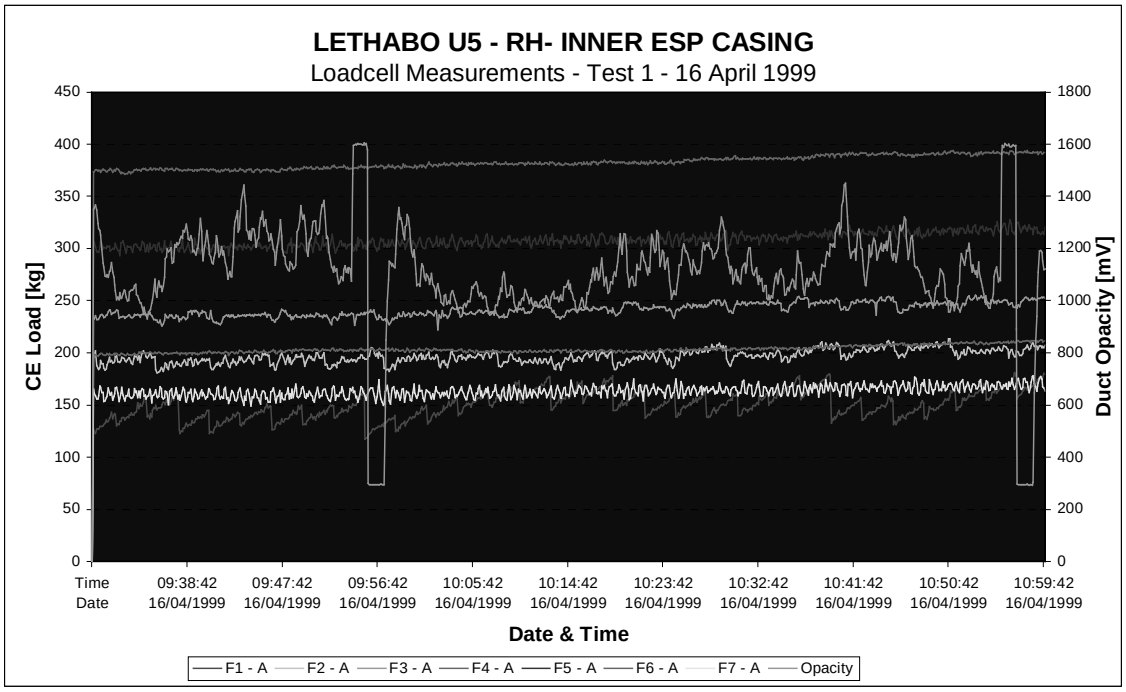

Figure 3.5 : Loadcell measurements – 16th April 1999 - All fields.

From Figure 3.5, above, it can be seen that rapping cleaning effects are clearly visible in fields 1 to 3. This corresponds to the rapper time intervals and the test time period. Fields 4 to 7 have longer rapping-off times and hence these are not visible. Figure 1 , also indicates the duct opacity meter (SICK RM41) “zero” and “100% range” checks. The average amount of ash discharged by each rap is 20 kg.

Figure 3.6, below, shows a clearer view of field 1’s precipitation characteristic. From this figure, it can be seen that a correlation exists between field 1 collection and outlet duct opacity. A cyclic pattern exists in the way field 1 operates – that is each rap does not seem to “remove” all the ash collected on it. This is due to the collection capability of

field 1 combined with too frequent rapping. This will be explained further in section 3.8.3 – Field 1 rapping optimisation.

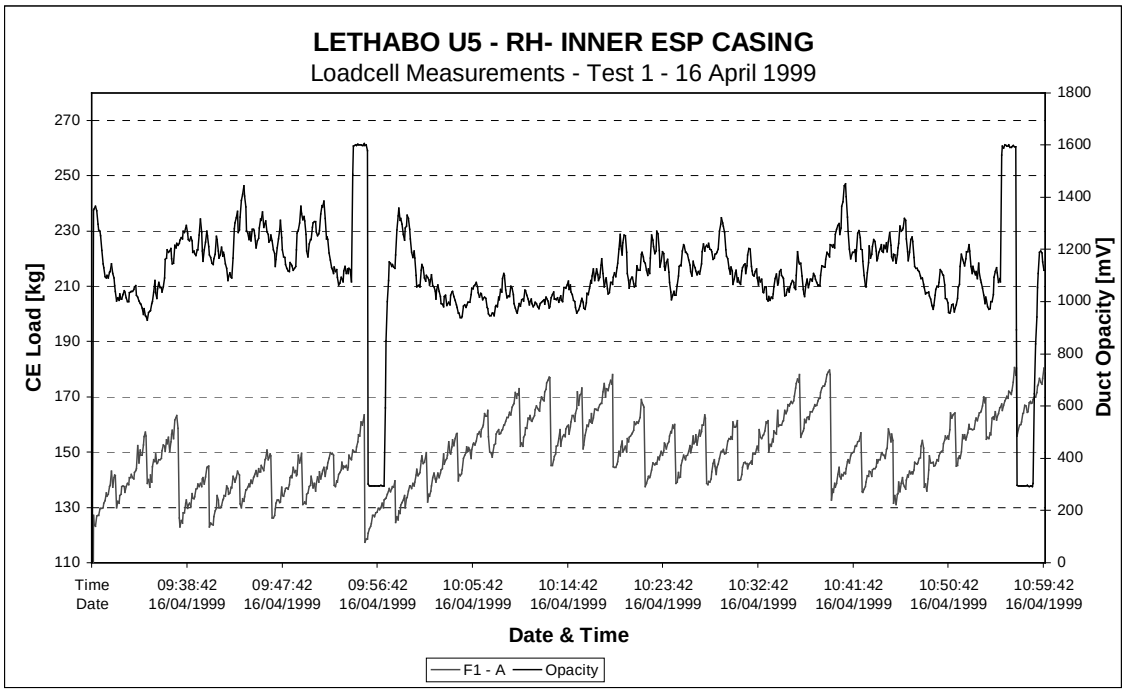

Figure 3.6 : Loadcell measurements – 16 April 1999 - Field 1

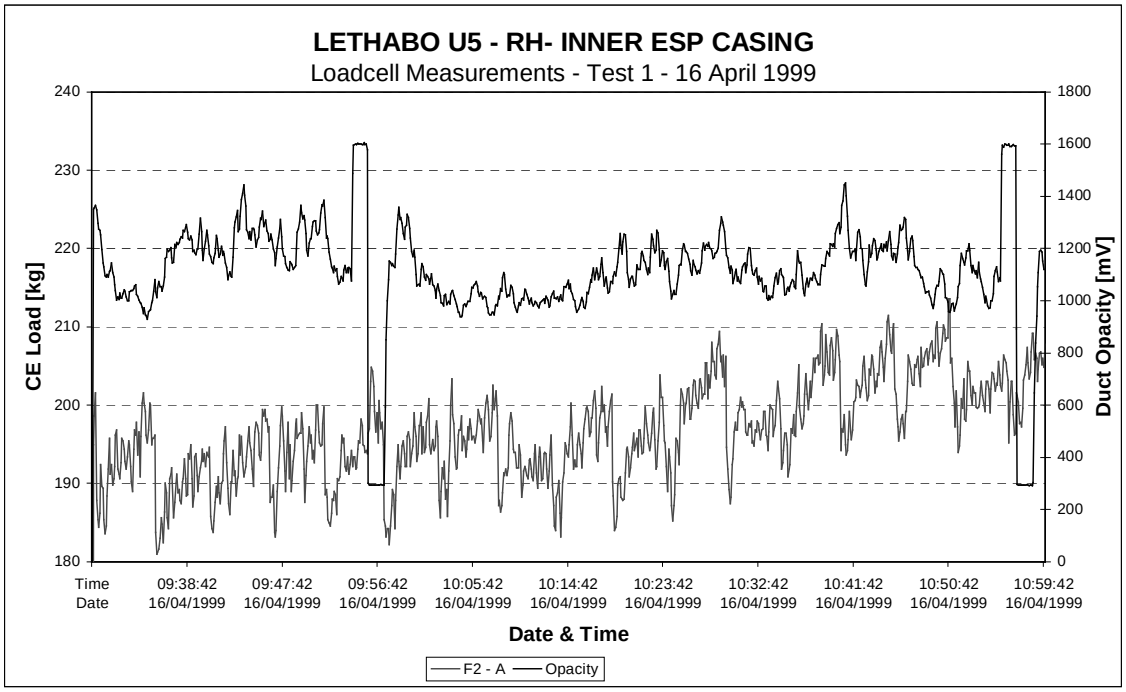

Figure 3.7 : Loadcell measurements – 16th April 1999 - Field 2

Figure 3.7, above, shows a clearer view of field 2's collecting characteristic. From this view no clear correlation exists between the field performance and outlet duct opacity. It can also be seen that the rapping times are not optimal – there seems to be a "flat-top" nature indicating that this field is reaching saturation despite having a fairly quick rapping cycle. This issue will be discussed further under section 3.8.4 - Field 2 rapping-off test .

Figure 3.8, below shows the collection characteristic of field 4. Note that there are no rapping spikes present in this test session due to the long rapping–off times. The variations (spikes) seen can be attributed to a combination of system noise as well as a "normal" ash collection and discharge from the CE due to flow assisted erosion/attrition known as scouring. These fluctuations range between 2 and 4 kg. The absence of a clearly defined collection curve/gradient is typical of the later fields of an ESP as the dust loading is fairly small and the field collects particles of a smaller/finer nature. Section 3.12 will show the percentages of ash collected by each field.

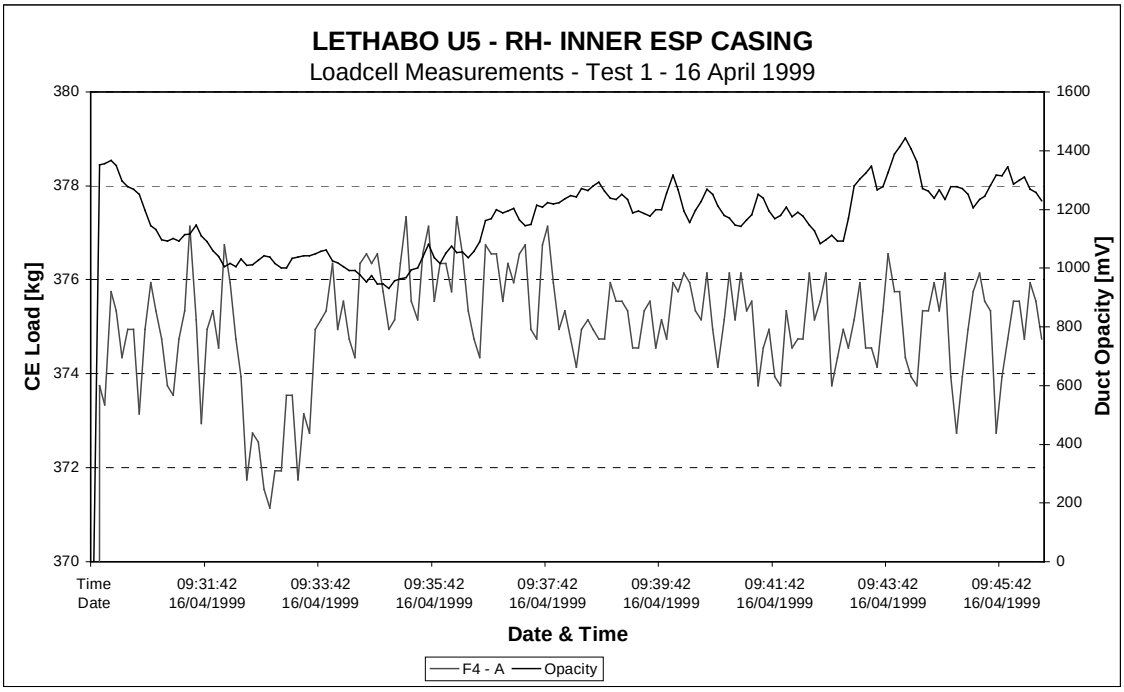

Figure 3.8 : Loadcell measurements – 16th April 1999 - Field 4

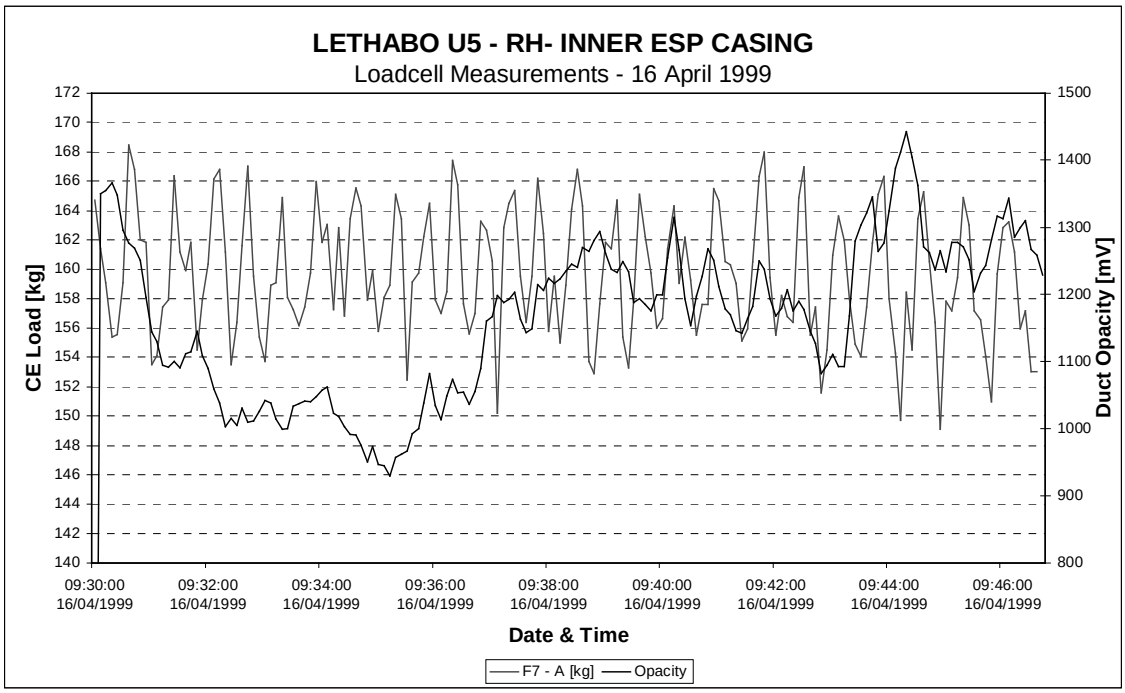

Figure 3.9 : Loadcell measurements – 16th April 1999 - Field 7

Figure 3.9, above, shows the collection characteristic of field 7(last field). As with field 4, no rapping has occurred during the test session due to its timing. However, variations of a large magnitude are visible – about 12 kg on average. This is considered large when considering that it is the last field and compared to field 1, with the full inlet burden only collects/discharges 20 kg. As mentioned above, a tolerance of 2 to 4 kg can be allowed for system noise. This would leave an amount of 8 kg unaccounted for. The above situation is one that cannot be precisely explained at this point in time. It nevertheless has serious implications if we are to believe that 8kg of ash per CE is being collected and then "re-entrained" into the gas stream, remembering that this is the last field. Differences in the last field hopper design (ESP last fields sometimes have different hopper slide gate mechanisms) were thought to be contributing to the effects but it was confirmed that all hoppers are identical, so hopper variations can be ruled out. At this stage, at least one possible explanation exists. Hopper cross-flow/swirl is strongly suspected as the quantities precipitated and discharged (20 kg) do not correlate with the

amount of dust flowing into the last field. (See section 3.12 later) Since the above variations occur randomly, and were not recorded again, it is likely that they occur with a combination of hopper swirl (provides ash quantities required since gas stream does not) as well as back corona (provides the mechanism promoting ash breakaway).

Figure 3.10 also shows two peculiar events, labeled Event 1 and Event 2. During these events, which occur over a period of approximately 40 minutes each, field 1's precipitation rate increases significantly. The rapping seems to not be able to clean the CE's efficiently and an ash cake develops. This ash cake development is correlated by a corresponding significant decrease in outlet duct opacity. These two quantities (F1 and outlet opacity) trend each other perfectly over these event periods. These events are not definitely explainable at this stage. A study of boiler conditions that usually affect ESP performance does not reveal any corresponding variations. No sootblowing was done during these tests and no mill changes occurred. One possible explanation, is that coal quality improved significantly over these two periods. This is possible if higher quality of coal occurred in a predominantly poor coal seam.

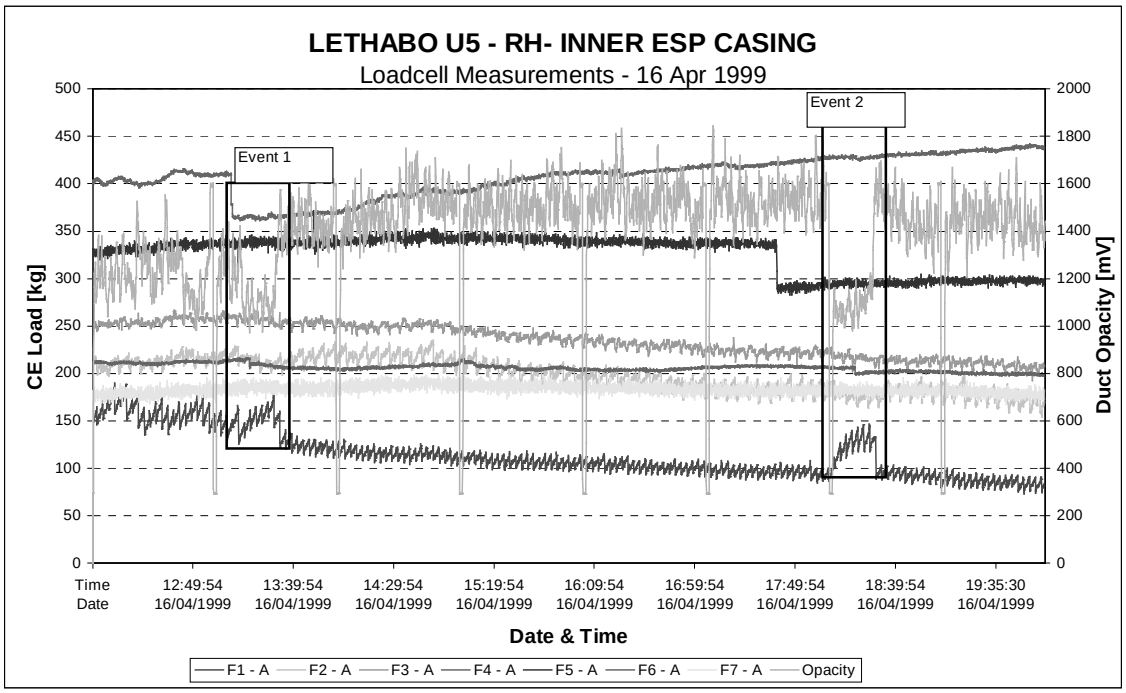

Figure 3.10 : Loadcell measurements – 16th April 1999 – All fields

3.7.3 De-energised/Off -Load Rapping

De-energised or power-off or even reduced power rapping is a technique used by many ESP operators where possible. It consists of some variations, however its basic concept is to better clean the CE by removing/reducing the electrical holding forces that tend to keep a residual ash layer on the CE. It is thought that the residual ash layer has a negative influence on energisation and hence collection.

De-energised rapping is a technique used by Lethabo Power Station for some time now. It is done once a week per casing. The process is manual and hence labour intensive and consists of:

- Closing the outlet damper on the applicable casing. (Usually done at low load/ flow conditions)

- Turning the electrical controllers (and hence transformers) off on all seven fields of the chosen ESP casing.
- Turning all rapper motors on (continuous operation) for two hours.

Figure 3.11, below shows the effects of de-energised rapping done on the night of 17th April. This was a few days after the previous tests, and the datalogger was kept running over the whole period.

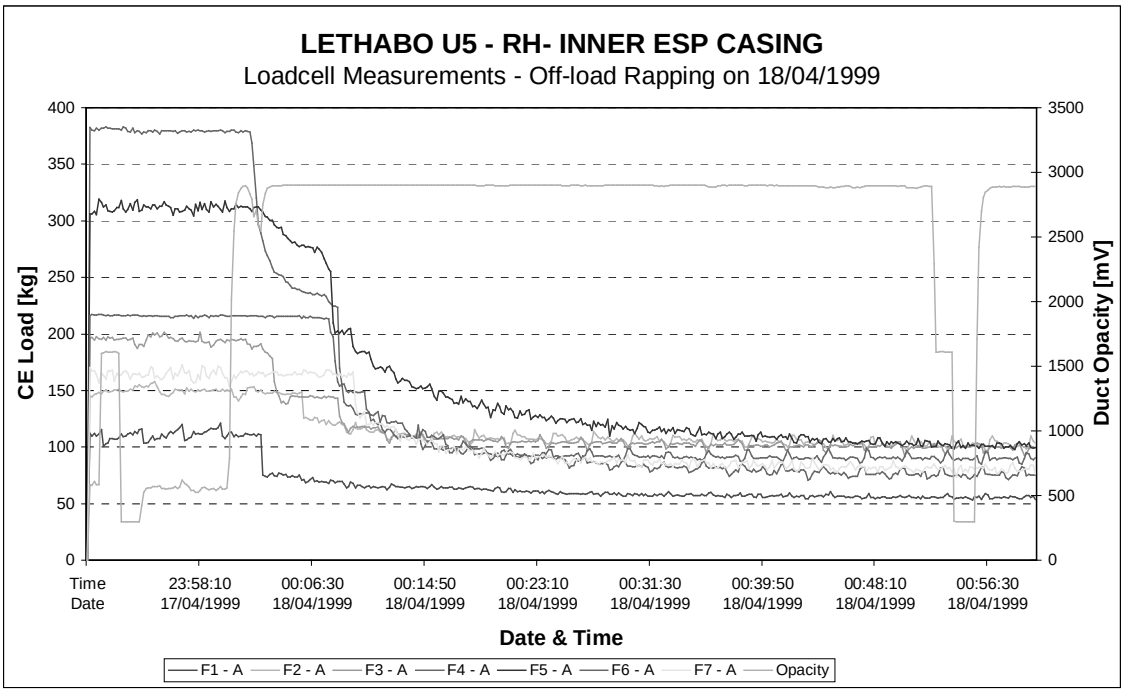

Figure 3.11 : Loadcell measurements – All fields showing de-energised rapping

From Figure 3.11 it can be seen that:

- De-energised/off load rapping commences at 0:00:00 on 18th April 1999 and is completed at 02:08:00, just over two hours later, in line with operating procedures

- All of the fields show a release of a residual dust layer that is not discharged during the normal rapping process. This varies from 40kg(field 2) to 280 kg(field 4). This proves and validates the effectiveness of de-energised rapping.

- All fields seem to reach their "cleaned" state within 20 minutes of the de-energised rapping process. Since de-energised rapping is done for two hours, it is now recommended that 30 minutes is enough to clean the fields.

- The over-range measurement from the opacity meter indicates that either the outlet damper does not seal perfectly, or was not closed during the cleaning process.

3.8 DETERMINATION OF OPTIMUM RAPPING SETTINGS

3.8.1 The Rapping-Off Test

The rapping-off test is a product of this research project. It essentially determines the field's collection and saturation capability, thus providing an indication as to what the rapping on-off times should be. It is a test that should be conducted cautiously, as the potential to cause blocked hoppers or more importantly, mechanical field damage is great if design structural loads are exceeded.

In the case of Lethabo Power Station, the design CE ash loading is 377kg each, for a field total of 46 x 377 kg = 17342 kg.

3.8.2 Field 1 (F1) Optimisation - Results and Discussion

On the 21st July 1999, rapping –off tests were done on field 1. Figure 3.12, below, shows the results of these tests. Three tests were done, and are labelled Test 1, Test 2 & Test

3 in the figure. For the periods in-between the 3 tests, the “normal” as found rapping times (continuous) for field 1 were used. For Test 1, the rapping was turned off for 17 minutes and the CE reached a load of 49 kg. When the rapping was turned on (for all tests), all hoppers were monitored for blockages. This combined with a collection pattern that indicated saturation had not occurred led to Test 2, where the rapping was turned off for 26 minutes. The CE reached a load of 78 kg, again without saturation. In Test 3, the rapping was turned off for 60 minutes, without reaching obvious saturation, but with indications that the controller was experiencing problems. Table 3, below shows a summary of the tests as well as the precipitation rates.

Table 3.5 : Summary of Field 1’s Rapping-Off Tests

Test	Time Rapping Off	Time Rapping On	Precipitation Duration [minutes]	Precipitated Ash [kg]	CE Precipitation Rate [kg/minute]
1	14:23	14:40	17	49	2,9
2	15:28	15:54	26	78	3
3	16:15	17:15	60	145	2,42

From Table 3.5 and Figure 3.12 it can be seen that a period up to 26 minutes a precipitation rate of 3kg/min is constantly attainable. Extending the period past 26 minutes leads to a gradual decrease in precipitation rate.

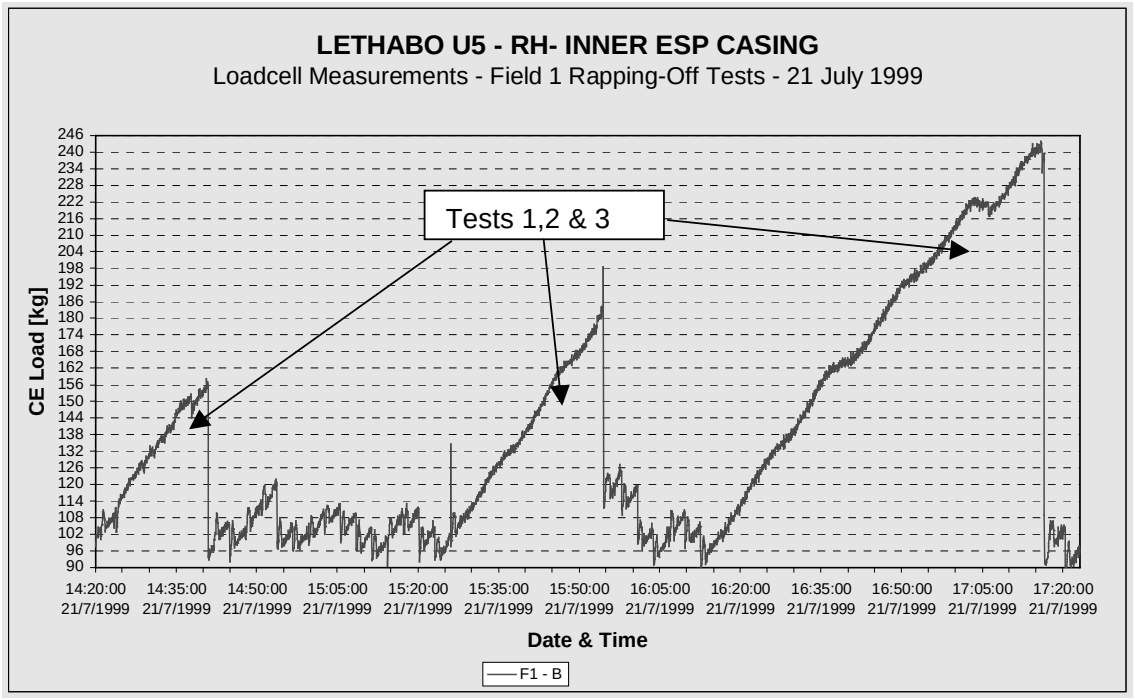

Figure 3.12 :Loadcell measurements – Rapping-Off Test – Field 1

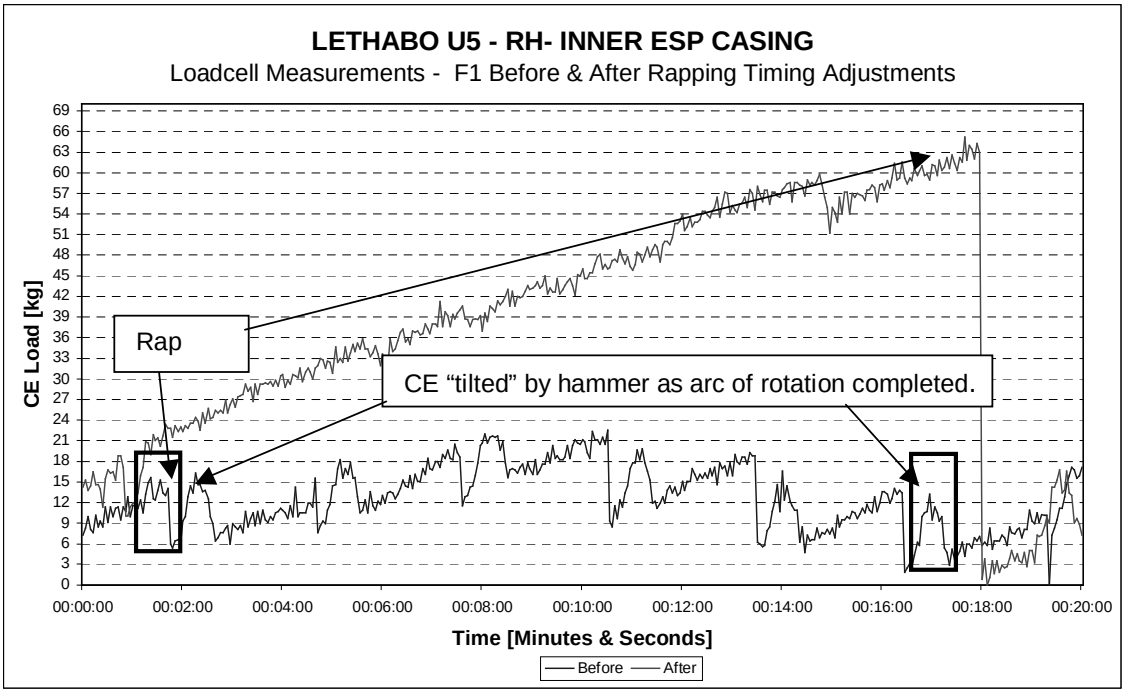

Figure 3.13a : Loadcell measurements – Rapping-Off Test 1 Comparison

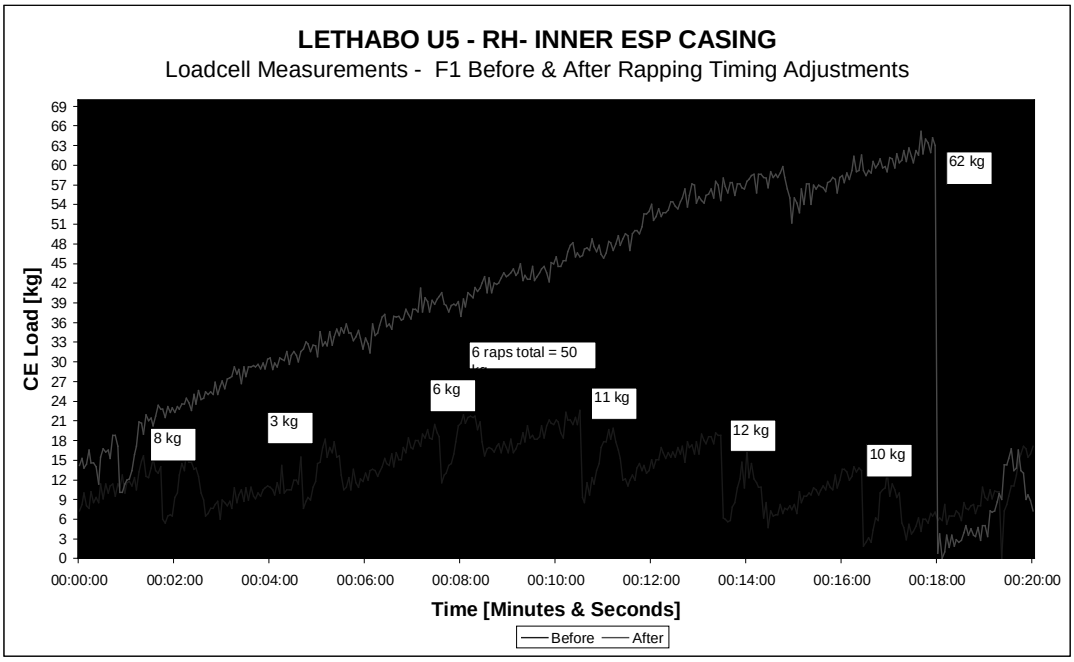

Figure 3.13b : Loadcell measurements – Rapping-Off Test 1 Comparison

Figure 3.13a and 3.13b (same data), above shows an exploded view of Test 1 from Figure 3.12 (labeled “After”) as well as a sample of the “as found” (labelled “before”) rapping collection pattern. These have been adjusted to a common time base for illustrative purposes.

From 3.13b, in the “Before” case, a total of six raps occurs during the test period of 18 minutes. A total of 50 kg is discharged during this period. In the “after” case 1 rap is used and this discharges 62 kg. Note that during this test session the collection rate increased to approximately 3,4 kg/minute as compared to a previous high of 3 kg/minute. A variation in coal is the likely cause of this.

It is also seen that from Figure 3.12, that the impact force to the CE is enough to discharge the collected ash, even after a collection period of 1 hour. However, in the “as found” condition, the CE is not completely cleaned by the same impact. This is probably

due its collection capability (for its ash treatment properties) being too strong at thin CE ash layers. As the ash layer increases, gravity as well as ash “caking” promotes the discharge of collected ash.

More frequent rapping, not just in total shaft rotation, but also in the continual on-off switching process leads to greater times of electrical as well as vibration instability in the field. This can be explained using the following two examples. Section 3.12, later, will also show how rapping re-entrainment is increased by the more frequent rapping.

Assume the same rapper shaft is used for both discussion cases and it has a speed of 3 minutes per 360° revolution.

Case 1

9 minutes OFF : 3 minutes ON

Case 2

60 seconds OFF : 20 seconds ON

Case 1 is an exact ratio of Case 2, therefore the number of raps in both cases are the same.

For Case 1:

- 9 minutes of stability or “quietness” in the field during which the field electrical controller/transformer energisation is uninterrupted.
- At the end of the 3 minutes rapping on cycle, the entire field is cleaned and the controller can start control on an entirely clean field where all CE’s are at an equal state. Arcing/sparking is kept to a minimum.
- The above state promotes a higher collection rate (kg collected/time) as well as causes less potential damage to the transformer/rectifier set.

- Rapping re-entrainment is minimised to 9 cycles of 3 minutes each. If rapping is controllable (by some automatic system), then remaining fields can be set to not rap during these periods. As seen before, outlet emissions are directly affected by the re-entrainment from the first field. It is also for this reason that MIGI rapping systems have become so popular. They can rap the entire field in 5 seconds and applied to the above case, over a 1 hour period, the 5 rapping cycles can be completed in a total of 45 seconds as opposed to 15 minutes with the rotary hammers.

For Case 2:

- 1 min of “quiet” in the field. Then the controller has to operate simultaneously with rapping and no rapping with alternating rapping at some position in the field. Hence, the controller never has a clean field to start control from. Ideally each CE should have its own controller, however this is not practical. As a result, field electrical control will always occur around the “dirtiest” CE(arcs/sparks), of which there will always be one or two. The entire field is at a disadvantage due to the presence of dirty CE’s.
- Collection rates are adversely affected by higher arc/spark rates.
- Rapping re-entrainment is higher in Case 2 as more rapping-on cycles are experienced (45 cycles compared to 5 in Case 1), despite being of shorter duration. It has been seen that even short cycles cause a “dust” cloud which result in increased emissions. Hence a constant dust cloud is present in the field due to near continuous rapping.
- So, it can be seen that despite both cases being equal in terms of rapping quantity, the influences on ESP performance are significantly different.

3.8.3 Field 2 (F2) Optimisation - Results and Discussion

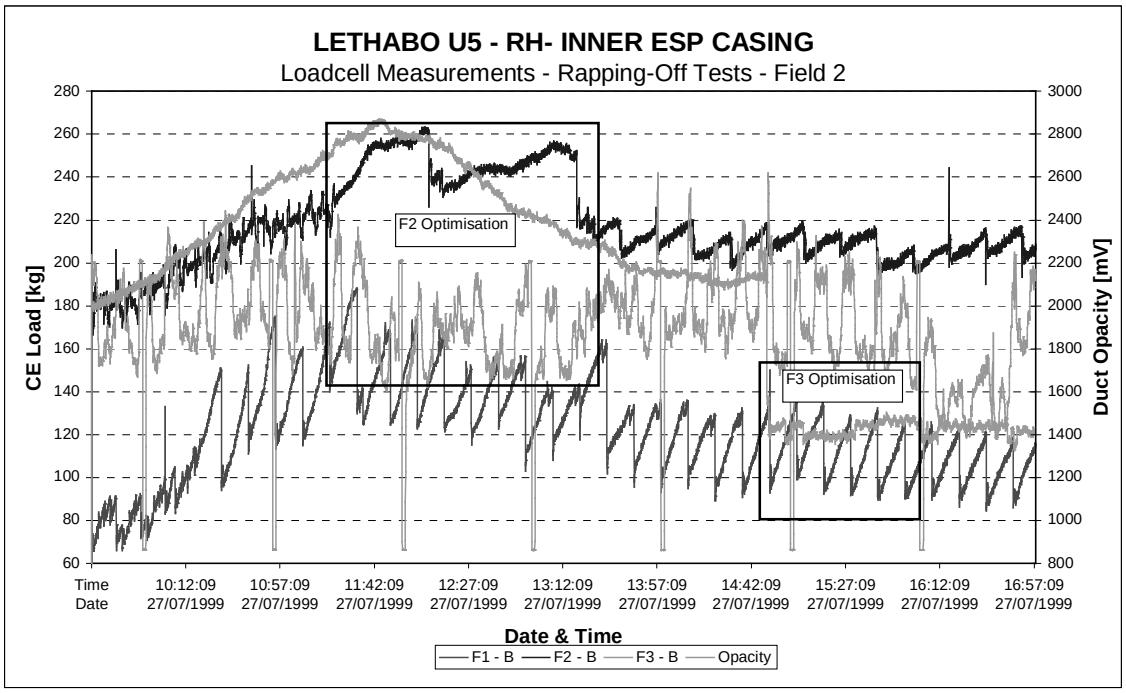

Figure 3.14 : Loadcell measurements – Field 2 Rapping-Off Test

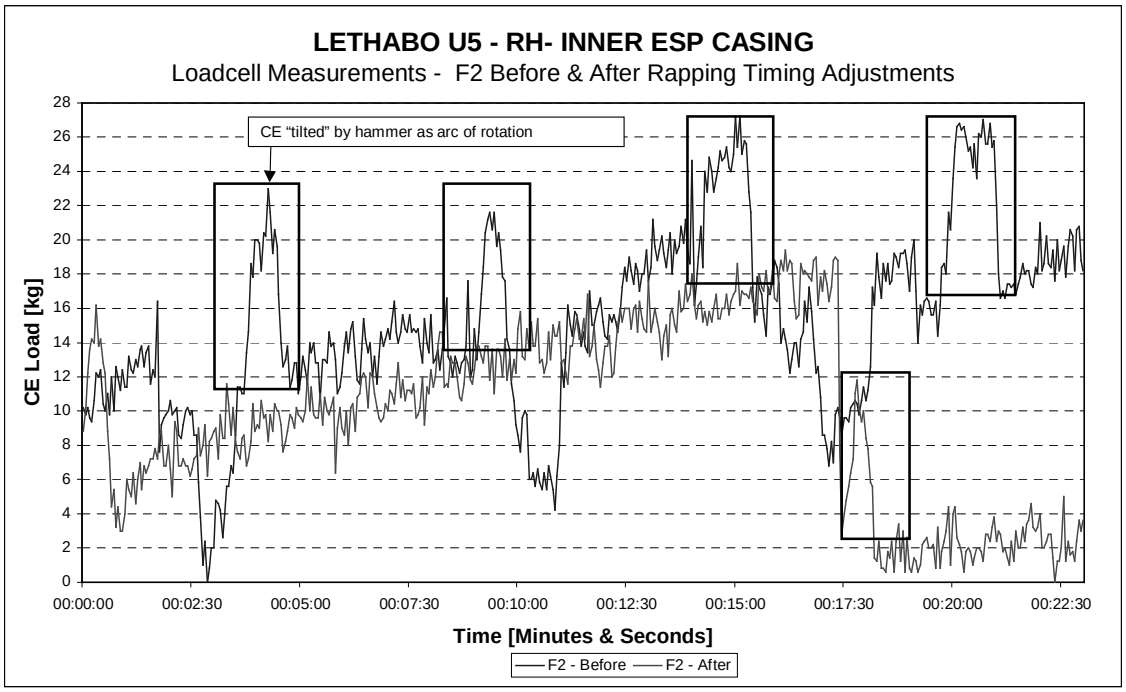

Figure 3.15 : Loadcell measurements – Field 2 Rapping-Off Test Comparison

Figure 3.14 shows field 2's rapping-off tests. Two rapping-off cycles were recorded and are labelled as "F2 Optimisation" in Figure 3.12. The general peaking at midday of all the loadcell channels is symptomatic of the problem discussed in 3.5.1 "Measurement System Fluctuation with Temperature".

In the first cycle it can be seen that the collection rate is relatively higher than the second. This is probably due to better electrical energisation of the dust burden by field 2. Field 1 shows this trend as well by looking at the amount of ash discharged by each rap. This condition changes over the next hour as shown by field 1. The field also reached a saturated state (flat top curve nature) in both of the tests. From these tests an optimised, precipitation time of 18 minutes between raps was set at approximately 13:12:00 (Figure 3.14). Thereafter this setting was monitored and 12 precipitation cycles as shown in Figure 3.14. An average of these cycles revealed a precipitation rate of 0,92 kg/minute per CE. This rate is 30 % of the precipitation rate of field 1.

Figure 3.15, shows one of these optimised cycles (18 minute precipitation interval) compared to the corresponding "as found" ("before") time period cycles. It should be noted that the steep spikes highlighted in Figure 3.15 are not precipitation of ash but rather the tilting of the CE after the hammer has struck the anvil and is completing its arc of rotation. This action provides a very useful indication of whether the dislodgment of precipitated ash was due to rapping or gravity induced breakaway, when interpreting these measurements. In the latter case, it would not be visible after a non-rapping influenced dislodgement of ash.

Considering the above, it is also seen that not all raps cause a dislodgement of ash. Now, it should be remembered that fields 2 to 7 have two rapper shafts. Depending on the location of a specific CE's front and rear hammers (their location can be totally random in nature due to lack of co-ordination between the two rapper shafts) rapping can

accordingly, vary considerably between the timer set cycles. If the front and rear hammers strike the CE at similar times, then interference can occur between the two raps.

The saturation of field 2 after a period shorter than field 1 means that its precipitation time should in all likelihood be shorter than field 1. Conventionally, an exponential increase in precipitation times is applied from the first to last fields of an ESP. This probably resulted from the logic that the first field was most likely to reach saturation the soonest. This does not occur, as seen from the loadcell measurements, at both Hendrina (flue gas conditioned) and Lethabo (no flue gas conditioning) Power Stations. This is most likely explained by field 1 being able to precipitate dust particles from the total input particle size spectrum. Later fields are dealing with “pre-filtered” ash particles, where the larger particles have already been removed by field 1. Even with a thick ash layer, it can continue collection. Field 2 and later fields do not have this entire ash particle spectrum to precipitate from. Hence they reach saturation even with thinner ash layers. Shorter precipitation intervals followed by raps are required to keep the CE’s in a clean condition to be able to collect the more “difficult” ash that front fields could not collect. These shorter precipitation intervals have to be evaluated against re-entrainment and rapping puffs. In smaller, shorter ESP’s with fewer fields (e.g. 3 field ESP), re-entrainment losses will outweigh the gains of shorter field 2 precipitation intervals. However, in the case of 5 or more field ESP’s, improvements should be seen. In the case of Lethabo, both field 2 and 3 can have progressively shorter intervals without rapping puffs becoming a limiting factor.

3.8.4 Field 3 [F3] Optimisation – Results and Discussion

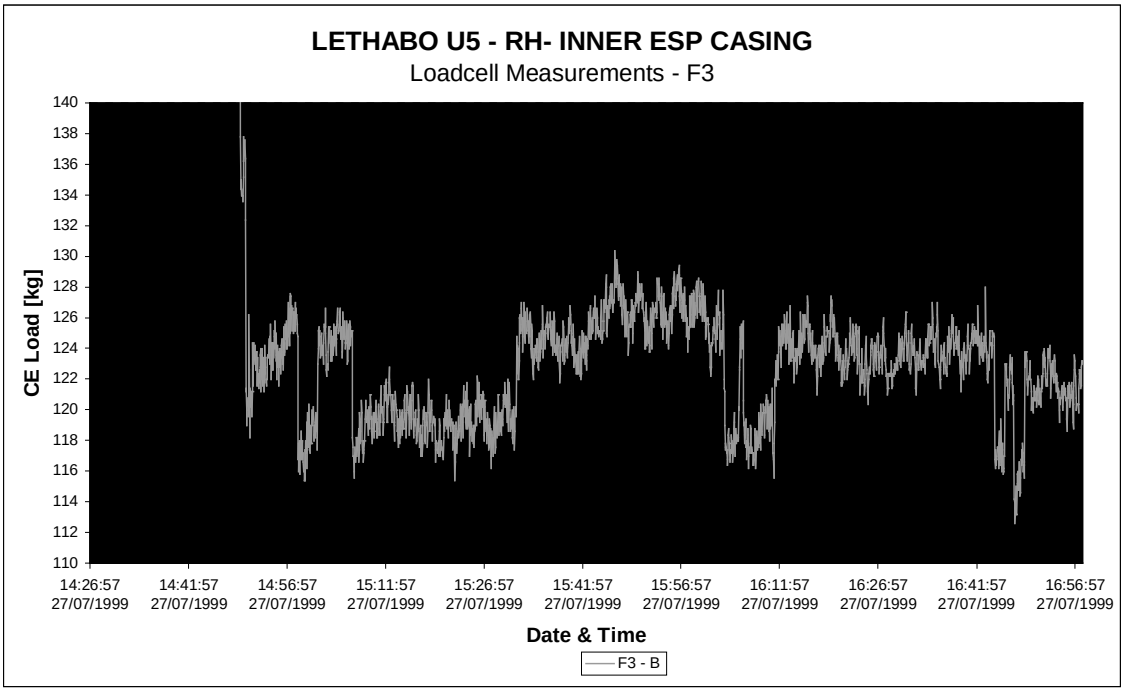

Figure 3.16 : Loadcell measurements – Field 3 Rapping-Off Test

Rapping-off tests were attempted for F3 as shown in Figure 3.14. Figure 3.16, above shows an exploded view of the event. The field was initially cleaned (continuous rapping using both rapper shafts for 10 minutes) and 60 kg of residual ash was discharged. For two cycles after this,(between 15:26 and 16:56) F3 appeared to be collecting fairly well, despite reaching saturation. As discussed previously, shorter precipitation times have to be balanced against rapping puffs. Of concern, however, were the sinusoidal cycles seen above. These cycles are approximately 4 kg peak to peak and suggest that while the CE has already precipitated a base ash layer, it has problems in developing an ash cake.

Since the above phenomenon also occurs when the CE is in a clean state, the problem could be the manner in which the electrical controller is energising the field. Too little

voltage, perhaps due to back corona could be responsible for the interference in the build up of the ash cake.

3.8.5 Field's 4 to 7 Optimisation - Results and Discussion

Rapping off tests were conducted in these fields, however, precipitation rates were not easily quantified. This is due to difficulty in viewing ramp cycles (as seen in F1,2,3) as result of low precipitation rates. Back corona is often a problem in these fields and to control this, lower voltages and currents are supplied by the controller, in a pulsing mode. While the pulsing mode is especially used to limit the negative effects of back corona, it may not be supplying enough power in these latter fields to precipitate the "difficult" ash particles. Electrical optimisation in these fields will have to be intensified to improve power delivery into these fields in the face of back corona conditions.

It has also been seen that these fields tend to build up a residual ash layer that is not cleaned by "normal" rapping. De-energised rapping has most benefit in these fields. The rapping sequences required by these fields cannot be presently programmed using mechanical timers.

3.8.6 Effects of a Broken Rapper Timer

Figure 3.17, below, shows what can possibly occur in an ESP if a rapper timer malfunctions. In this case, the device is of the mechanical type (rotary set-points). It should be noted that this was not a specific test, but rather a random event recorded co-incidentally. The event occurred during one of the remote data capturing sessions. In these sessions the logging equipment is set on a slower sampling rate and left to record over a two week period without personnel being present.

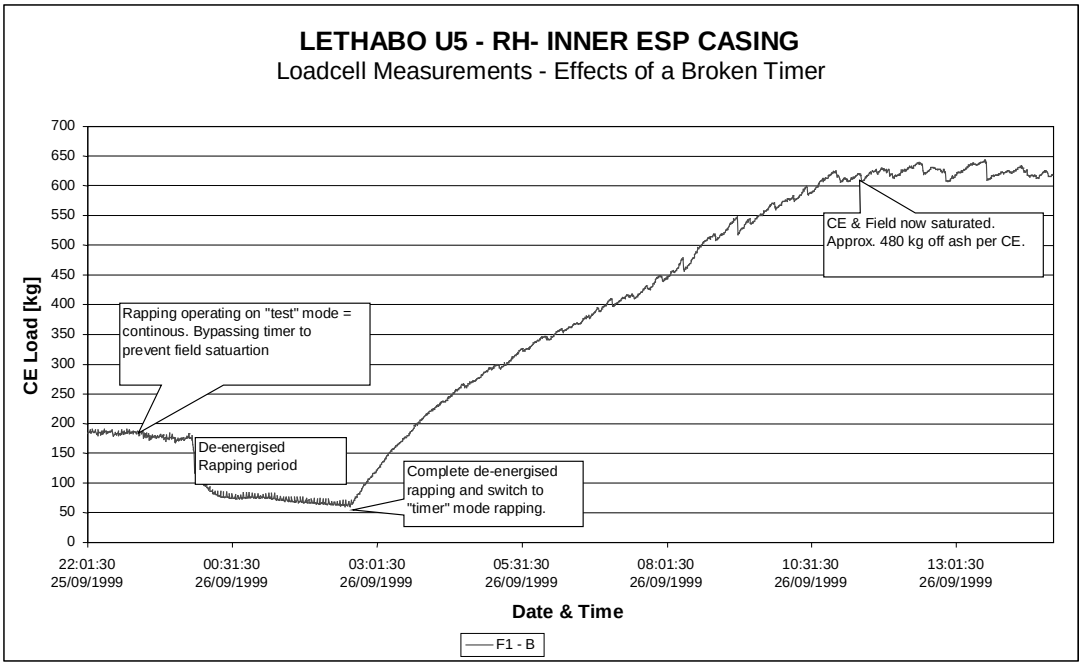

Figure 3.17 : Loadcell measurements – Effects of a malfunctioning Rapper Timer.

Below, is a description of what most likely occurred.

Prior to the start of the recording session in question, it was noticed that the rapper timer controlling field 1's only rapper shaft was malfunctioning. This was then reported to the relevant site personnel and the repair/replacement process was initiated. In the interim, however, it was decided to leave the field on "test" mode rapping. In this mode, the timer is bypassed and the rapper motor operates continuously. This was very acceptable, though not ideal from an efficiency perspective, as it was the first field and previously optimised settings had the field operating continuously. Figure 3.17 shows, that despite not cleaning the CE totally (maintaining a residual ash load of approximately 190 kg), it was nevertheless satisfactory.

On the night of 25th September, de-energised rapping was done by Lethabo P/S boiler operators. This commenced at about midnight on the 25th and continued into the early hours of the morning of the 26th. After the normal de-energised rapping session (about 2 hours), the fields were energised and rapping "reinstated". This occurred at about 02:45

on the 26th. However, at this stage, the rapping was switched to the failed "timer" mode instead of "test" mode. Figure 3.17 shows that with no rapping, (remembering field 1's collection capability from previous rapping-off tests), the field continued collection for 10 hours before reaching a saturated state. This saturated state was reached with an indicated CE ash load of 600 kg. Now considering section 3.5.1 'Measurement System Fluctuation with Temperature", it has been quantified that between morning and midday, system drift amounts to 120 kg. Subtracting this value gives an actual CE saturated load of 480 kg. This is approximately 100 kg above the design CE ash load. Unfortunately, the data recording ended (storage full) shortly after this period, so data showing the discharge of this thick ash layer is not available. Lethabo P/S site personnel did report blocked first field hoppers for this day.

Considering the above precipitation behaviour, particularly when dealing with the first fields caution should be exercised with broken timers as well as rapper motors and shafts. The possibility of design loads being exceeded, leading to main roof beam and CE failures must be investigated further. A more commonly experienced problem is blocked hoppers due to dislodgement of large ash cakes when rappers/timers are repaired. Flue gas conditioned units are more prone to these problems as their precipitation rates are much higher. Second fields in ESP units are also at risk from this problem.

3.9 MEASUREMENT OF ESP "OPTIMISED" CHARACTERISTICS

3.9.1 Introduction

Tests were conducted on the 2nd and 3rd November with the objective of determining the effects of using the optimisation rapping times determined from previous tests. Isokinetic tests were not conducted at this stage as the costs could not be justified against what

could be described as the project's "interim state". However, monitoring of the outlet duct opacity meter in conjunction with the loadcells for boiler full load conditions would provide as indication of present efforts.

Constant boiler full load conditions (620 MW) were had on the 2nd and 3rd November 1999. Other parameters, which are enforced during isokinetic sampling tests were also maintained.

3.9.2 Measurements : 2nd November 1999 – Results and Discussion

Figure 3.18, below, shows the measurements obtained during this time period. It should be noted that boiler load was a stable 620 MW with no mill changes and sootblowing. Also, air flows and flue gas temperatures were monitored and considered normal for the duration of this as well as following tests.

For this test, the rapping conditions of the ESP's "as found" state, that is before the project commenced and as indicated in Table 3.3 were implemented. Electrical settings as used in the "as found" state were also implemented.

From Figure 3.18, it can be seen that the duct opacity levels correlate well to those tested in back in April 1999. The emission monitor output (trend indications only) visually average approximately 1100 mV. Also, compared to the "As Found" April 1999 tests, opacity seems to trend most significantly with field 1's precipitation, as can be seen from the three highlighted areas in Figure 3.18 and the exploded view in Figure 3.19. Some system noise is visible in Figure 3.18, field 5B.

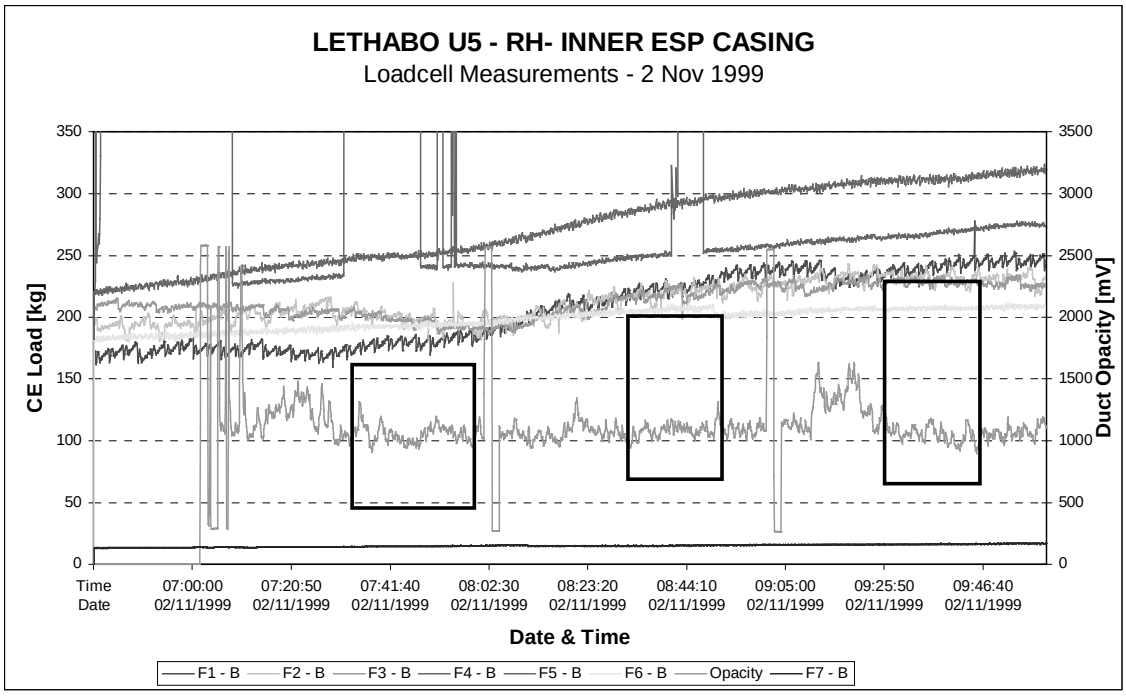

Figure 3.18 :Loadcell measurements – 2 November 1999 - 07:00 to 10:00

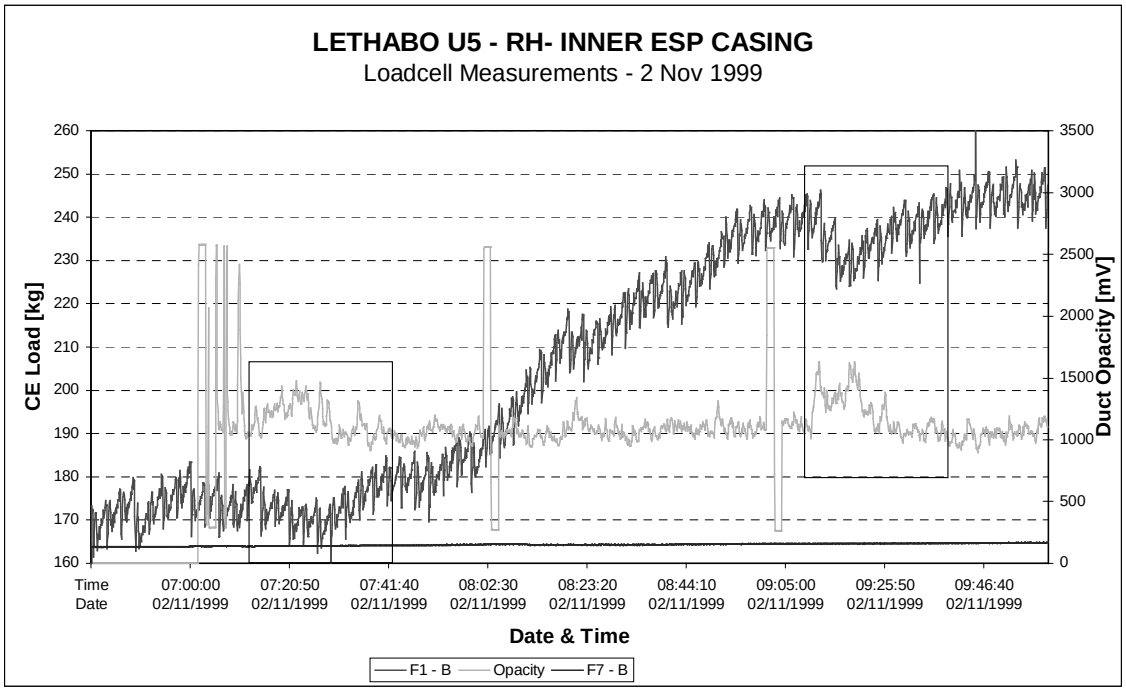

Figure 3.19 : Loadcell measurements – 2 November 1999 - 07:00 to 10:00 – Field 1

Test 2 (2nd November 1999, 10:00 to 18:00)

During this test, optimised settings resulting from previous tests were implemented. Again boiler conditions were stable. Figure 3.20, below, shows the test period measurements with Figure 3.21 showing an exploded view of the first two hours of testing.

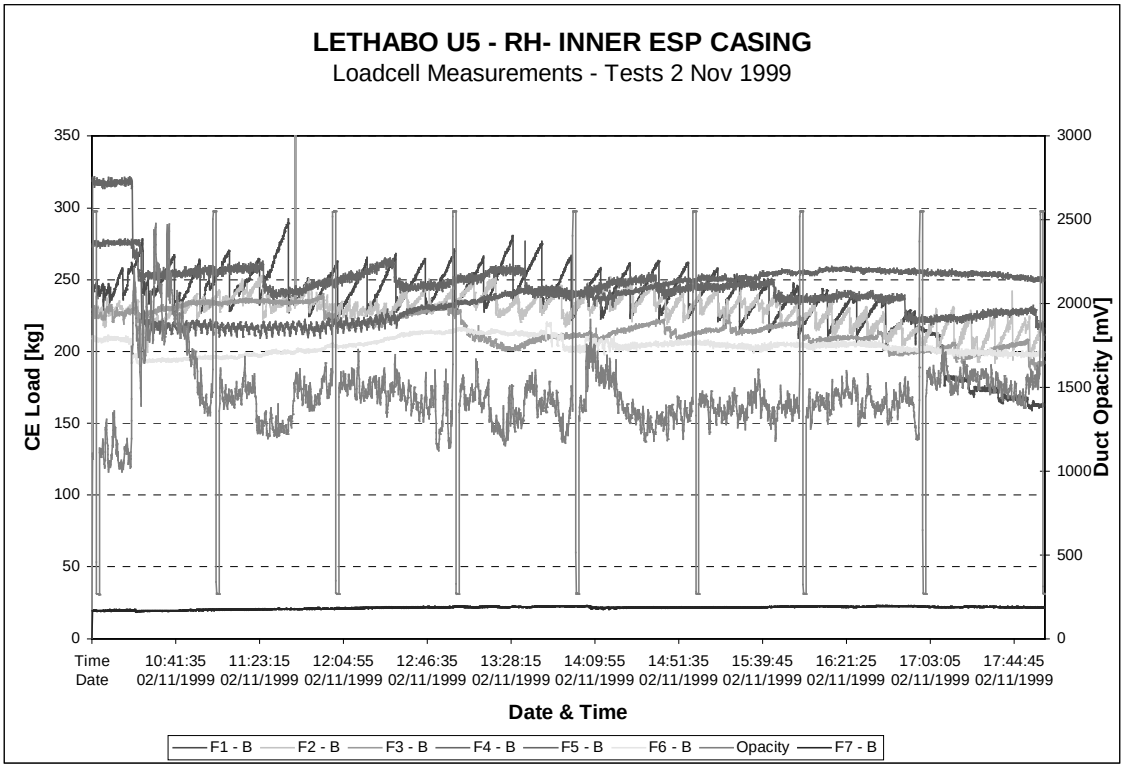

Figure 3.20 :Loadcell measurements – 2 November 1999 – 10:00 to 18:00

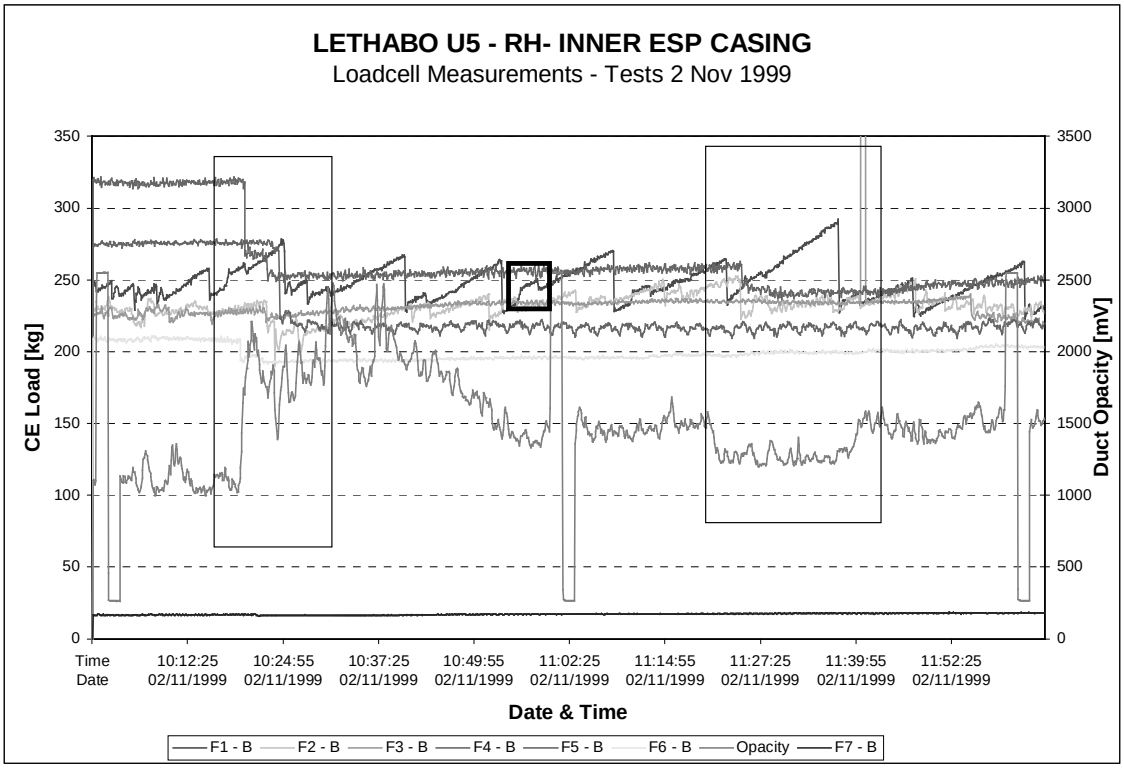

Figure 3.21 : Loadcell measurements – 2nd November 1999 - 10:00 to 12:00

In the first hour, all fields seemed to be responding well to optimised settings, from an energisation and corresponding precipitation perspective. Comparing to the “As Found” April 1999, tests, opacity was now down to a trend indication of about 1200 mV (1150mV for this time of day back in April) and trending downwards when electrical problems started appearing in field 1.

Field 1, from an electrical energisation perspective, seemed to develop what was likely an internal problem. Due to the unit being on load, it was impossible to verify this. It could only be concluded that field 1 was not being sufficiently energised. The electrical characteristics indicated an partial “short” in the field which led to arcing. This could possibly have been due to a clinker of ash present on an electrode. Field 1, earlier on in the day seemed to performing well from a collection precipitation view. However, it could have performed significantly better (precipitation rate higher than 3 kg/minute/CE) if the

desired power could be delivered to its electrodes. This problem continued for the rest of the test session, leading to final field failure at approximately 17:03 (Figure 3.20).

Despite this problem, the optimised rapping/electrical settings for remaining fields showed an average opacity trend of 1300 mV as compared to 1500 mV for the corresponding time of day back in April.

3.9.3 Measurements : 3rd November 1999 – Results and Discussion

(3rd November 1999, 08:00 to 14:00)

Since the boiler had been scheduled for full load conditions for this day, it was decided to continue testing despite the problem with field 1 from the previous day.

From 08:00 to 10:20, field 1 was switched-off due to its problem. Figure 3.22 shows that field's 2 and 3 were now behaving as fields 1 and 2 would respectively operate Interestingly, for the period 08:00 to 10:20, when field 1 was not energised, collection occurred, albeit at a very low rate. This is due to the "natural" static levels present in the gas flow.

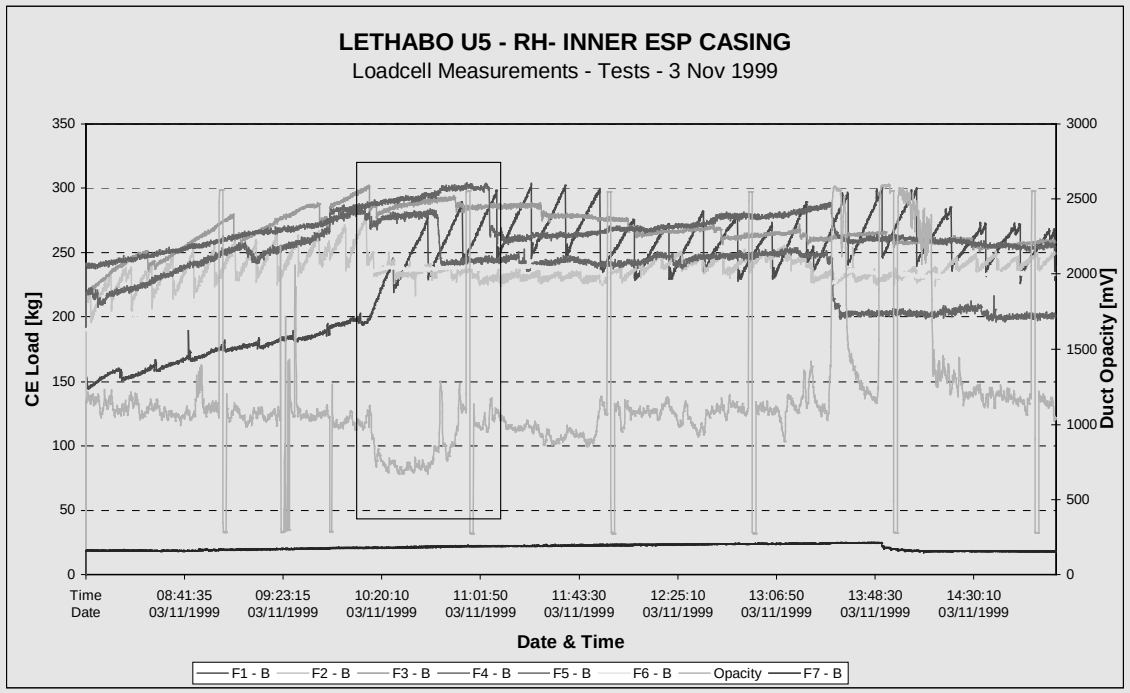

Figure 3.22 : Loadcell measurements – 3rd November 1999

At 10:20, (see area highlighted in Figure 3.22) it was decided to check the operation of field 1 and the controller was switched on. The problem from the previous day was now not present anymore. Since field 1 seemed to be operating extremely well electrically, testing continued. Between 10:20 and 11:00, the lowest duct opacity seen thus far was measured. This trend averaged 700mV. However, this decrease cannot be totally attributed to rapping and electrical optimisations. A study of Unit 5's boiler records showed that stack opacity for the period 08:00 to 12:00 was an average 33,05 %. Consider that optimisations are only carried out in 1 of the 4 casings feeding the stack. For the same period on the 2nd November, stack opacity averaged 40 %. So coal quality was definitely better on the 3rd November. This variation in coal quality made quantification of rapping optimisation improvements on these days difficult, but nevertheless illustrated the variable conditions present when optimising ESP units.

At approximately 12:00, there seemed to be a be another change in coal quality, this time for the worse. Duct opacity increased to 1200 mV, and it was confirmed that power input into all fields was again difficult. Boiler logs confirmed the change in coal quality by showing an average stack opacity of 42,02 % for the period 12:00 to 18:00. This was an increase of 7% from the morning average.

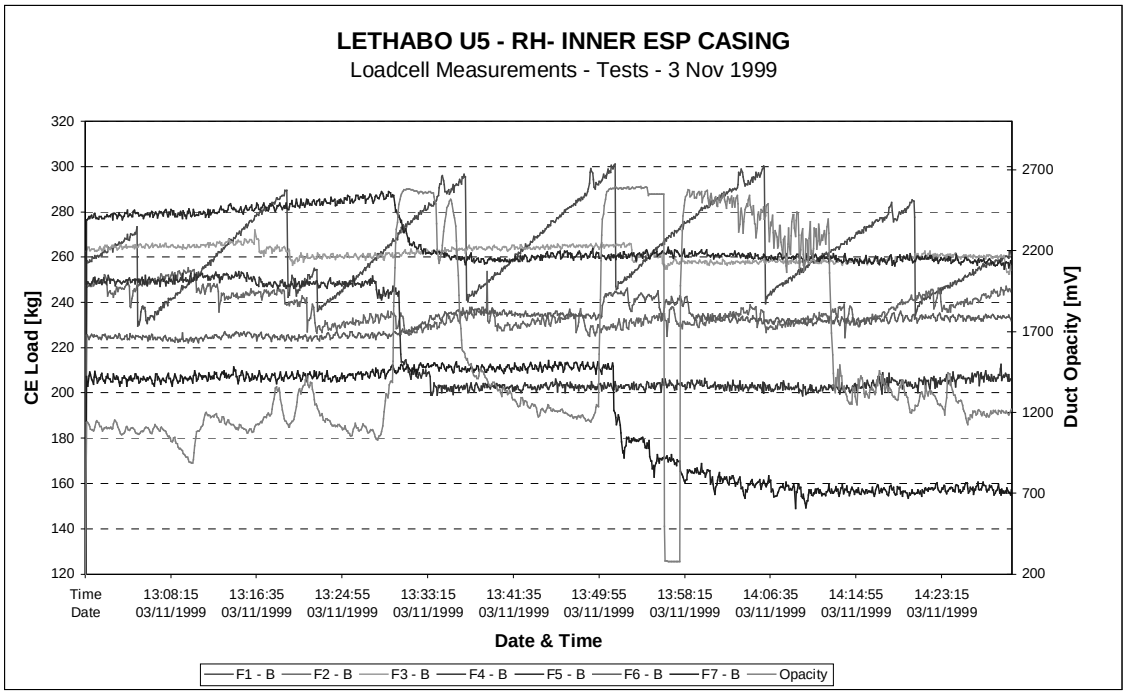

Figure 3.23 : Loadcell measurements – 3rd November 1999

The high duct opacity levels between 13:24 and 14:14 (Figure 3.23, above) is due to a "force cleaning" of fields 4 to 7 with continuous rapping (for short periods of ten minutes per field). This was done with the fields energised and not energised and the results indicate that, with an automatic control system, de-energised rapping can be performed over short time periods without closing the outlet damper, and without significant emission excursions. These ten minute cleaning sessions commenced at 13:50 and by 14:20, a period of 30 minutes, had settled down. This information will be useful for all ESP units considering de-energised rapping but not having the ability to isolate casings.

3.10 MEASUREMENT OF ESP "OPTIMISED" EMISSION LEVELS

3.10.1 Introduction

In order to measure the effectiveness of the projects efforts thus far, it was an isokinetic sampling test (as performed to determine the ESP's "as found") was required.

Also the opacity meter currently installed in the outlet duct (SICK RM41) proved to be extremely problematic. Considering that it's model type is now over 20 years old, and that it's production was discontinued approximately 8 years ago, spares and hence repairs became very expensive. Considering the valuable, online trend indications provided by the outlet duct opacity meter, it was decided to replace the opacity meter with a more modern one. This new opacity meter needed to be correlated to provide a calibration of its output (electrical signal) versus mass particulate emissions.

The above two reasons provided the motivation to conduct isokinetic tests on the test unit. However, for cost saving reasons, these tests were only performed on the outlet duct rather than both inlet and outlet ducts. Opacity meter correlations only require outlet duct measurements. It was also decided, that for the issue of ESP efficiency measurement, outlet duct emissions will be compared to initial measurements.

3.10.2 Optimised Rapper Settings

Table 3.6, below shows the optimised rapping settings used for the test. It also shows the "as found" rapping settings used for the previous isokinetic test.

Table 3.6 : As Found and Optimised Rapping Settings

Lethabo Power Station - Unit 5 RH Inner Casing **Rapping Analysis**

Time for full revolution (seconds) 180

As Found Conditions

	Front/Leading Edge Rapper Shaft						Back/Trailing Edge Rapper shaft					
FIELD	Off/Pause	On/Run	On/Off Cycles	1 Full Rev.	1 Full Rev.	1 Full Rev.	Off/Pause	On/Run	On/Off Cycles	1 Full Rev.	1 Full Rev.	1 Full Rev.
			[Rev]	[Seconds]	[Minutes]	[Hours]			[Rev]	[Seconds]	[Minutes]	[Hours]
1	No Shaft						6	21600	0.01	180.05	3.00	0.05
2	5	30	6.00	210.00	3.50	0.06	35	40	4.50	337.50	5.63	0.09
3	3	20	9.00	207.00	3.45	0.06	23	30	6.00	318.00	5.30	0.09
4	5400	20	9.00	48780.00	813.00	13.55	5420	30	6.00	32700.00	545.00	9.08
5	14400	20	9.00	129780.00	2163.00	36.05	14420	30	6.00	86700.00	1445.00	24.08
6	18000	20	9.00	162180.00	2703.00	45.05	18020	30	6.00	108300.00	1805.00	30.08
7	3600	4	45.00	162180.00	2703.00	45.05	3604	6	30.00	108300.00	1805.00	30.08

Optimised Times - 17 Novmber 1999

	Front/Leading Edge Rapper Shaft						Back/Trailing Edge Rapper shaft					
FIELD	Off/Pause	On/Run	On/Off Cycles	1 Full Rev.	1 Full Rev.	1 Full Rev.	Off/Pause	On/Run	On/Off Cycles	1 Full Rev.	1 Full Rev.	1 Full Rev.
			[Rev]	[Seconds]	[Minutes]	[Hours]			[Rev]	[Seconds]	[Minutes]	[Hours]
1	No Shaft						600	180	1.00	780.00	13.00	0.22
2							360	180	1.00	540.00	9.00	0.15
3							1800	360	0.50	1080.00	18.00	0.30
4							3600	360	0.50	1980.00	33.00	0.55
5				0			7200	360	0.50	3780.00	63.00	1.05
6							21600	540	0.33	7380.00	123.00	2.05
7							86400	720	0.25	21780.00	363.00	6.05

3.10.3 Results and Discussion

Table 3.7, below shows a summary of the measurements conducted on the outlet duct. Nine tests were conducted, at varying boiler loads, to provide a correlation at different particulate emissions for the new opacity meter.

Table 3.7 : Post Optimisation Isokinetic Test Results

EMISSION MEASUREMENTS										
Power Station		Lethabo								
Unit No.		ESP 5								
Location		RH Inner Outlet								
Test No.		1	2	3	4	5	6	7	8	9
Date	dd-mm-yy	30-May-00	30-May-00	30-May-00	31-May-00	1-Jun-00	1-Jun-00	1-Jun-00	2-Jun-00	2-Jun-00
Start Time	HH:mm	10:00	13:23	16:00	22:42	1:10	3:41	22:40	1:13	3:40
End Time	HH:mm	11:50	15:25	17:49	0:30	3:00	4:59	0:31	3:00	4:55
Boiler Load	T/HR	618	618	618	450	450	450	550	550	550
Electrostatic Precipitator Outlet Conditions.										
Gas Temperature	°C	132.0	134.9	134.9	123.2	119.0	117.0	133.2	132.4	130.4
Moisture	%v/v	9.0	8.8	8.2	8.2	8.6	7.7	8.6	8.3	8.9
Oxygen	% (d)	5.0	5.0	5.0	5.0	5.0	5.0	8.8	8.8	8.8
Velocity	m/s	19.6	20.0	19.9	15.6	15.2	15.2	17.9	18.2	18.4
Gas Volume Flow (Qact)	Am3/s	277.4	283.4	281.3	220.0	215.6	215.1	253.3	257.9	260.1
Gas Volume Flow (Qnw)	Nm3/s	153.9	155.7	154.4	126.4	125.2	125.6	141.3	144.0	145.9
Thimbles used		N22	N21	N20	N19	N18	N17	N16	N15	N14
Nozzle diameter	mm	11.0	9.0	9.0	10.0	10.0	10.0	10.0	10.0	10.0
Dust mass	mg	748.1	635.6	600.6	394.3	358.0	230.8	486.9	537.5	349.8
Gas Volume Sampled (Vact)	Am3	12.1542	8.3538	8.2844	7.1037	7.0570	4.6775	7.9814	8.0637	5.4572
Gas Volume Sampled (Vnw)	Nm3	6.7413	4.5912	4.5475	4.0805	4.0962	2.7327	4.4514	4.5032	3.0623
Gas Volume Sampled (Vad)	Am3 (d)	11.0926	7.6400	7.6233	6.5380	6.4672	4.3248	7.3152	7.4117	4.9803
Gas Volume Sampled (Vnd)	Nm3 (d)	6.1524	4.1990	4.1846	3.7556	3.7538	2.5266	4.0798	4.1391	2.7947
Dust Concentration	mg/Am3 (w)	61.6	76.1	72.5	55.5	50.7	49.3	61.0	66.7	64.1
Dust Concentration	mg/Nm3 (w)	111.0	138.4	132.1	96.6	87.4	84.5	109.4	119.4	114.2
Dust Concentration	mg/Am3 (d)	67.4	83.2	78.8	60.3	55.4	53.4	66.6	72.5	70.2
Dust Concentration	mg/Nm3 (d)	121.6	151.4	143.5	105.0	95.4	91.4	119.3	129.9	125.2
Outlet Dust Flowrate	mg/s	17077.9	21560.5	20394.2	12211.5	10940.9	10612.0	15452.5	17193.0	16668.1
Isokineticity	%	121.3	121.9	122.0	108.3	109.6	109.3	105.5	104.6	105.2
Average O/M Signal	% of output	30	30	30	10	10	10	20	20	20

Table 3.8 below shows the efficiency measurements of the experimental unit. At the start of the test work, emission measurements were done to determine the ESP casing's baseline, "as found" condition. These were done at boiler full load conditions (620MW) and are shown in Table 5, as "PRE-EFFICIENCY" measurements. Three tests were done to provide a suitable average. For the presently optimised state (shown as "POST EFFICIENCY" in the table), outlet emission measurements used for the correlation of the dust emission monitor mentioned in section 9.1 were used for analysis. Again, three measurements were averaged.

Table 3.8: Lethabo Unit 5 RH Inner Casing Efficiency Measurements

		PRE EFFICIENCY - 620 MW			POST EFFICIENCY - 620 MW		
		Test 1	Test 2	Test 3	Test 1	Test 2	Test 3
GAS FLOW (ACTUAL)	m3/s	1060.00	1080.00	1060.00	1109.00	1133.00	1125.00
EFF CORR FOR GAS FLOW	%	99.85	99.84	99.85	99.73	99.69	99.70
CARBON	%	0.80	0.80	0.80	0.80	0.80	0.80
K1(CARBON)		1.00	1.00	1.00	1.00	1.00	1.00
SULPHUR	%	0.67	0.71	0.58	0.73	0.73	0.73
K2(SULPHUR)		0.90	0.80	1.00	0.75	0.75	0.75
GAS TEMP	Degrees C	142.00	143.00	131.00	138.00	141.00	141.00
K3(GAS TEMP)		1.34	1.38	1.00	1.18	1.30	1.30
MOISTURE	%	10.00	10.00	10.00	10.00	10.00	10.00
K4(MOISTURE)		0.95	0.95	0.95	0.95	0.95	0.95
DESIGN EFF	%	99.83	99.83	99.86	99.77	99.71	99.72
Measured Dust concentration	mg/m3 (STP)	165.00	180.00	188.60	111.00	138.40	132.10
Average	mg/m3 (STP)		178			127	
Predicted Dust concentration	mg/m3 (STP)	144	148	118	191	239	229
Average	mg/m3 (STP)		137			220	
Average difference (mg/Sm3)between measured and predicted :			41.04			-92.87	(133mg/sm3)
Average Difference	mg/m3 (STP)		41			-93	
As a percentage of the predicted design outlet dust concentrations :							
Average difference to Design	%		29.99			-42.21	
Difference in percentage points before and after is							
Difference	% points			-72.20			
				Reduction			

Due to variable conditions found during in-situ tests, it is widely accepted that efficiency measurements be corrected for these factors to enable proper comparisons to be made. The manufacturer's correction curves have been used for this purpose where :

$$E_{corr} = 100 - [(K_1.K_2.K_3.K_4).(100 - E_G)]$$

where:

E_{corr} = Corrected ESP efficiency in percentage.

K_1 = Carbon in grits correction factor.

K_2 = Sulphur in coal correction factor.

K_3 = Gas temperature correction factor.

K_4 = Moisture in gas correction factor.

E_G = Efficiency corrected for gas flow in percentage.

The factor having most influence on the corrected efficiency values is gas volume correction. The table initially shows a comparison between "Pre-Efficiency" measurements and design efficiency and "Post-Efficiency" design efficiency. Design efficiency then becomes a common reference point and this allows "PRE-Efficiency" to be compared to "POST-Efficiency" measurements.

For the "Pre-Efficiency" case, the average measured dust concentration was 178mg/Sm^3 compared to a predicted design emission of 137mg/Sm^3. The difference between measured and predicted (design) emissions is 41.04 mg/Sm^3 or 29.99 %.

For the "Post-Efficiency" case, the average measured dust concentration was 127 mg/Sm^3 compared to a predicted design emission of 220 mg/Sm^3. It should be noted that in the "Post-Efficiency" measurements the first field was out of service due to a defective transformer. The manufacturer's gas flow correction curve for 6 fields was used and this is reflected in the "EFF CORR FOR GAS FLOW" data. The difference between measured and predicted emissions is –92.87 mg/Sm^3 or –42.21 %.

Now comparing the "PRE" to "POST" emission levels, we see that the ESP casings levels reduced by 133mg/Sm^3 or 72.2 %.

In order to obtain confidence in the above calculations, the Deutsch equation, as shown below, is used to perform the corrections. This calculation will only correct for gas volume flow rate changes and not for other ESP factors (temperature, sulphur etc.). Gas volume flow rate changes, nevertheless have the greatest influence on ESP efficiency corrections.

Deutsch equation :

$$\text{Efficiency} = 1 - e^{-Ac/Q} * 100\%$$

Where:	Efficiency	=	ESP collection ffficiency. (%)
	e	=	log constant.
	A	=	Collecting electrode plate area (m^2)
	c	=	Particle migration velocity (m/s)
	Q	=	Gas volume flow rate (m^3/s)

Table 3.9, below shows the correction of the measured values for both “Pre” and “Post” efficiency measurements. For the “Post” efficiency measurements, plate area has been adjusted due to one field being out of service.

Table 3.9 : Isokinetic easurements Compared to Design Efficiency Using Deutsch Equation

EFFICIENCY COMPARISONS USING DEUTSCH EQUATION									
		7 fields	Pre-Efficiency - 620 MW			Post Efficiency - 620 MW			6 fields
TEST #		Given	1	2	3	1	2	3	
PLATE AREA	m2	47 656							40848
DESIGN MIGRATION VELOCITY (worst coal)	m/s	0.0344							
AVERAGE VOLUME FLOW RATE	m3/s		265.00	270.00	265.00	277.25	283.25	281.25	
DESIGN EFFICIENCY	%		99.79	99.77	99.79	99.37	99.30	99.32	
MEASURED MIGRATION VELOCITY	m/s		0.0346	0.0350	0.0338	0.0385	0.0380	0.0380	
DIFFERENCE (measured compared to design)	%		0.45	1.66	-1.86	11.91	10.51	10.54	
AVERAGE DIFFERENCE [measured compared to design]	%			0.08			10.99		
DESIGN EMISSION	mg/Sm3		169.62	199.09	168.05	522.36	581.56	561.40	
DIFFERENCE (measured compared to design)	%		2.74	9.61	-12.22	78.75	76.19	76.47	
AVERAGE DIFFERENCE [measured compared to design]	%			0.04			77.14		
AVERAGE DIFFERENCE[Post to Pre Efficiency = Reduction]	%				77.10				

Similarly to the previous correction shown in Table 5, measured values to compared to predicted design values. With the predicted design value being a constant, measured values for the “Post Efficiency state can be compared to that of the “Pre” efficiency state. Using this method, it can be seen that an emission reduction of 77.10% is realised. This correlates very well with the emission reduction of 72.2 % (with other correction factors) shown in Table 3.8. Hence the emission reduction of 133 mg/Sm^3 or 72 % is verified.

3.10.4 Correlation of Emission (Opacity) Monitor

A newer, more modern emission monitor was purchased due to the previous ones failure. This monitor was also to be used for re-entrainment tests, to be discussed in section 3.11. As before, it needed to be correlated.

Figure 3.24, below, shows the opacity meter correlation against mass emissions. The trend line indicates a very linear relationship between its output and mass emission and this is dictated by the equation shown in the figure. This relationship will be used in future tests to indicate particulate mass emissions.

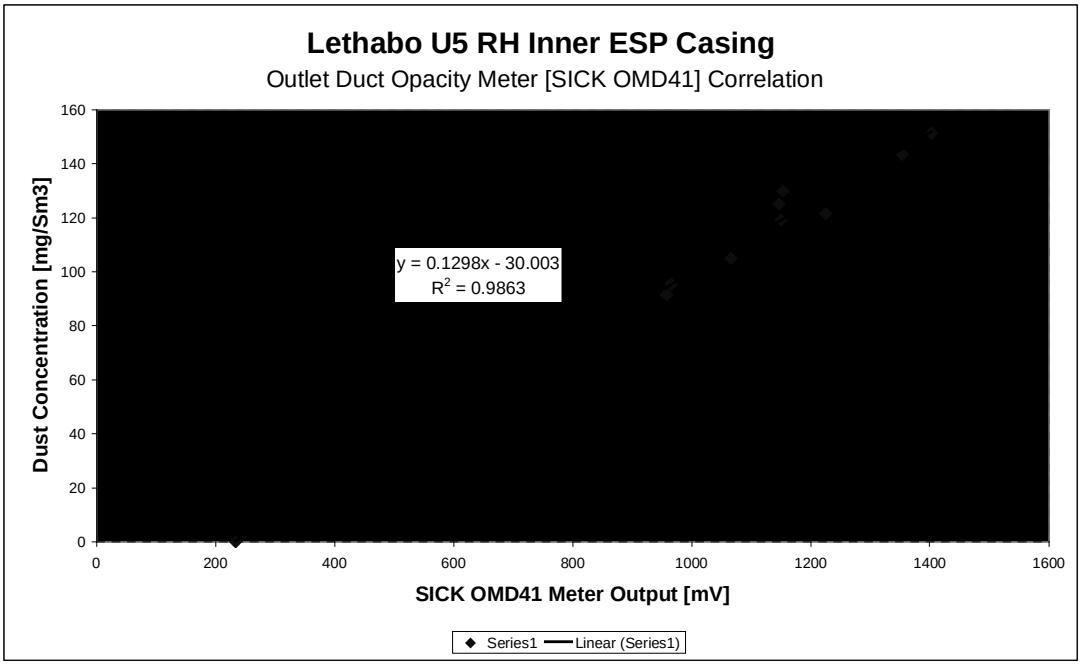

Figure 3.24 : SICK OMD41 Emission Monitor Correlation

3.10.5 Sustainability of Optimised Rapping Settings

The question as to whether the emission reductions seen are sustainable over longer periods of time led to an attempt to trend the test casings emission monitors outputs against boiler load. Since it is not feasible to conduct iso-kinetic sampling tests over these time periods, this approach is probably the best information we can gather under the circumstances.

Lethabo and other Eskom Power Stations current operational load characteristics are variable based on system demand. Figure 3.25, below, shows an example of the boiler load variations that can be experienced over a period of six days.

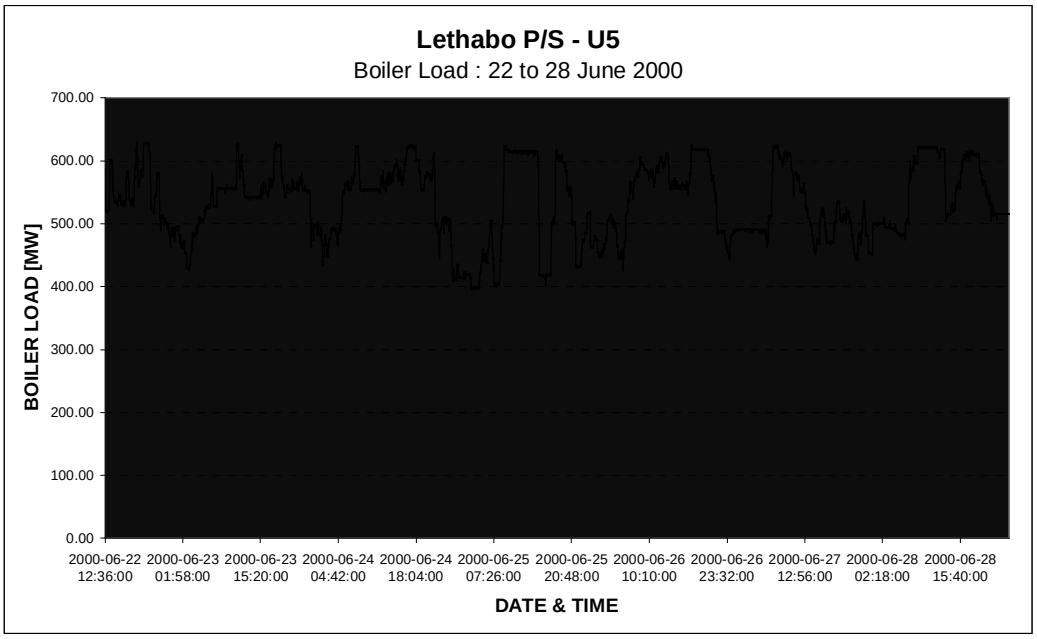

Figure 3.25 : Example of Boiler Variable Load Conditions

It was decided to compare average boiler loads to average dust emission monitor outputs to establish if optimised ESP emission levels were consistent over longer time periods. Table 3.10, below, shows this comparison for different time periods over the different months of the 2000 year. It should be noted that the emission measurements

were recorded from the monitor, and as such cannot be corrected for gas volume flow rate. The average emission levels are also effected greatly increased by boiler process conditions (mill changes, sootblowing, temperatures etc.) and these are not accounted for when comparing to constant boiler load conditions.

Table 3.10: Comparison Of Average Boiler Load to Average Emissions

	AVERAGE	
TIME PERIOD	**Boiler Load [MW]**	**U5 DUCT OPACITY [mg/Sm^3]**
10th to 18th May 2000	559	123
30th May to 1st June 2000	556	117
2nd to 9th June 2000	545	134
22nd to 29th June 2000	534	120
1st to 8th August 2000	525	81
29th Aug to 6th Sep 2000	554	110
12th to 20th October 2000	549	114
21st to 25th October 2000	544	120

From Table 3.10, it can be concluded that despite the limitations of this averaging approach, the optimisation process has produced results that can be consistently maintained. No emission excursions over 140 mg/Sm^3 are experienced.

3.11 RAPPING RE-ENTRAINMENT AND FIELD COLLECTION QUANTITIES

Results from the dust emission monitor correlation tests were analysed to determine rapping re-entrainment effects of the ESP unit. Specific tests were conducted on 30th

May 2000 and 12th October 2000, under full load conditions to determine these characteristics.

3.11.1 Measurements on 30th May 2000

It should be noted that during these full load (620MW) dust emission monitor correlation tests, rapping changes could not be implemented/tested. However, a review of the data showed some of the required characteristics coinciding with the test sessions and these are shown below.

During these test sessions (30th May), the first field was out of service due to a transformer malfunction. Hence field 2, behaved as the first field, field 3 as the second field and so on.

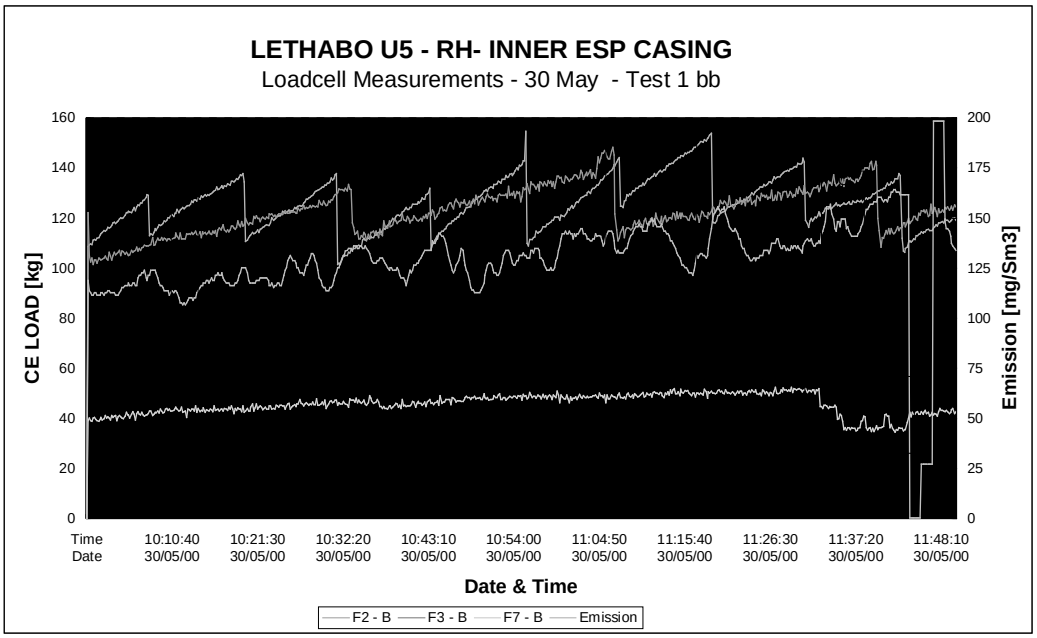

Figure 3.26: Rapping Re-entrainment Measurements

Figure 3.26, above shows the fields collection during the first test session. Here it can be seen that duct outlet emission trends field's 2 (1) and field's 3(2) are rapping very well. Re-entrainment caused by rapping the front fields (even in their optimised state)

still remains a problem. In Figure 3.26, from the area highlighted as “A”, it can be seen that when the front fields (2 and 3) are collecting, emission levels drop to about 106 mg/Sm^3.

In the area highlighted as “B”, two interesting conclusions can be made. Firstly, rapping two front fields almost simultanously, does not necessarily produce a larger re-entrainment spike in the outlet emission. Secondly, the ESP casing reacts/settles down very quickly after this re-entrainment event. Within 8 minutes of the two rapping events, outlet emission has returned to pre-rapping levels.

The areas highlighted as “C” and “D” reflect the same event, field 7’s(last field) rapping re-entrainment characteristic. This is measured at 20 mg/Sm^3. Area “D” illustrates the effectiveness of rapping the later fields with the regime discussed in 3.8.3.

The times for field 7 are :

Pause (collect) : 24 hours

Run (clean/dislodge) : 12 minutes continuous (4 rap cycles)

This shows that due to the nature of the ash, one rap is not sufficient to adequately clean the CE. The first rap removes 50% of the ash, the second the remaining 50%. The following two raps do not remove any more, but are available should they be needed.

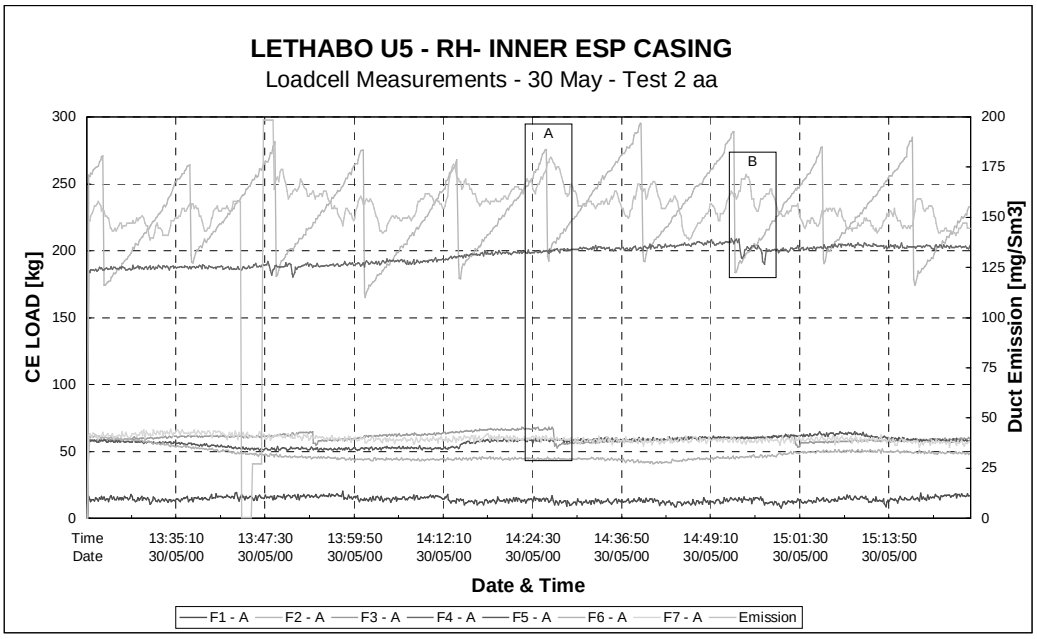

Figure 3.27: Rapping Re-entrainment Measurements

Figure 3.27, above shows the rapping characteristics during the second test session, also at 620 MW. During this period field 3(2) and field 4(3) re-entrainment effects are seen. When rapped, both these fields produce re-entrainment spikes of approximately 20 mg/Sm^3. Field 3(2) collection rate during this period is 0.42 kg/min while field 4(3) collection rate is 0.13 kg/min.

3.11.2 Measurements on 12th October 2000

The emission monitor correlation tests on 30th May 2000 did not provide all re-entrainment and collection rate information required. Besides, the malfunctioning first field complicated the analysis somewhat. Full load (620 MW), isokinetic tests were conducted on the 12th October 2000. Due to this, field manipulations could be carried out as they would interfere with the isokinetic test results.

Figure 6, below shows the boiler load for the test session. Between 14:00 and 15:30, there was a drop in boiler load from 620 MW to 480 MW. This however, did not impact

too much on the tests. Figure 3.29, shows the overall loadcell data for the test period. Various tests were carried out during this session and these will be analysed on an individual basis. These are shown in the subsequent figures.

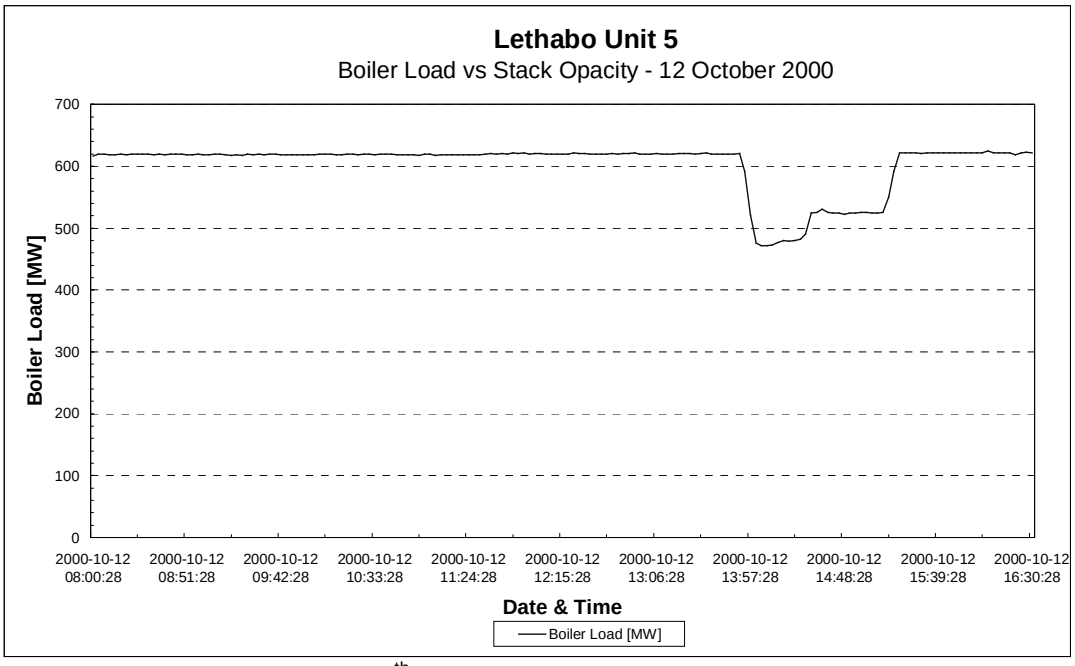

Figure 3.28 : Boiler Load for 12th October 2000 Test Period

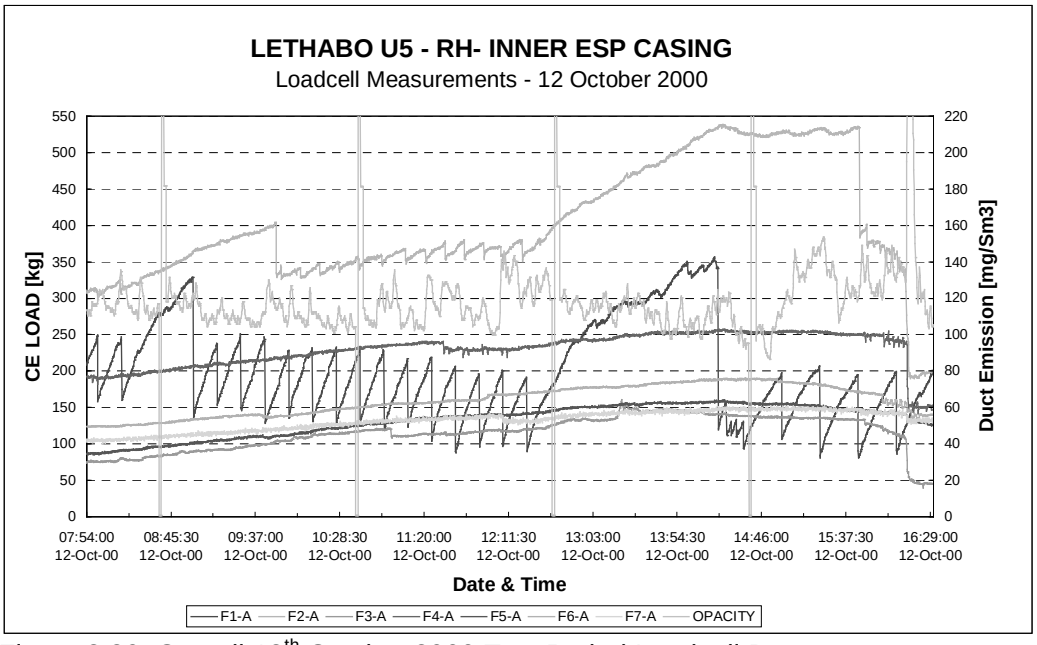

Figure 3.29: Overall 12th October 2000 Test Period Loadcell Data

In the first test, between 08:20 and 08:57, all fields rapping were turned off (collection in all fields). Figure 8, below shows this test session with some pre-test data. Window A in Figure 8, shows the rapping of fields 1 & 2 coinciding and this produces an emission spike of approximately 23 mg/Sm^3.

Window B shows the data between 08:20 and 08:57. It can be seen that rapping spikes are absent and outlet emission decreases to 109 mg/Sm^3. The surge in emission in this window is the monitor conducting its zero and range checks.

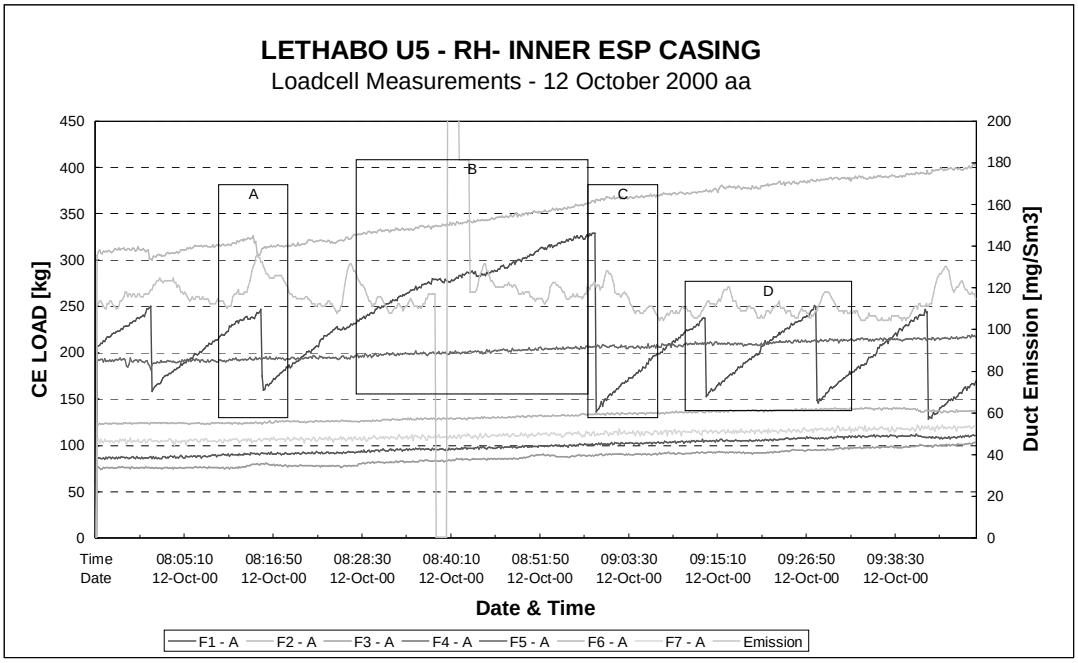

Figure 3.30: Rapping re-entrainment of Field 1

Window C in Figure 3.30 shows the rapping of field 1, with its large ash layer and the re-entrainment effect it solely produces on outlet emission. Note that all remaining fields(2 to 7) rapping are still off. The emission spike of approximately 16 mg/Sm^3 for the dislodgement of 190kg of ash compares very favourably with the rap shown in Window D. Here, the dislodgement of 81 kg of ash produces a re-entrainment spike of 12mg/Sm^3.

This provides further evidence that the less frequent rapping and dislodgement of larger ash layers causes lower re-entrainment than the more frequent dislodgement of smaller ash layers. This difference can be as much as 40 % less.

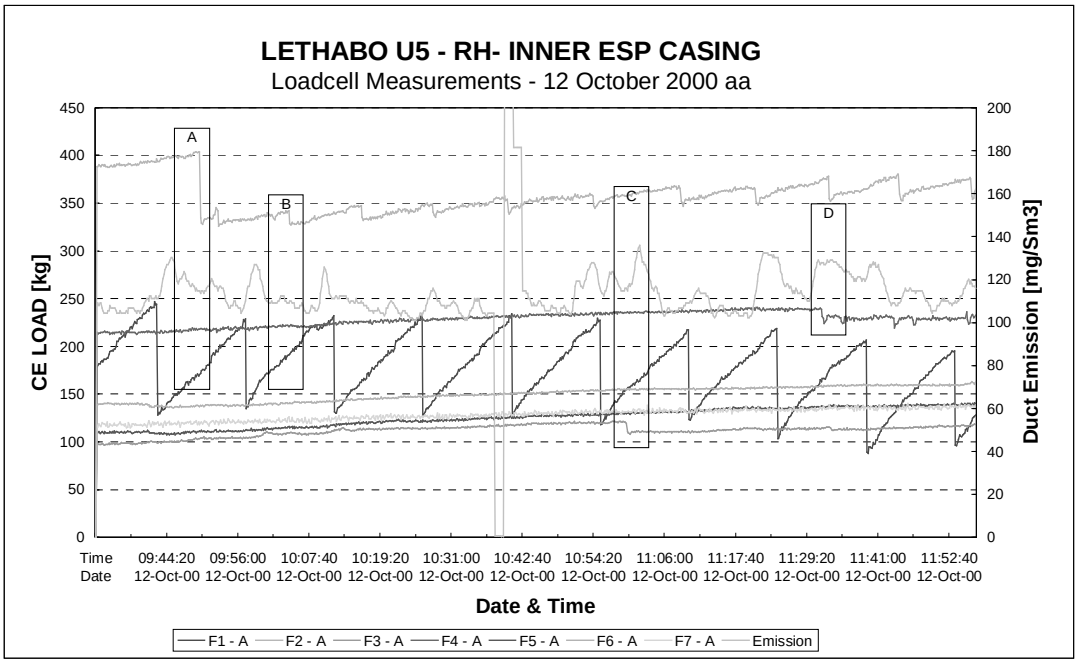

Figure 3.31: Rapping re-entrainment of fields 2, 3 and 4.

Figure 3.31, above continues with determining the re-entrainment of subsequent fields. From the previous test, field 1's rapping was turned on and the subsequent fields were off. In this figure, fields 2, 3,and 4's rapping was turned on and the corresponding emission spike on the monitor noted. Window A, in Figure 3.31 shows that when field 2 is rapped after its extended collection period, almost no rapping spike is seen. However, when field 2's "normal" rapping is re-instated (Window B and rest of Figure 3.31) a rapping spike of up to 4mg/Sm^3 can be seen. From this we can conclude that rapping-off larger ash layers/cakes produces less re-entrainment.

Unfortunately, due to field 5's rapping gear being out of service, it was not tested.

Figure 3.32, below shows the re-entrainment tests for fields 6 and 7. Window A, shows the period when field 7 was rapped. A rapping spike of approximately 25 mg/Sm^3 was produced. Field 6 was rapped between 11:58 and 12:03. However, no rapping significant spike is seen and this cannot be explained.

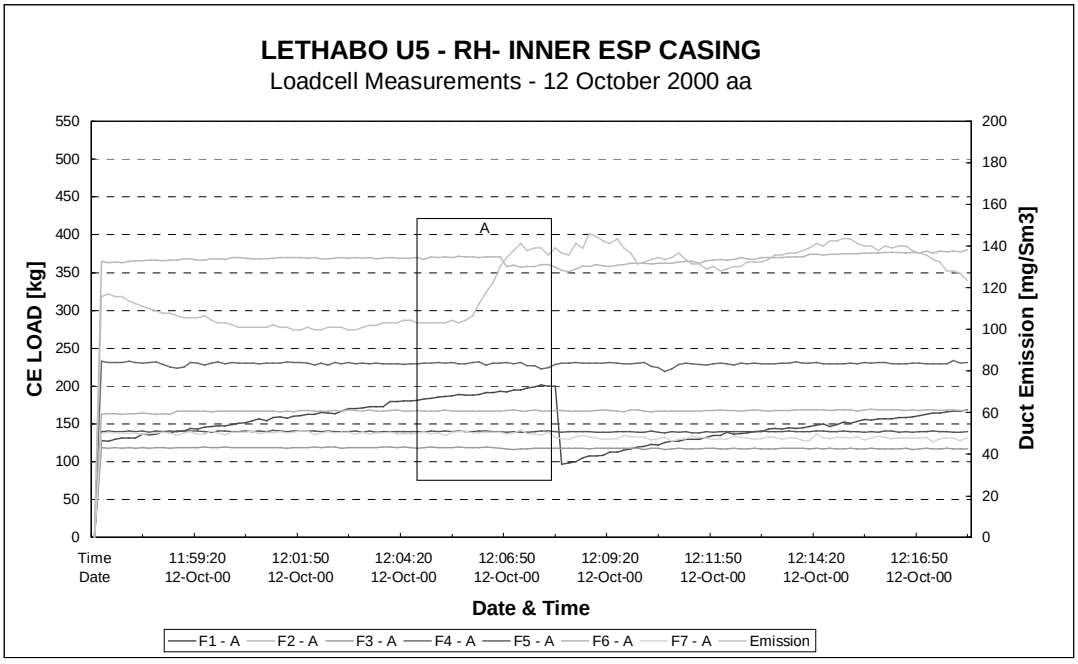

Figure 3.32: Field 6 and 7 re-entrainment

Generally it has been found that rapping of thinner CE ash layers causes greater re-entrainment spikes than thicker ash layers. Considering that the rapping of thinner ash layers is the result of more frequent rapping, this accumulation causes the re-entrainment efficiency losses to be amplified.

In order to understand the collection quantities of the different fields, an analysis was done on data from isokinetic efficiency tests as well as loadcell data. Table 3.13, below, shows the collection rates measured in each of the fields, based on the inlet and outlet emissions as well loadcell rates.

Table 3.11: Lethabo U5 Collection Rate Measurement

Field	COLLECTED ASH - [kg/s]			COLLECTED
	Per CE	Per CE Area [m2]	Per Total Field	%
1	0.083333333	0.000566893	3.8333	32.54
2	0.017676768	0.00012025	0.8131	6.90
3	0.002380952	1.6197E-05	0.1095	0.93
4	0.001165981	7.93184E-06	0.0536	0.46
5	0.000694444	4.72411E-06	0.0319	0.27
6	0.000231	1.57143E-06	0.0106	0.09
7	0.000144525	9.83166E-07	0.0066	0.06
Total Field Collected			4.8588	41.24
Collected by Dropout [By Difference]			6.9223	58.76
Total Ash Collected by ESP [From measurements below]			11.7811	100.00
From Isokinetic Efficiency Measurements				
Gas Flow			265	Am3/s
Inlet			44500	mg/Am3
Outlet			43	mg/Am3
ESP Collected Ash			11781105	mg/s
ESP Collected Ash			11.781105	kg/s

Collection due to gravitational assisted ash drop-out has been estimated (by difference) at 58.3%. From the table, it can be seen that field 1 accounts for approximately 68% of the total ash collected by the ESP. Most of the ash drop-out (of the large particles) generally occurs in the first fields of ESP's and 13.5% can be added to the 68% to provide a total collection of 81,5%. Field 2 collects 14,5% with fields 3 to 7 (5 fields) collecting a total of 4% of the total ESP collected ash. The percentage ash collected per field decreases exponentially from field 1 to field 7, in accordance with the theory suggested by Deutsch.

3.12 ESP RAPPING WEAR ANALYSIS

Table 3.12, below shows "as found" compared to "presently optimised" rapping time schedules. It should be noted that with the exception of field 1, all other fields have two rapper shafts. These shafts are located at the bottom of the CE's, just above the top of the hoppers, one on the leading/front edge of the CE and the other on the trailing/back edge.

The rapping “off” tests indicated that with the optimised longer collection times, the fields were properly cleaned using one rapper shaft (trailing/rear shaft). Hence in the optimised section of the table, the front shafts were not used.

Table 3.12 : Lethabo Unit 5 ESP Rapping Analysis

Lethabo Power Station - Unit 5 RH Inner Casing Rapping Analysis

Time for full revolution (seconds) 180

As Found Rapping Times

	Front/Leading Edge Rapper Shaft						Back/Trailing Edge Rapper shaft					
FIELD	Off/Pause	On/Run	On/Off Cycles	1 Full Rev.	1 Full Rev.	1 Full Rev.	Off/Pause	On/Run	On/Off Cycles	1 Full Rev.	1 Full Rev.	1 Full Rev.
			[Rev]	[Seconds]	[Minutes]	[Hours]			[Rev]	[Seconds]	[Minutes]	[Hours]
1	No Shaft						6	21600	0.01	180.05	3.00	0.05
2	5	30	6.00	210.00	3.50	0.06	35	40	4.50	337.50	5.63	0.09
3	3	20	9.00	207.00	3.45	0.06	23	30	6.00	318.00	5.30	0.09
4	5400	20	9.00	48780.00	813.00	13.55	5420	30	6.00	32700.00	545.00	9.08
5	14400	20	9.00	129780.00	2163.00	36.05	14420	30	6.00	86700.00	1445.00	24.08
6	18000	20	9.00	162180.00	2703.00	45.05	18020	30	6.00	108300.00	1805.00	30.08
7	3600	4	45.00	162180.00	2703.00	45.05	3604	6	30.00	108300.00	1805.00	30.08

Optimised Rapping Times

	Front/Leading Edge Rapper Shaft						Back/Trailing Edge Rapper shaft					
FIELD	Off/Pause	On/Run	On/Off Cycles	1 Full Rev.	1 Full Rev.	1 Full Rev.	Off/Pause	On/Run	On/Off Cycles	1 Full Rev.	1 Full Rev.	1 Full Rev.
			[Rev]	[Seconds]	[Minutes]	[Hours]			[Rev]	[Seconds]	[Minutes]	[Hours]
1	No Shaft						1200	180	1.00	1380	23	0.38
2							1800	180	1.00	1980	33	0.55
3							3600	360	0.50	1980	33	0.55
4							14400	360	0.50	7380	123	2.05
5	0						43200	360	0.50	21780	363	6.05
6							86400	540	0.33	28980	483	8.05
7							172800	720	0.25	43380	723	12.05

While there has been an increase in the last four fields shaft rotation in percentage terms, it is not significant in overall terms as the results show.

The “as found” section reveals that the first three fields(Field 1, 2, and 3) were being rapped too frequently than was necessary. A comparison of the times shows this. Figure 3.32, and Table 3.12 shows a graph and tabular summary of the “as found” and “optimised” rapping impacts to the CE (1 CE used for analysis) as well as shaft rotation as a function of time. Impacts and shaft rotation were the two quantities used in the analysis as from a rapping point of view, they predominantly influence wear and tear

rates. A reduction in shaft rotation also has an influence in power saving considering Lethabo Power Station has a total of 312 rapper motors.

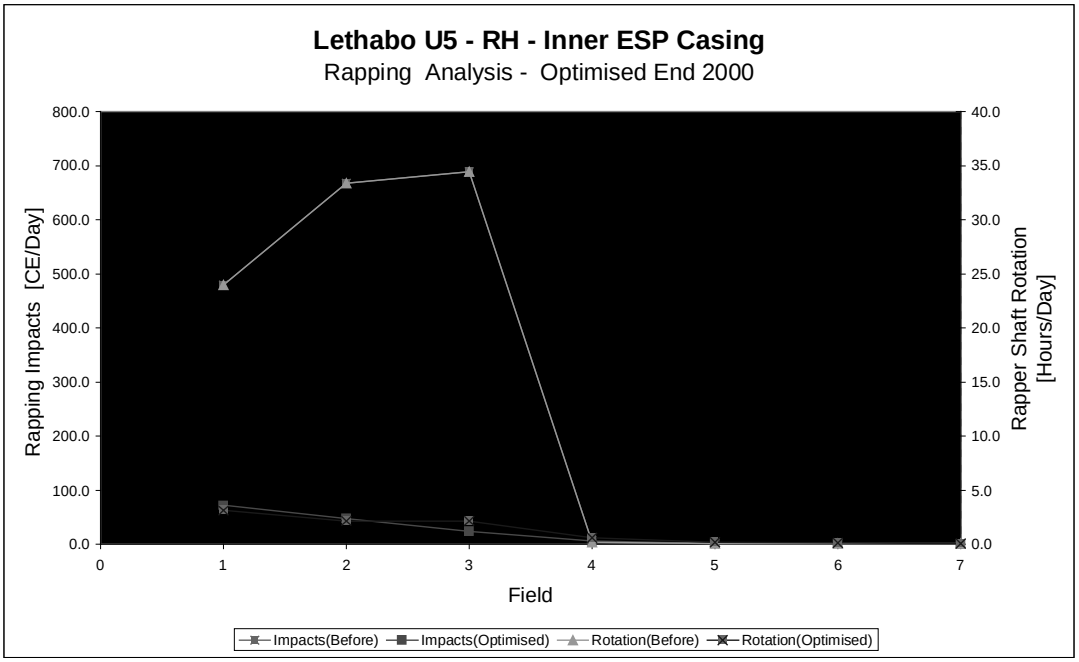

Figure 3.33 : Comparison of Rapping Analysis Times

From Figure 3.33, it can be seen that the “as found” use of the rapper shafts (both sides) resulted in excessive impacts and shaft rotation when compared to the “optimised” times. This is especially true for the first three fields. A study of present maintenance schedules correlate this excessive wear trend in the first three fields by showing that rapper shaft bearings and split bushes need to be replaced more frequently in these fields. Rapper hammers in the first field also have to be refurbished most frequently due to the previous near continuous rapping.

Table 3.13: Rapping Wear Related Analysis

IMPACTS AND SHAFT ROTATION

IMPACT BLOWS

As Found - Start 1999

Impacts per CE [over 24 hrs]

Front shaft	Back shaft	Total
0.0	479.9	479.9
411.4	256.0	667.4
417.4	271.7	689.1
1.8	2.6	4.4
0.7	1.0	1.7
0.5	0.8	1.3
0.5	0.8	1.3
	Total	1845.1

Optimised - End 2000

Impacts per CE [over 24 hrs]

Front shaft	Back shaft	Total
0.0	72	72.0
	48	48.0
	24	24.0
	6	6.0
	2	2.0
	1	1.0
	0.5	0.5
	Total	153.5

SHAFT ROTATION

As Found - Start 1999

Rotation per shaft [over 24 hrs]

Front shaft	Back shaft	Total
0.0	24.0	24.0
20.6	12.8	33.4
20.9	13.6	34.5
0.089	0.132	0.221
0.033	0.050	0.083
0.027	0.040	0.067
0.027	0.040	0.067
	Total	92.3

Optimised - End 2000

Rotation per shaft [over 24 hrs]

Front shaft	Back shaft	Total	% Reduction
0.0	3.1	3.1	86.95
	2.2	2.2	93.46
	2.2	2.2	93.67
	0.585	0.585	-165.27
	0.198	0.198	-138.64
	0.149	0.149	-124.07
	0.100	0.100	-49.69
	Total	8.5	90.76

Table 3.13 shows the influence of these times into the primary wear and tear factors, namely CE impacts and rapper shaft rotation.

Table 3.12, above shows that originally, in the “As Found” situation, each CE was subjected to 1845 impacts during a 24 hour period. This is generally constant for the whole lifetime of the plant (minor exceptions being outages). At the end of 2000 this had been reduced to 153 impacts. Similarly, on an ESP casing basis, the “As Found’s” total rapper shaft rotation of 92 hours running time per day (13 shafts per casing) was reduced to 8 hours.

This immense reduction in rapping has a correspondingly significant reduction in day to day running (auxiliary power) and maintenance costs (bushes, bearings, hammers,

anvils etc). This is especially significant when one considers the amount of components installed in all six boiler unit ESP's at Lethabo P/S.

CE's	7728
Rapper Hammers	14352
Anvils	14352
Bushes	78960
Rapper shaft bearings	2184
Rapper motors	312

The above are changed/repaired on average once every 8 years and these costs amount to R2.1m for 6 ESP units. Now considering that, these are now being rapped 75% less, a potential cost saving of R 6,3m over 24 years can be realised. Power savings resulting from reduced rapper shaft operation have been calculated at R1,42m over the next 20 years of operation. These savings however, will be minimal when compared to long term savings in damage to ESP CE's. Refurbishment/replacement of CE's is considered the major cost portion of ESP rebuilds when plant life extension procedures are implemented.

A reduction in rapping will be especially welcome in older ESP's. Examples of these are Eskom's Arnot, Hendrina, and Kriel Power Stations which are already 20 and more years old. It would extend the life of these ESP's, while at the newer Eskom stations will protect the mechanical integrity of fairly good ESP's. Plant life extension objectives are already being implemented at the older power stations and the costs are exorbitant.

3.13 SUMMARY

There has been a successful measurement of ash collection patterns at Lethabo P/S Previous loadcell problems experienced at Hendrina P/S have been eliminated using the external loadcell installation technique. A new problem of the loadcell measurement system variation with ambient temperature has been seen. Steps are however available to eliminate this. Despite having dual CE rapping hammer shafts, it has been found that one CE side rapping produces sufficient vibration intensities to adequately clean even the thickest ash layers.

The inlet dust loading loading at Lethabo Power Station is relatively high, averaging 84 g/m^3 (STP). In the “as found” conditions, the ESP collection efficiencies ranged from 99,77 to 99,84 %.

Lethabo U5 RH Inner ESP casing operating efficiencies appear to be at their highest during time period up to 11:00. Thereafter operating efficiencies decrease despite fairly constant boiler conditions. Ambient temperatures seem to have the greatest influence on this situation

ESP outlet dust burden trends field 1’s precipitation rate most closely. When field 1 experiences a cycling of its CE ash cake layer, this trend is correlated by the outlet opacity. This cycling nature of the ash cake layer is usually a result of too frequent rapping on the front fields which carry a larger ash load. This is contrary to conventional wisdom, especially in a large 7 field, high aspect ratio ESP as Lethabo. This phenomenon could be more pronounced on smaller ESP units.

De-energised rapping is very beneficial to improving ESP performance and has the greatest influence in cleaning the rear fields of an ESP which build up thicker residual

ash layers. Again, this phenomenon is contrary to general thoughts which does not predict the build up of very large residual ash layers in the last fields.

Hopper swirl, with or without a combination of back corona can have significant influences on last field's gravity induced re-entrainment. This condition most likely occurs randomly as a result of a combination of high hopper levels, back corona and coal quality variations.

Rapping-off tests in which field precipitation rates and saturation levels are determined are very useful and perhaps the most accurate method of :

- Calculating optimum rapping time intervals (minimising re-entrainment and wear by fewer, more effective raps)
- Determining field precipitation rates and using them as a benchmark to diagnose the presence of operational problems.
- Setting up controller energisation parameters.
- Determining if existing rapper hammer forces are enough to clean the CE's. If forces are not enough, then rapping time schedules and sequencing can be optimised so existing rapping forces are made to act upon a thicker ash cake, which is dislodged easier. Expensive hammer changes can thus be avoided. At Lethabo Power Station it was shown that rear rapper shafts provide sufficient vibration intensity for CE cleaning. Front rapper shafts can be considered "spare". If part of an automatic control system, front and rear rapper shafts can be used in tandem to equally share system rapping.

The research has shown that it is relatively easy to optimise the front fields of an ESP using only timing schedule changes. On the last fields, timing changes must be

accompanied by de-energised rapping and electrical optimisation for significant changes to be seen.

Despite rapping precipitation time ratio's being the same, re-entrainment is increased with more frequent on-off cycles. It is advantageous to rap the entire field with one continuous rapper shaft revolution than smaller equally proportioned increments. Rapping off larger ash layers produces, cumulatively lesser re-entrainment than rapping thinner ash layers.

Electrical controller operation is enhanced and rapping re-entrainment is minimised by completing rapping in the shortest time period. Sonic horns and Magnetic Impulse Gravity Impact (MIGI) systems take advantage of this phenomenon. Higher speed rapping shafts, via rapper gearbox ratio changes should be investigated as a cheaper alternative to minimise re-entrainment.

The reduction of rapping times correspondingly produces a reduction in rapping impacts to CE's. This will minimise repairs/retrofits the ESP will require after twenty to thirty years of operation.

Mechanical timers controlling rapping must be constantly inspected for integrity. Rapper timer failures lead to a variety of problems. This is most critical for the first fields of ESP's. The possibility of exceeding design loads for CE's and supporting structure during timer and/or rapper system failures should be investigated further. This problem can be quite severe in flue gas conditioned ESP's where thicker ash layers can be collected. Hopper blockages when large ash layers are dislodged from the entire field (after timer or rapper motor repairs) can easily occur. Flue gas conditioned units, with their higher collection rates/ash layers are highest at risk from this phenomenon.

Damage to older hopper structures is also possible from the impacts generated by large ash layers being dislodged.

The emphasis on reducing or even maintaining present emission levels and decreasing rapping frequencies must be investigated further as it is beneficial from a wear and tear perspective.

Coal variations, on a frequent basis (sometimes within 2 hours) mean that manual, optimised settings are not always in tune with ESP conditions. Operator intervention is not practical considering the number of fields, controllers and timers present at power stations. Optimised settings might result in only small emission reductions on a daily basis. However, when these small reductions are sustainable over longer periods of time, significant overall reductions can be achieved. Power station's monthly emission levels (tons emitted) can benefit from these reductions if emission reductions are sustainable.

Equipment failures, specifically mechanical rapper timers are a threat to maintaining optimised settings. Controller failures occur, though less frequently. Mechanical timers limit the optimisation of particularly the back fields where the timing cycles required cannot be achieved without an operator being present. This can be a seriously limiting factor if all units at a power station need these timing cycles on a daily basis. An automatic control system can eliminate many of the above problems and lead to sustainable, constantly optimised, settings. The loadcell system can be directly linked to such a system, thus producing an ESP that is able to continuously optimise its rapping as well as electrical energisation based on prevailing, real time conditions.

Optimisation efforts and results using CE mass measurement at Lethabo P/S show an emission decrease of approximately 70% and a corresponding decrease in rapping induced wear and tear of 90%.

Chapter 4 : Conclusion

4.1 CONCLUSION

4.1.1 The use of collecting electrode mass measurement to optimise an electrostatic precipitator has been successfully investigated and developed.

4.1.2 Rapping optimisation with the use of loadcells has been shown to be successful in terms of both reducing emissions as well as reducing wear and tear. Emission reductions of 133 mg/Sm^3 (70%) and rapping induced wear and tear reduction of 90 % have been realised at the Lethabo Power Station test facility.

4.1.3 Rapping of thinner ash layers causes greater re-entrainment than the rapping of thicker ash layers. Rapping of thinner ash layers occurs more frequently (faster times) and hence, cumulatively also results in greater re-entrainment losses.

4.2 RECOMMENDATIONS

4.2.1 The use of collecting electrode mass measurement to optimise an ESP is recommended for both new as well as existing plant.

4.2.2 ESP externally located loadcells are preferred over internally located loadcells due to the high risk of damage and the corresponding accessibility problems.

4.2.3 The possibilities of patenting the concept or any other aspect of the project should be studied. The technique was originally tested by the EPRI as presented in the reference 2. However to, the best of our knowledge, we are the first to use data

obtained to see the areas of inactivity in an ESP. As the project progresses, we will also be the first to logically optimise other parameters, besides rapping.

4.2.4 Considering the positive results obtained thus far, and the capital spent in setting up the test facility at Lethabo Power Station, it is recommended that it be used to conduct further research and development. Topics that need to be researched are detailed below, in “Future Research”.

4.2.5 There has been much interest for collaborative ESP research, development and joint ventures by ESP Original Equipment Manufacturers (OEM’s), repairers, vendors etc. These potential alliances must be investigated.

4.3 FUTURE RESEARCH

4.3.1 Further testing and analysis must be conducted to fully understand the re-entrainment phenomenon. Emphasis must be placed on rapping induced re-entrainment since it is widely considered to have a major influence on ESP efficiency. Actual, in-situ results as obtained from the loadcell measurements must be used in conjunction with CFD modelling. CFD modelling will provide the benefit of being able to overcome some of the limitations of full scale “live” testing (e.g. transient temperature fluctuations, high hopper levels and sneakages etc.). This relationship will allow correlation/verification of CFD results with real plant data.

4.3.2 The use of the loadcells in conjunction with other ESP control parameters (electrical controllers, rapper timers etc.) to develop one complete ESP control and management system must be investigated. This has huge benefit to ESP operators and as such will provide a viable commercial entity for Eskom TSI.

4.3.3 A study must be undertaken to correlate rapping intensity and ash dislodgment, so as to optimise this process. Excessive, unnecessary rapping causes undue, costly mechanical wear on ESP plant. This study must also consider the optimum positioning/location of rapping hammers.

4.3.4 The loadcell system must be used to evaluate the control of ESP FGC plant and more specifically the injection rates of conditioning agents. In many ESP plants, over-injection does not necessarily increase collection efficiency – rather the opposite occurs. Besides conditioning agent cost savings can be realised by not over-injecting.

4.3.5 Similar work must be investigated for DE's. The interaction between discharges electrodes (DE's) and CE's has not been considered up to now. Some of the problems seen in the data at Hendrina could be related to problems in the rapping of the DE's. Now that we have enough confidence we should consider the difficult task of measuring the collecting loads of DE's which have high DC voltages. This is something that has not been attempted by any party in the world due to its complex nature. However, if the data from CE's are anything to go by, then improvements in efficiency can be effected by monitoring DE ash loads.

4.3.6 The experience gained in optimising an ESP thus far must be attempted to be applied at other Eskom ESP units. This could take the form with/without loadcells. The development of a generic rapping optimisation procedure must also be investigated. Ideally loadcells would be recommended, but it finances do not allow this, then attempts must be made to apply the lessons learned at Lethabo P/S ESP's to other ESP's.

4.3.7 Future investigations must be done to optimise rapper hammer masses and configurations as well as their positioning on the electrodes. Again, this can be

investigated at the Lethabo P/S test facility. different hammer configurations. Reduction of the rapping forces can greatly reduce ESP wear and tear.

Chapter 5 : References

5.1 References

1. Tassicker O J ; Control of an electrostatic precipitator by continuous measurement of plate dust load ; Prepared by Flow Research Company for The Electric Power Research Institute, June 1978

2. Bowman H, et al ; Selecting and defining rapping schedules to prevent sodium depletion on hot side precipitators ; Arkansas Power & Light Redfield, Arkansas.

3. Yamamoto T, et al ; Studies of rapping re-entrainment from electrostatic precipitators ; Sumitomo Heavy Industries Ltd ; Proceedings : ICESP 7 Conference ; September 1998 ; Kyongiu, Korea ; pp.163-166

4. Lee J, et al ; Experimental study of electrostatic precipitator plate rapping and re-entrainment ; Pusan National University, Korea ; Proceedings : ICESP 7 Conference ; September 1998 ; Kyongiu, Korea ; pp.155-162

5. Bosch F J ; Particulate Emission Control Technology Evaluation and Database ; Eskom Technology Group ; Report No. TRR/P93/034.

6. Geecom (Pty) Ltd ; Electrostatic precipitator – Advanced training course notes ; 1999 ; Johannesburg, SA.

7. White H J ; Industrial Electrostatic Precipitation ; Addison – Wesley Publishing 1963, Chapter 6 ; pp105-117.

8. McCullough M ; Minor modifications and operating techniques to enhance precipitator performance : Experience report of Southwestern Public Service ; Southwestern Public Service Co.

9. Saito Y ; The latest dust collecting technique ; Technical Institute, Mitsubishi Heavy Industries Ltd Technical Review ; Vol. 13, No 3 ; October 1976.

10. Sproull W T ; Fundamentals of electrode rapping in industrial electrical precipitators ; Journal of the Air pollution control association ; February 1965.

11. Crynack R R ; Rigid frame and rigid discharge electrode electrostatic precipitator design comparison relating to upgrade technology ; An Introduction to United States of America Electrostatic Precipitator Rebuild Technology, WPCA and Eskom ; January 1998 ; Johannesburg, SA.

12. Electrostatic Precipitators – 50 Years Technology for Energy and the Environment, Rothemühle brochure

5.2 Additional Reading

1. Humbert C O ; Electrostatic precipitator rappers – Their function, operation and maintenance ; 76th Annual Meeting of Air Pollution Control Association ; June 1983.

2. Goland Y ; Mechanical and structural design consideration for internals in electrostatic precipitators ; ASME publication.

3. Miller S J, et al ; Measurement of re-entrainment effects in electrostatic precipitators and fabric filters ; Energy and Environmental Research Center – University of North Dakota.

4. Maziarz M ; Electrostatic precipitator rapping with sonic horns at Atlantic Electric's B.L England generating station ; Belco Technologies Corporation ; Power-Gen America 1995 conference.

5. Nicholas D M ; A structural design philosophy specific to electrostatic precipitators and fabric filter casings ; American Power Conference proceedings volume 56-II ; 1994

6. Perevodchikov V I, et al ; Research in formation of a dust layer on precipitation electrodes of the electric precipitator at an alternating polarity power supply ; Proceedings ICESP VII, September 1998 ; Kyongiu, Korea.

7. Engelbrecht H L ; Rapping systems for collecting surfaces in an electrostatic precipitator ; Environment International, volume 6, pp 297-305 ; 1981

8. Fukuzawa K, et al ; Rapping characteristics of electrodes in dry electrostatic precipitators ; Mitsubishi Heavy Industries Ltd technical review, volume 25 – number 3 ; October 1988.

9. Barrett A A, et al ; Gas cleaning in Central Electricity Generating Board Power Stations ; Second International Clean Air Congress of the International Union of Air Pollution Prevention Association ; December 1970 ; Washington USA.

10. Stewart L L, et al ; A back to basics approach to solve and avoid electrostatic precipitator performance problems associated with the firing of coals with high resistivity

and/or highly adhesive ashes ; Peabody Sturtevant Corporation ; Princeton, New Jersey ; USA.

11. Juricic D, et al ; Modeling and simulation of dust dislodgement on collecting plates in electrostatic precipitators ; Mechanical Engineering Department – University of Texas ; USA.

12. Ashworth R A, et al ; Cost effective ESP performance enhancement by flue gas humidification ; 10th annual international Pittsburhg coal conference ; University of Pittsburgh ; September 1993; Pittsburgh, USA.

13. Riehl R T ; New air flow uniformity data analysis for predicting the presence of hopper re-entrainment losses in electrostatic precipitators ; Proceedings of the Ninth particulate control symposium ; volume 1 ; October 1991 ; Virginia, USA.

14. Trinward J ; Electrostatic precipitator performance improvement with frame stabilization ; Power-Gen America 1995 conference ; Book V, volume 1 ; December 1995 ; California, USA.

15. Gallego J A, et al ; Pilot scale acoustic preconditioning of coal combustion fumes to enhance electrostatic precipitator performance ; 3rd International symposium on gas cleaning at high temperatures, pp 60-68 ; September 1996 ; Karlsruhe, Germany.

Chapter 6 : Appendices

Appendix A

Hendrina Loadcell Design Calculations

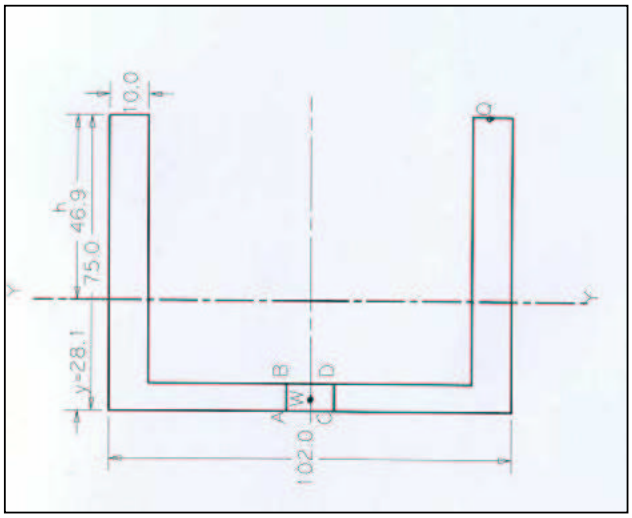

Moment of Inertia

$$\Sigma M_m = 0 \qquad \therefore y = \frac{A_1 y_1 + 2A_2 y_2}{A_T}$$

$$= \frac{(102\times 7)(3{,}5) + 2(68\times 10)(41)}{2074}$$

$$= 28{,}090 \text{ mm}$$

$$I_{x_1} = \frac{bd^3}{12} + Ah^2$$

$$= \frac{102\times 7^3}{12} + (102\times 7)(24{,}590)^2$$

$$= 434{,}648\times 10^3 \text{ mm}^4$$

$$I_{x_2} = 2\left[\frac{bd^3}{12} + Ah^2\right]$$

$$= 2\left[\frac{(10\times 68^3)}{12} + (10\times 68)(12{,}91)^2\right]$$

$$= 750{,}722\times 10^3 \text{ mm}^4$$

$$I_{X_T} = I_{X_1} + I_{X_2}$$
$$= (434{,}648 \times 10^3) + (750{,}722 \times 10^3)$$
$$= 1{,}185 \times 10^{-6}\ \text{mm}^4$$

Area of Channel A
$$= (102 \times 75) - (68 \times 82)$$
$$= 20{,}74\ \text{mm}^2$$
$$= 20{,}74 - (12 \times 8)$$
$$= 1978\ \text{mm}^2$$
$$= 1{,}978 \times 10^{-3}\ \text{m}^2$$

Maximum Load W
$$= 1000\ \text{kg} \times 9{,}81\ \text{m/s}^2$$
$$= 9810\ \text{N}$$
$$= 9{,}81\ \text{kN}$$

Using the Relation

δ at point a as shown in above diagram

$$\delta_A = \frac{W}{A} - \frac{Whx}{I_{yy}}$$
$$= \frac{(9810)}{1{,}978 \times 10^{-3}} - \frac{(9810)(46{,}910 \times 10^{-3})(28{,}090 \times 10^{-3})}{1{,}185 \times 10^{-6}}$$
$$= 5{,}949\ \text{MPa (C)} \qquad = \delta_C$$

$$\delta_B = \frac{W}{A} + \frac{Whx}{I_{yy}}$$
$$= \frac{(9810)}{1{,}978 \times 10^{-3}} + \frac{(9810)(46{,}910 \times 10^{-3})(21{,}090 \times 10^{-3})}{1{,}185 \times 10^{-6}}$$
$$= 13{,}150\ \text{MPa (T)} \qquad = \delta_D$$

Direct Stress
$$= \frac{(9810)}{1{,}978 \times 10^{-3}}$$
$$= 4{,}960\ \text{MPa}$$

$$\delta_{B\&D} = 13{,}150\ \text{MPa}$$

$$\delta_{A\&C} = 5{,}949\ \text{MPa}$$

$$\delta_Q = \frac{W}{A} + \frac{Whx}{I_y}$$
$$= \frac{(9810)}{1{,}978 \times 10^{-3}} + \frac{(9810)(46{,}910 \times 10^{-3})^2}{1{,}185 \times 10^{-6}}$$
$$= 23{,}177\ \text{MPa (Tensile)}$$

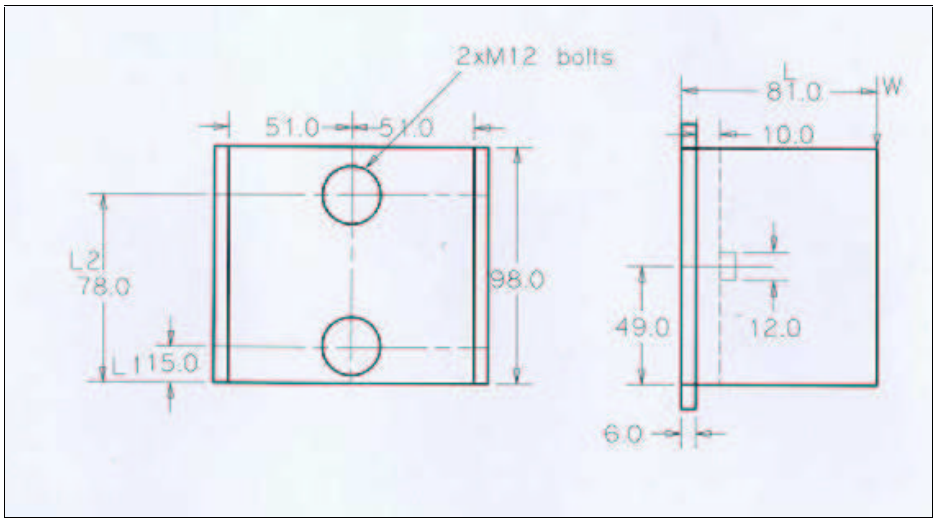

Using two bolts (M12)

Maximum Load on Channel $= W$

$= 1000 \times 9{,}81$

$= 9810$ N

Using the Theory of Eccentric Loading.

Given :

	L	= Distance of the load from the face of column.
	W	= Maximum load on bracket
	L_1	= Distance of the bottom bolt from lower edge of channel
	L_2	= Number of bolts
	3	= Channel
Let	L	= 81mm
	L_2	= 78 mm
	L_1	= 15 mm

Shear Load on each bolt (Top Bolt)

$$W_s = \frac{W}{N}$$

$$= \frac{9810}{2}$$

$$= 4905 \text{ N}$$

Maximum Tensile Load on bolts No.1 & 2

$$W_{t2} = W_t = \frac{WLL_2}{2(L_1^2 + L_2^2}$$

$$= \frac{(9810)(81\times10^{-3})(78\times10^{-3})}{2(0{,}015^2 + 0{,}078^2)}$$

$$= 4{,}912\ \text{kN}$$

Bolts Subjected to Shear & Tensile Load which is Equivalent load.

$$W_{te} = \frac{1}{2}(W_t + \sqrt{W_t^{\,2} + 4W_s^{\,2}}$$

$$= \frac{1}{2}(4{,}912\times10^3 + \sqrt{4912^2 + 4(4905)^2}$$

$$= 7{,}942\ \text{kN} \quad = \text{Equivalent Tensile Load}$$

Equivalent Shear Load $= W_{se}$

$$W_{se} = \frac{1}{2}\left(\sqrt{W_t + 4W_s^2}\right)$$

$$= \frac{1}{2}\left(\sqrt{4912 + 4(4905)^2}\right)$$

$$= 4905{,}125\ \text{N}$$

Using M12 bolts Metric (Top Bolt)

dc = core diameter = 12 mm

Using the Relation.

$$\frac{\pi}{4} d\,c^2 \times ft = W_{te}$$

$$\frac{\pi}{4}(0{,}012)^2 \times ft = 7{,}942\ \text{kN}$$

$$\therefore ft = 70{,}222\ \text{MPa} = \text{Tensile Stress on bolt}$$

Shear Load on bolt = 4905 N

$$\therefore \delta_{Shear} = \frac{F}{A} = \frac{4905\times4}{\pi(0{,}012)^2}$$

$$= 43{,}4\ \text{MPa}$$

Using M12 bolts

a) Stresses at bottom bolt

b) Increasing the distance L by 5 mm

a) $W_{t1} = \frac{W\,L\,L_1}{2(L_1^2 + L_2^2)}$

$= \frac{(9810)(81\times10^{-3})(0,015)}{2(0,015^2 + 0,078^2)}$

$= 944,615\,N$

$W_t = \frac{1}{2}(944,615 + \sqrt{944,615^2 + 4(4905)^2}$

$= 5,399\,kN$

$W_{se} = \frac{1}{2}\left(\sqrt{W_t + 4W_s^2}\right)$

$= \frac{1}{2}\left(\sqrt{5399 + 4(4905)^2}\right)$

$= 4905,138\,N$

Consider Stresses at bottom bolt (Using M12).

$\frac{\pi}{4}dc^2 \times ft = W_{te}$

$\frac{\pi}{4}(0,012)^2 \times ft = 5,399\times10^3$

$ft = 47,8\,MPa$

$\delta_{SHEAR} = \frac{F}{A}$

$= \frac{4905\times4}{\pi(0,012)^2}$

$= 43,4\,MPa$

b) Stresses at bottom bolt by increasing distance L by 5 mm.

$W_t = \frac{W\,L\,L_1}{2(L_1^2 + L_2^2)}$

$= \frac{(9810)(0,086)(0,015)}{2(0,015^2 + 0,078^2)}$

$= 1,003\,kN$

$$W_{te} = \frac{1}{2}\left(W_t + \sqrt{W_t^2 + 4W_s^2}\right)$$
$$= \frac{1}{2}\left(1{,}003\times10^3 + \sqrt{1003^2 + 4(4905)^2}\right)$$
$$= 5{,}432\,\text{kN}$$

$$W_{se} = \frac{1}{2}\left(\sqrt{W_t + 4W_s^2}\right)$$
$$= \frac{1}{2}\left(\sqrt{1003 + 4(4905)^2}\right)$$
$$= 4905{,}026\,\text{N}$$

Consider Stresses at bottom bolt (Using M12).

$$\frac{\pi}{4}dc^2 \times ft = W_{te}$$
$$\frac{\pi}{4}(0{,}012)^2 \times ft = 5{,}432\,\text{kN}$$
$$ft = 48{,}029\,\text{MPa}$$
$$\delta_{SHEAR} = \frac{F}{A}$$
$$= \frac{4905\times4}{\pi(0{,}012)^2}$$
$$= 43{,}4\,\text{MPa}$$

Stresses on top bolt using M12 bolt when distance L is increased by 5 mm.

$$W_t = \frac{W\,L\,L_2}{2(L_1^2 + L_2^2)}$$
$$= \frac{(9810)(0{,}086)(0{,}078)}{2(0{,}015^2 + 0{,}078^2)}$$
$$= 5{,}215\,\text{kN}$$

$$W_{te} = \frac{1}{2}\left(5215 + \sqrt{5215^2 + 4(4905)^2}\right)$$
$$= 8{,}163\,\text{kN}$$

$$W_{se} = \frac{1}{2}\left(\sqrt{5215 + 4(4905)^2}\right)$$
$$= 4905{,}132\,\text{N}$$

Using M12 bolt (Top bolt).

$$\frac{\pi}{4} dc^2 \times ft = W_{te}$$

$$\frac{\pi}{4} (0{,}012)^2 \times ft = 5{,}432\,kN$$

$$ft = 72{,}176\,MPa$$

$$\delta_{SHEAR} = \frac{F}{A}$$

$$= \frac{(4905 \times 4)}{\pi (0{,}012)^2}$$

$$= 43{,}4\,MPa$$

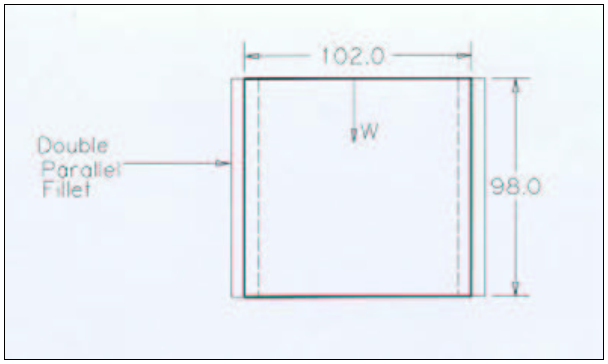

Transverse and Double parallel Welding Calculations.

Let : W = Maximum Load = 1000 kg

Width of channel = 102 mm

Thickness of channel = 6 mm

L_1 = Length of Weld

= 102 - 12,5

= 89,5 mm

ft = Maximum Tensile Stress

Using the Weld formular.

$P = b \times t \times ft$

$9810 = 0{,}102 \times 0{,}006 \times ft$

$\therefore ft = 16{,}03\ MPa$ = Maximum Tensile Stress

Let the Load carried by Single Transverse Weld

$$= P_1 = \frac{t\,l_1}{\sqrt{2}} \times ft$$

where $\frac{t\,l_1}{\sqrt{2}}$ = Maximum Area of Weld

$$\therefore P_1 = \frac{(0{,}006)(89{,}5 \times 10^{-3})}{\sqrt{2}} \times (16{,}03 \times 10^{6})$$

$$= 6{,}087\ kN$$

Let the Load carried by double fillet weld

$= \quad P_2 \quad = \quad \sqrt{2} \times t.l_2 \times fs$

The Load carried by JOINT

$P_T \quad = \quad P_1 + P_2$

where P_T = Sum of strengths of Joints

ie. $P_T \quad = \quad P_1 + P_2$

$9810 \quad = \quad \left(6{,}087 \times 10^3\right) + \left(\sqrt{2} \times 0{,}006 \times l_2 \times fs\right)$

where $l_2 \quad = \quad 0{,}098\,mm$

$\therefore \quad fs \quad = \quad 4{,}48\,MPa \quad = \quad$ Maximum Shear Stress

$\therefore \quad P_2 \quad = \quad 3{,}73\,kN$

For fatique loading consider the following table.

Type of JOINT	Stress concentration factor
Toe of Transverse fillet Welds	1,5
End of parallel fillet welds	2,7

Permissible Tensile Stress $=$ ft

$= \quad \frac{16{,}03}{1{,}5}$

$= \quad 10{,}687\,MPa$

Permissible Shear Stress $=$ fs

$= \quad \frac{4{,}48}{2{,}7}$

$= \quad 1{,}659\,MPa$

$\therefore$ Load Carried by Single Transverse LOad

$= \quad P_1 \quad = \quad \sqrt{2} \times t.l_2 \times fs$

$= \quad \sqrt{2}\,(\,0{,}006)(0{,}098)\left(1{,}659 \times 10^6\right)$

$= \quad 1{,}379\,kN$

$\therefore$ Load Carried by Joint

$= \quad P_T \quad = \quad P_1 + P_2$

$= \quad (4058) + (1379)$

$= \quad 5{,}437\,kN$

$\therefore$ The Direct Stress on Welds

$\delta \quad = \quad \frac{\text{Force}}{\text{Area}} \quad = \quad \frac{\left(5{,}437 \times 10^3\right)}{(0{,}006)(0{,}098)}$

$= \quad 9{,}247\,MPa$

Appendix B

Lethabo Loadcell Design Calculations

Empty CE mass

Ash loaded CE mass

Assumptions:

$Bulk\ Density\ of\ \ flyash\left(\rho_{ash}\right)$	=	$1200\frac{kg}{m^3}$
$Density\ of\ steel\left(\rho_{steel}\right)$	=	$7800\frac{kg}{m^3}$
$CE\ plate\ thickness$	=	$1,XX\ mm$
$Area\left(1\ side\ of\ CE\right)$	=	$Height\times Length$
	=	$15m\times 5,1m$
	=	$76,5m^2$
$Area\left(both\ sides\ of\ CE\right)$	=	$\underline{153m^2}$
$\therefore\ldots Mass\ of\ Clean\ CE$	=	$\rho_{steel}\times CE\ Volume$
	=	$7800\times\ 76,5\times 0.0015$
	=	$895kg\left(excluding\ bolts, etc.\right)$
$Total\ CE\ mass$	=	

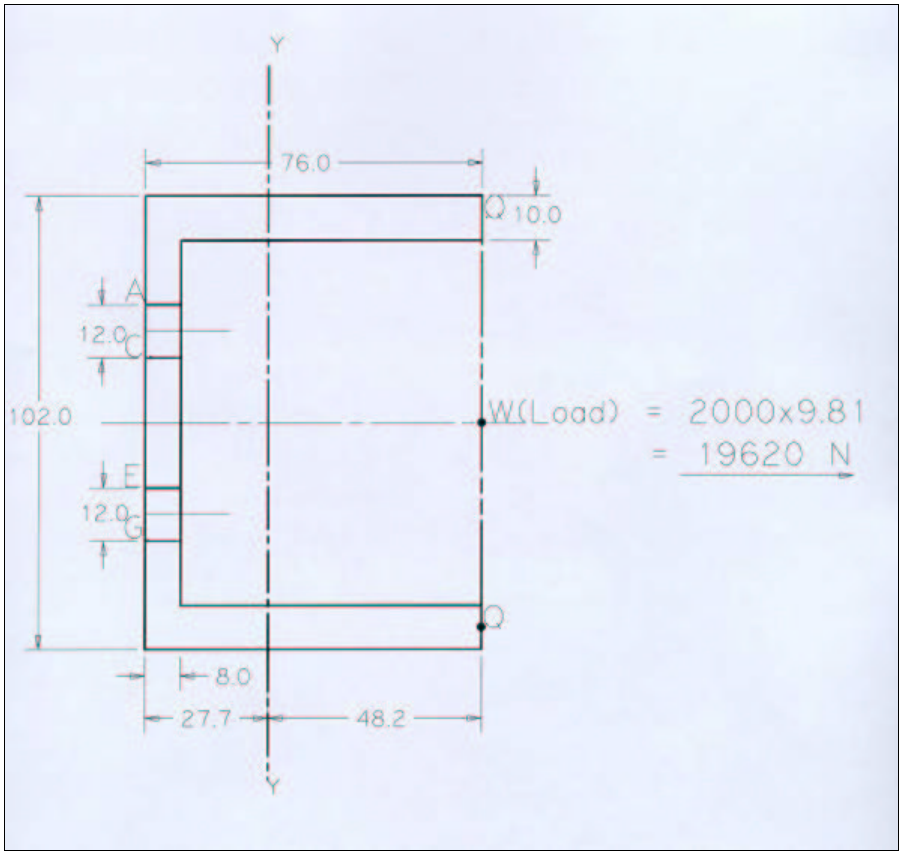

Moment of Inertia $y = \dfrac{A_1y_1 + 2A_2y_2}{A_T}$

$= \dfrac{(102\times 8)(4) + 2(68\times 10)(42)}{2176}$

$= 27{,}75 \text{ mm}$

$I_{x1} = \dfrac{bd^3}{12} + Ah^2$

$= \dfrac{(102\times 8^3)}{12} + (102\times 8)(23{,}75)^2$

$= 464{,}627\times 10^3 \text{ mm}^4$

$I_{x2} = 2\left[\dfrac{bd^3}{12} + Ah^2\right]$

$= 2\left[\dfrac{(10\times 68^3)}{12} + (68\times 10)(14{,}25)^2\right]$

$= 800{,}218\times 10^3 \text{ mm}^4$

$I_{x_T} = I_{x1} + I_{x2}$

$= 1264{,}485\times 10^{-6} \text{ mm}^4$

$\therefore \quad I_{yy} = I_{x_T} = 1{,}265\times 10^{-6} \text{ m}^4$

Using the relation $\delta = \frac{W}{A} \pm \frac{Whx}{I_y}$

where h = distance of load from neutral axis in meters

x = distance of stress from the YY axis in metrs

W = applied load in Newtons

I_{yy} = moment of inertia in meters^4

A = area of channel asin top view in m^2

Calculations

Area of channel A $= (102 \times 76) - (68 \times 82)$

$= 2176 \text{ mm}^2$

$= 2176 - [2(12 \times 10)]$

$= 1936 \text{ mm}^2$

$= 1{,}936 \times 10^{-3} \text{ m}^2$

δ at point B as shown in diagram

$$\delta_B = \frac{W}{A} - \frac{Whx}{I_{yy}}$$

$$= \left(\frac{2000 \times 9{,}81}{1{,}936 \times 10^{-3}}\right) - \left(\frac{2000 \times 9{,}81 \times 0{,}04825 \times 0{,}01975}{1{,}265 \times 10^{-6}}\right)$$

$= 4{,}646 \text{ MPa (C)} = \delta_D$

δ at point A as shown in the diagram

$$\delta_A = \frac{W}{A} + \frac{Whx}{I_{yy}}$$

$$= \left(\frac{2000 \times 9{,}81}{1{,}936 \times 10^{-3}}\right) + \left(\frac{2000 \times 9{,}81 \times 0{,}02775 \times 0{,}04825}{1{,}265 \times 10^{-6}}\right)$$

$= 30{,}901 \text{MPa (T)} = \delta_C$

$$\delta_F \,\&\, \delta_H = \frac{W}{A} - \frac{Whx}{I_{yy}}$$

$$= \left(\frac{2000 \times 9{,}81}{1{,}936 \times 10^{-3}}\right) - \left(\frac{2000 \times 9{,}81 \times 0{,}04825 \times 0{,}01975}{1{,}265 \times 10^{-6}}\right)$$

$= 4{,}646 \text{ MPa (C)}$

$$\delta_E \,\&\, \delta_G = \frac{W}{A} + \frac{Whx}{I_{yy}}$$

$$= \left(\frac{2000 \times 9{,}81}{1{,}936 \times 10^{-3}}\right) + \left(\frac{2000 \times 9{,}81 \times 0{,}02775 \times 0{,}04825}{1{,}265 \times 10^{-6}}\right)$$

$= 30{,}901 \text{MPa (T)}$

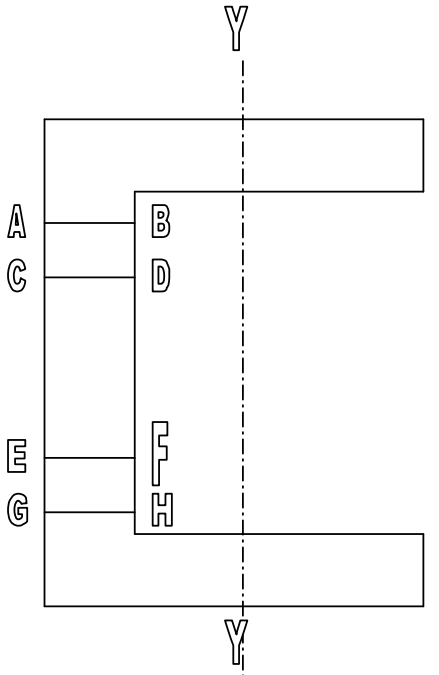

Graph of stresses

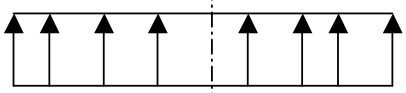

$$\text{Direct Stress} = \frac{F}{A} = \frac{2000 \times 9{,}81}{1{,}936 \times 10^{-3}}$$

$$= 10{,}134 \text{ MPa}$$

10,134 MPa

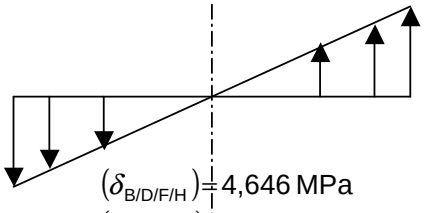

$(\delta_{B/D/F/H}) = 4{,}646 \text{ MPa}$

$(\delta_{A/E/C/G}) = 30{,}901 \text{ MPa}$

Bending Stresses

$$\delta_Q = \frac{W}{A} - \frac{Whx}{I_{yy}}$$

$$= \left(\frac{2000 \times 9{,}81}{1{,}936 \times 10^{-3}}\right) - \left(\frac{2000 \times 9{,}81 \times 0{,}04825 \times 0{,}04825}{1{,}265 \times 10^{-6}}\right)$$

$$= 25{,}974 \text{ MPa (Compressive)}$$

Scale : 10 mm = 10 MPa

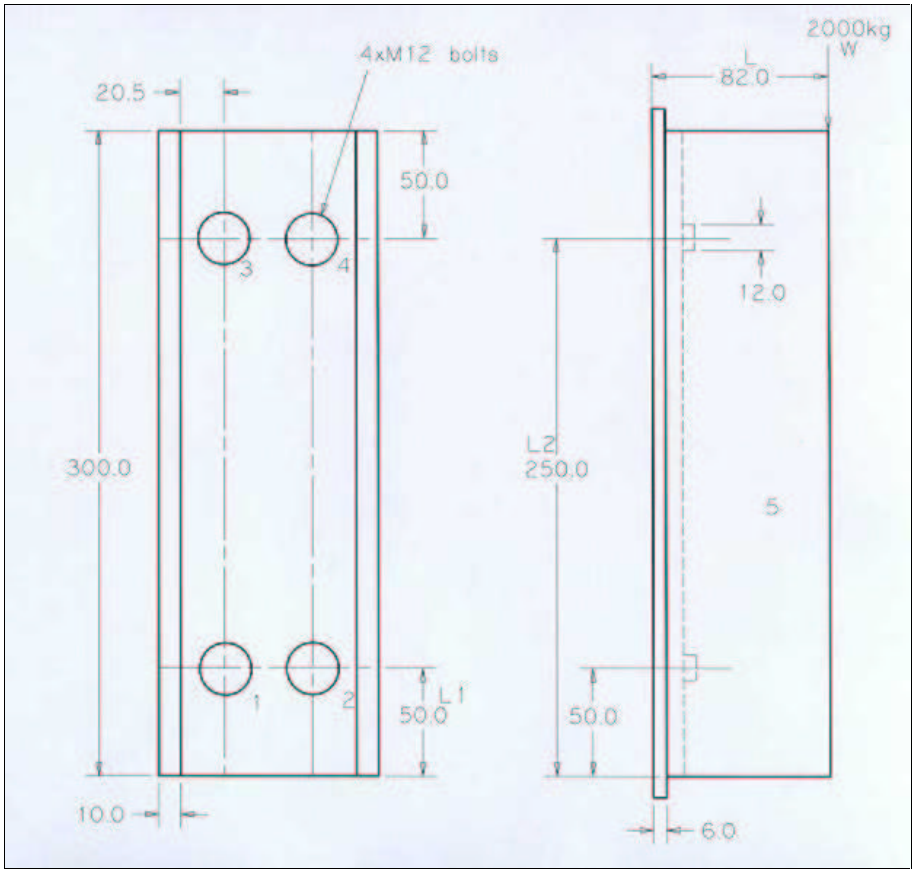

Channel Calculations (Using four bolts only)

Using four M16 bolt & using four M12 bolts

Maximum Load on Channel = $2000 \times 9{,}81$

= 19,6 kN

Using the Theory Eccentric Loading Perpendicular to the axis of the bolt.

Given :

L = distance of the load from the face of the column.

W = maximum load on bracket.

L_1 = distance of the bottom bolts from the lower edge of the bracket.

L_2 = distance of the upper bolts from lower edge of channel.

N = number of bolts

5 = channel

Let $L = 82\,mm$

$L_2 = 250\,mm$

$L_1 = 50\,mm$

$W = 2000\,kg$

Using an M16 bolt (Top Bolts) from British Standard ISO Metric Hexagon Bolts.

dc = core diameter

$dc = 16\,mm$

Using the Relation $Wte = \frac{\pi}{4} \times dc^2 \times ft$

$6690,1 = \frac{\pi}{4} \times dc^2 \times ft$

$ft = 33,3\,MPa = $ Tensile Stress on Bolt.

For Shear Stress on Bolts.

$$\delta_{Shear} = \frac{Wse}{A}$$
$$= \frac{4905 \times 4}{\pi(0,016)^2}$$
$$= 24,4\,MPa$$

Shear Load on each bolt (Top Bolts).

$$Ws = \frac{W}{n}$$
$$= \frac{2000 \times 9,81}{4}$$
$$= 4905\,N$$

The maximum tensile load on bolts numbers 3 & 4.

$$Wt_2 = Wt = \frac{W\,L\,L_1}{2(L_1^2 + L_2^2)}$$
$$= \frac{2000 \times 9,81 \times 0,082 \times 0,250}{2\left([0,25]^2 + [0,050]^2\right)}$$
$$= 3093,92\,N$$

Bolts subjected to shear and tensile load which is equivalent load = Wte

$$Wte = \frac{1}{2}\left(Wt + \sqrt{Wte^2 + 4Ws^2}\right) = \text{Equivalent}$$

$$\text{Tensile Load} = \frac{1}{2}\left(3093,92 + \sqrt{3093,92^2 + 4 \times 4905^2}\right)$$

$$Wte = 6690,1\,N$$

Equivalent Shear Load.

$$\text{Wse} = \frac{1}{2}\left(\sqrt{\text{Wt} + 4\text{Ws}^2}\right)$$

$$= \frac{1}{2}\left(\sqrt{3093{,}92 + 4 \times 4905^2}\right)$$

$$\text{Wse} = 4905\,\text{N}$$

Using M12 bolts metric (Top Bolts)

dc = core diameter 12 mm

Using the relation $\text{Wt} = \frac{\pi}{4} \times \text{dc}^2 \times \text{ft}$

$$6690{,}1\text{N} = \frac{\pi}{4} \times \text{dc}^2 \times \text{ft}$$

$$\text{ft} = 59{,}15\,\text{MPa} = \text{Tensile Stress on Bolt}$$

Shear load on bolt $= 4905\,\text{N}$

$$\delta_{\text{Shear on bolts}} = \frac{\text{F}}{\text{A}}$$

$$= \frac{4905 \times 4}{\pi(0{,}012)^2} = \frac{\text{Wse}}{\text{A}}$$

Shear stress on bolts $= 43{,}4\,\text{MPa}$

Using four M16 bolts and using four M12 bolts (Bottom Bolts)

Required to calculate

a) The stresses at the bottom bolts

b) Increaseing the distance of L (ie. distance of the load from the face of channel) by 5 mm.

a) $Wt = \frac{W\,L\,L_1}{2(L_1^2+L_2^2)}$ $\quad L_1 = 50\,mm$

$Wt = \frac{2000\times 9{,}81\times 0{,}082\times 0{,}05}{2\left([0.25]^2+[0{,}05]^2\right)}$

$= 618{,}78\,N$

$Wte = \frac{1}{2}\left(618{,}78+\sqrt{618{,}78^2+4(4905)^2}\right)$

$Wte = 5224{,}14\,N$

$Wse = \frac{1}{2}\sqrt{618{,}78+4(4905)^2}$

$Wse = 4905{,}01N$

Stresses at the bottom bolts when $L = 0{,}082\,m$

Using M12

$Wte = \frac{\pi}{4}\times dc^2\times ft$

$5224{,}14 = \frac{\pi}{4}\times 0{,}012^2\times ft$

$ft = 46{,}19\,MPa$

$\delta_{Shear\ on\ bolts} = \frac{F}{A}$

$= \frac{4905\times 4}{\pi(0{,}012)^2}$

$\delta_{Shear} = 43{,}4\,MPa$

Using M16

$Wte = \frac{\pi}{4}\times dc^2\times ft$

$5224{,}14 = \frac{\pi}{4}\times 0{,}016^2\times ft$

$= 25{,}98\,MPa$

$\delta_S = \frac{F}{A}$

$= \frac{4905\times 4}{\pi(0{,}016)^2}$

$= 24{,}4\,MPa$

Stresses on the bottom bolts by increases distance L by 5 mm.

$Wt = \frac{W\,L\,L_1}{2(L_1^2+L_2^2)}$ $\quad L = 87\,mm$

$Wt = \frac{2000\times 9{,}81\times 0{,}087\times 0{,}05}{2(0{,}05^2+0{,}250^2)}$

$= 656{,}52\,N$

$Wte = \frac{1}{2}\left(656{,}52+\sqrt{656{,}52^2+4(4905)^2}\right)$

$= 5244{,}23\,N$

$Wse = \frac{1}{2}\sqrt{656{,}52+4(4905)^2}$

$= 4905{,}02\,N$

Using M12

$$\frac{\pi}{4}(0{,}012)^2 \times ft = 5244{,}23\ N$$

$$ft = 46{,}37\ MPa$$

$$\delta_{Shear} = \frac{4905 \times 4}{\pi(0{,}012)^2}$$

$$= 43{,}4\ MPa$$

Using M16

$$\frac{\pi}{4}(0{,}016)^2 \times ft = 5244{,}23\ N$$

$$ft = 26{,}08\ MPa$$

$$\delta_{Shear} = \frac{4905 \times 4}{\pi(0.016)^2}$$

$$= 24{,}4\ MPa$$

Top Bolts

Stresses on the top bolts using four M16 bolt and using four M12 bolts when distance L is increased by 5 mm.

$$Wt = \frac{W\ L\ L_1}{2(L_1^2 + L_2^2)}$$

$$= \frac{2000 \times 9{,}81 \times 0{,}087 \times 0{,}250}{2(0{,}25^2 + 0{,}05^2)}$$

$$= 3282{,}57\ N$$

$$Wte = \frac{1}{2}\left(3282{,}57 + \sqrt{3282{,}57^2 + 4(4905)^2}\right)$$

$$= 6813{,}6\ N$$

$$Wse = \frac{1}{2}\sqrt{3282{,}57 + 4(4905)^2}$$

$$= 4905{,}08\ N$$

Using M12

$$\frac{\pi}{4} \times d^2 \times ft = Wte$$

$$\frac{\pi}{4}(0{,}012)^2 \times ft = 6813{,}6\ N$$

$$ft = 60{,}25\ MPa$$

$$\delta_{Shear} = \frac{F}{A}$$

$$= \frac{4905 \times 4}{\pi(0{,}012)^2}$$

$$= 43{,}4\ MPa$$

Using M16

Similarly

$$ft = \frac{6813{,}6 \times 4}{\pi(0{,}016)^2}$$

$$= 33{,}89\ MPa$$

$$\delta_{Shear} = 24{,}4\ MPa$$

Appendix C

Lethabo P/S Loadcell & Supporting Structure Design Drawings

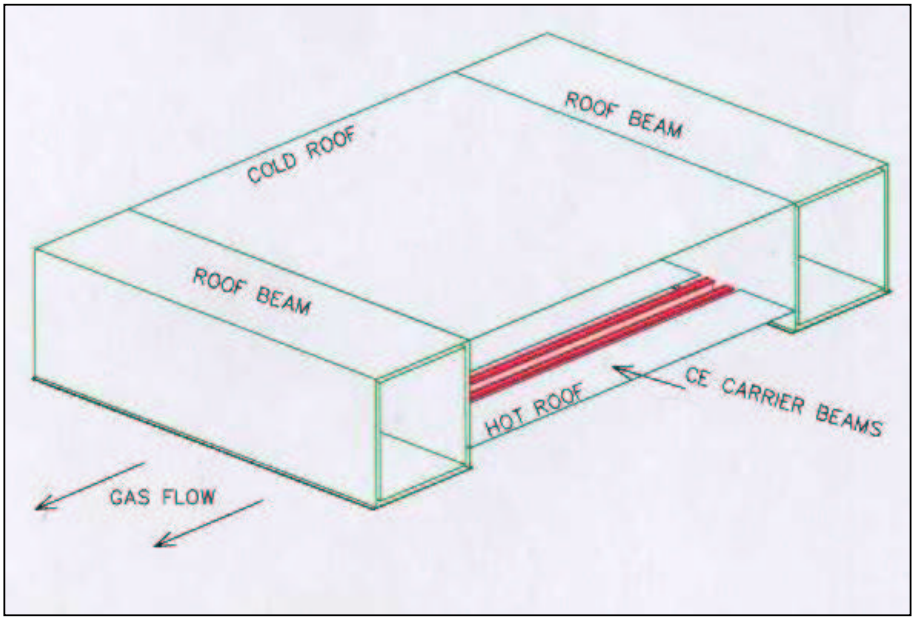

Isometric view of main roof beams.

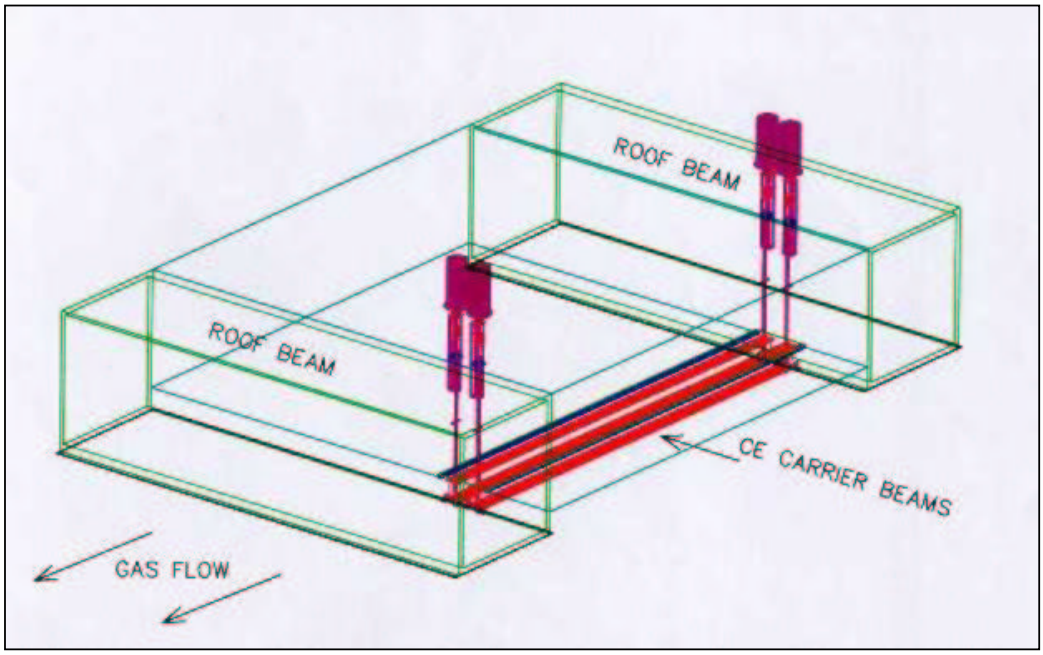

Isometric view of main beams and tow tests CE's

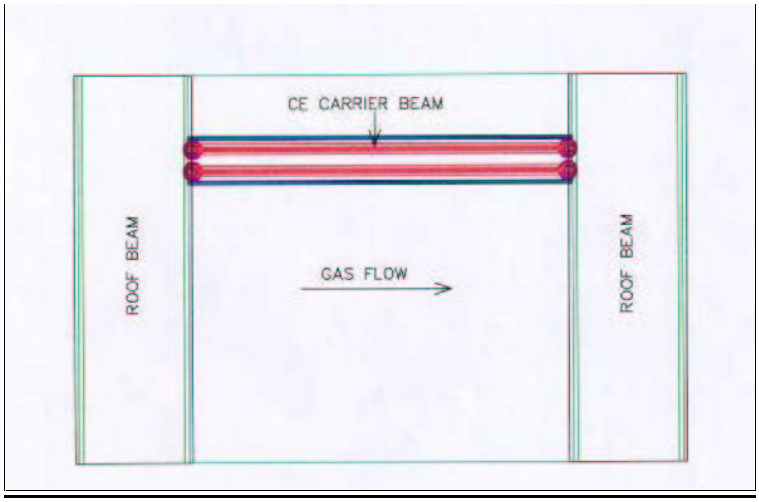

Top View of Main Beams

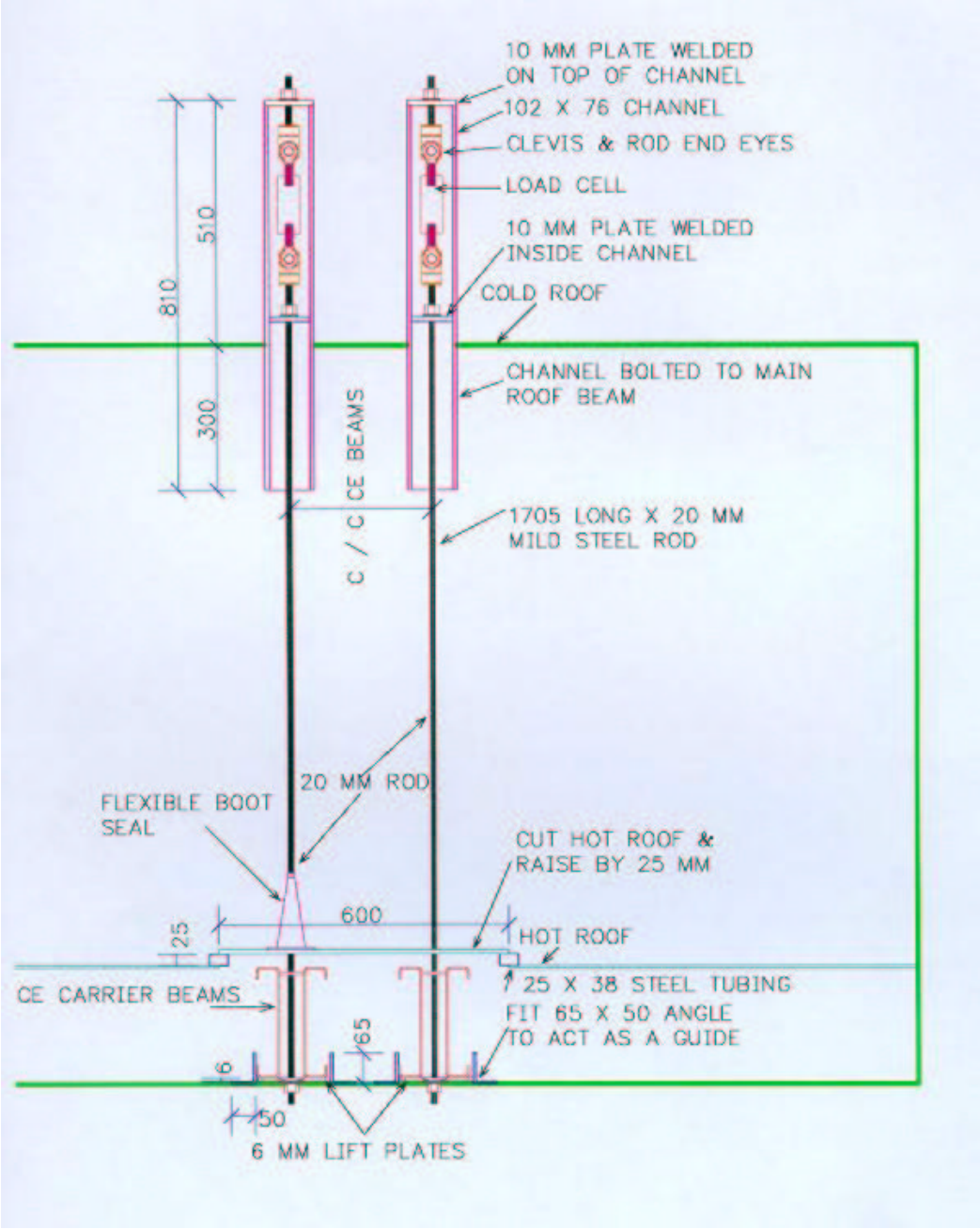

Detailed front view of loadcell and support structure installation.

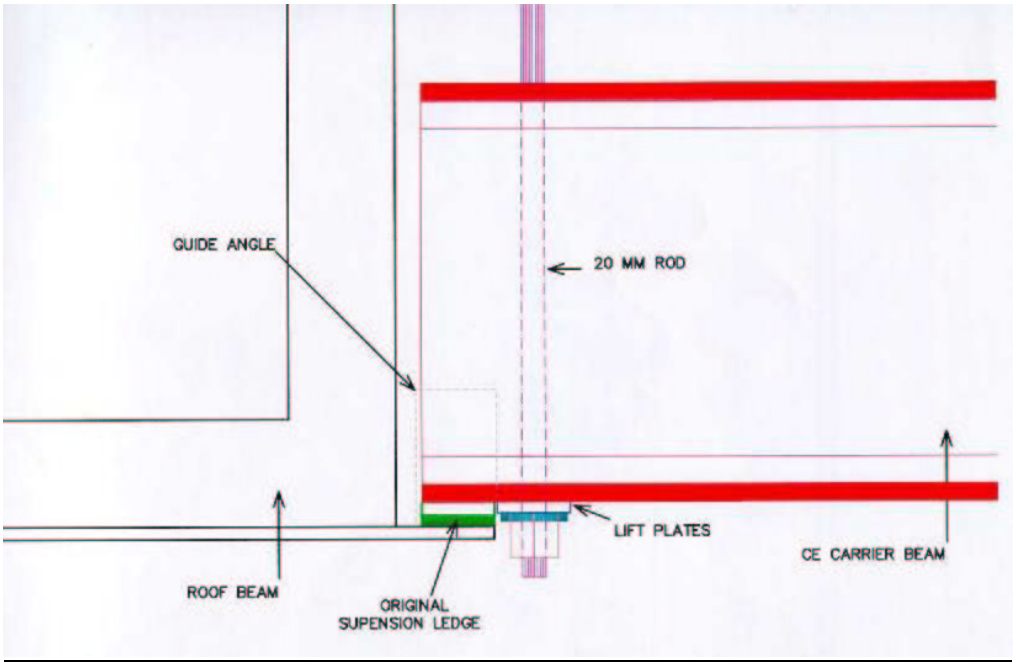

Side view of suspension edgeand lift plates

Appendix D

Paper Presented at South African Strain Society (SSSA)

AN INVESTIGATION INTO THE USE OF ELECTRODE MASS MEASUREMENT TO OPTIMISE AN ELECTROSTATIC PRECIPITATOR UNIT.

By

Shaun Pershad

Eskom TSI

Presented at the Strain Society of South Africa – Feature Event
Thursday. 8th June 2000

1. INTRODUCTION

Electrostatic precipitators (ESP's) can be simply described as particle collection devices. This particulate collection occurs for two basic reasons, either pollution control or product recovery or both. In the power industry, it is used primarily as a pollution control device. Other industries using them are municipal incinerators, air conditioning systems, pulp and paper plants, rock products (cement, lime, gypsum), chemical and petroleum industries (detarrers, deoilers, acids), iron and steel plants (coke ovens, blast furnaces, sinter plants) , and non-ferrous metal plants (aluminium, copper, gold).

ESP's have been around for approximately 70 years and their fundamental principle of operation has not changed much during this time. What has changed is the demand on their operating efficiency. Environmental pressure in the form of stricter reductions in emission levels as well as the need for increased product recovery has necessitated optimal ESP performance. ESP's can be large devices with many costly, high maintenance components. ESP downtime usually critically affects the overall plant process. In power generation plant, a defective ESP causing higher than licensed emission levels can cause the enforcement of a generation load loss to bring emission levels down. Alternate devices to ESP's have been cyclones in the past, and fabric filters currently.

In power generation plant, the ESP is usually located after the airheaters and before the induced draft fans and smoke stacks. Flue gases from the boiler, after exiting the airheaters are cleaned by the ESP before being released into the atmosphere via the stacks.

2. BASIC COMPONENTS AND OPERATION OF AN ESP

Figure 1 shows a front view of an ESP as well as the general components located within it. Figure 2 shows an arrangement of collecting electrodes (CE's) and discharge electrodes (DE's). CE's are constructed from plate steel (typically 1.2 to 1.8 mm thick) and shaped so as resist buckling. DE's are constructed from strips of metal (various shapes and sizes) suspended between a rigid frame.

Dust laden gases flow through a system of parallel passages of DE's and CE's as shown in Figure 2 below. CE's are grounded whilst a negative voltage (typically 30-50 kV and 400-1000 mA) is applied to the DE's. A corona is then generated from the DE to the CE. The dust flowing within the passage is electrostatically charged and migrates towards the CE (relatively positive). Dust/ash collects on the CE until it is dislodged by rapping (impacted upon), where it then falls into a hopper and is carried away by some type of ash handling plant.

Table 1 shows typical design and operating data of an ESP unit.

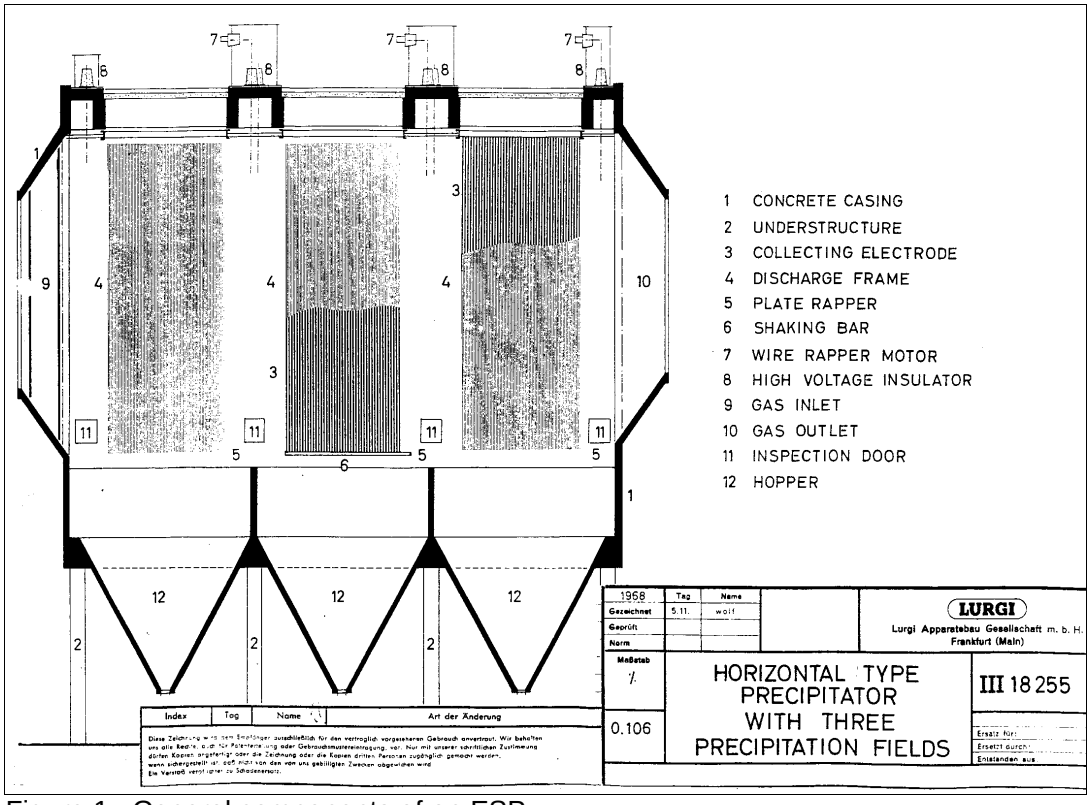

Figure 1 : General components of an ESP.

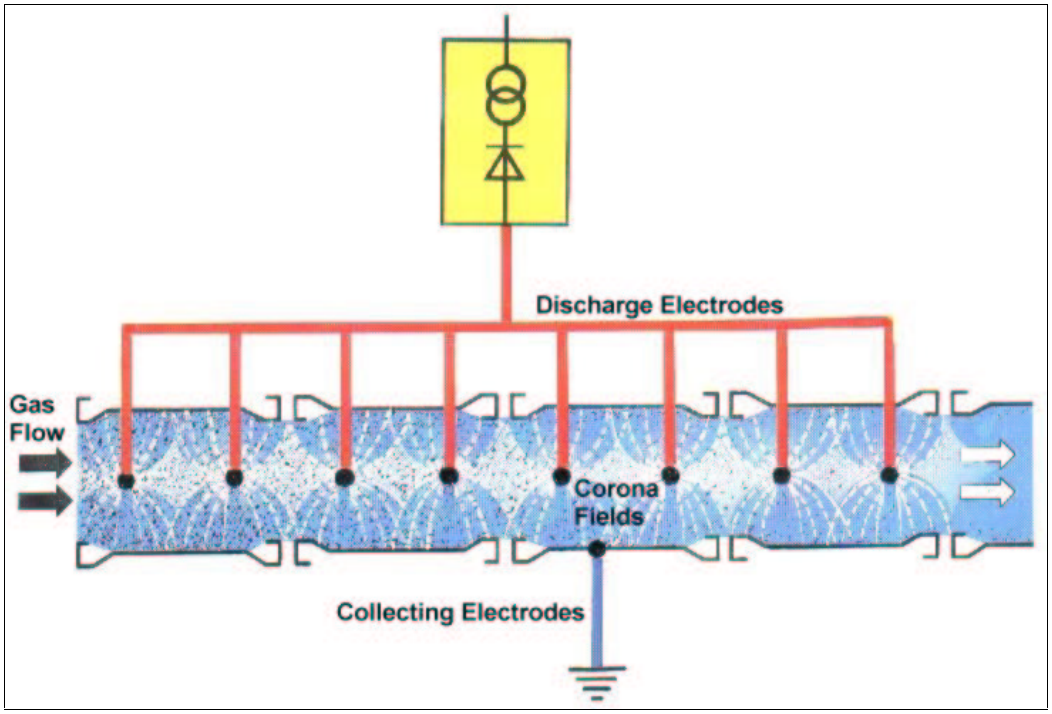

Figure 2 : CE's and DE's and principle of ash collection

Table 1 : Typical design and operating specifications of an ESP

Design Data	
Boiler rating (at 97% MCR)	600 MW
Efficiency (at 97% MCR) for all fields in service	99.88
Parallel Casings	4
Plate (CE) Height	15 m
Plate (CE) Length	5.1 m
Lanes per filter casing	46
Pitch between lanes	300 mm
Fields in series per pass	7
Plate (CE) area total	190 000 m^2
Flow area (total)	817 m^2
Specific collecting area (SCA)	191.6 s/m
Aspect Ratio	2.4
Casing Construction	Steel
Operating Data	
Gas volume flow rate	997 m^3/s
Gas temperature	130 °C
Dust Burden	50 g/Sm^3
Treatment time	28.7 s
Migration velocity (Deutsch)	35.1 mm/s
Gas velocity at electrodes	1.2 m/s
Coal Specification	
Ash content	35-42 %
Sulphur	1 %
Net C.V	16.8 MJ/kg

3. THE PROBLEM STATEMENT & OBJECTIVES

This project objectives are to investigate and if necessary, develop the use of electrode mass measurement in optimising ESP performance. Optimisation of ESP performance can be further divided into the following areas:

- Increase of ESP collection efficiency and reduce particulate emissions.
- Minimise wear and tear on ESP.
- Reduce electrical energy consumption of ESP plant.

4. FACTORS AFFECTING EFFICIENCY AND OPTIMISATION METHODS

The primary factors affecting the efficiency of an ESP unit can be broadly grouped under the following areas.

- ESP type (design, mechanical condition).
- Electrical energisation.
- Flow distribution.
- Rapping.
- Process before ESP (boiler parameters, temperatures, mill charge rates etc).

Once investigations have identified which of the above are problem areas, then appropriate action can be taken to improve efficiency. These can take the form of the following :

- Electrical controller upgrade.
- Electrode modification.
- Electrical sectionalisation.
- Flow and particle distribution/manipulation.
- Minimising hopper sneakage.
- Rapping optimisation.
- Gas conditioning (resistivity modification, SO_3,Ammonia etc.).
- Temperature adjustments.(lowering it,)
- Increasing aspect ratio.
- Compact Hybrid Particulate Collector (COHPAC - v1 & 2).

5. RAPPING OPTIMISATION

In general, rapping optimisation can consist of one or more of the following :

- Schedule/timing change(ON-OFF times).
- Hammer change.
- Power-off rapping.
- Incremental rapping.
- High speed rapper shafts.
- Magnetic Impulse Gravity Impact (MIGI).
- Sonic horns.
- Process control system.

However, the problem arises in knowing the exact nature, location, process condition, and time of specific problems. Without this knowledge, finding solutions are very difficult.

The use of loadcells for CE mass measurement eliminates the above difficulties by providing an:

- Online (hence process/condition/ specific),
- Unit/plant and field specific,
- Real time(can be part of process control),

"gauge" of operational behaviour. This is turn provides insight into what problems exist, suitable appropriate optimisation methods, fine-tuning of applied upgrade methods and finally the effectiveness of upgrades. This "gauge" is not limited to rapping optimisation but can also be applied to the other factors affecting ESP efficiency mentioned previously .

6. LOADCELL CONSIDERATIONS

The ESP presents a very hostile and difficult environment in which to operate a loadcell in.
Depending on the location of loadcell, the conditions faced can be a combination of most of the following

- Work/install in very confined spaces.
- Erosive/abrasive conditions (ash).
- High temperatures (up to 160 °C).
- Corrosive flue gases (acids).
- High voltage corona discharge in close proximity (close as 150 mm).
- Amplifiers and recording equipment usually located far away (control room, 120 m away). Amplifiers must be capable of operating with these lengths of cable with suitable compensation.
- Considering the above (cable length and corona discharge), electrical noise can be a problem. Suitable instrumentation and installation procedures need to be used to minimise this.
- All instrumentation needs to be protected against surges (sparkovers, arcing, lightning)

7. RESULTS

Some sample graphs are shown in Figures 3 to 7. from the experimentation conducted at Eskom's Hendrina and Lethabo Power Stations.

Hendrina Power Station Results

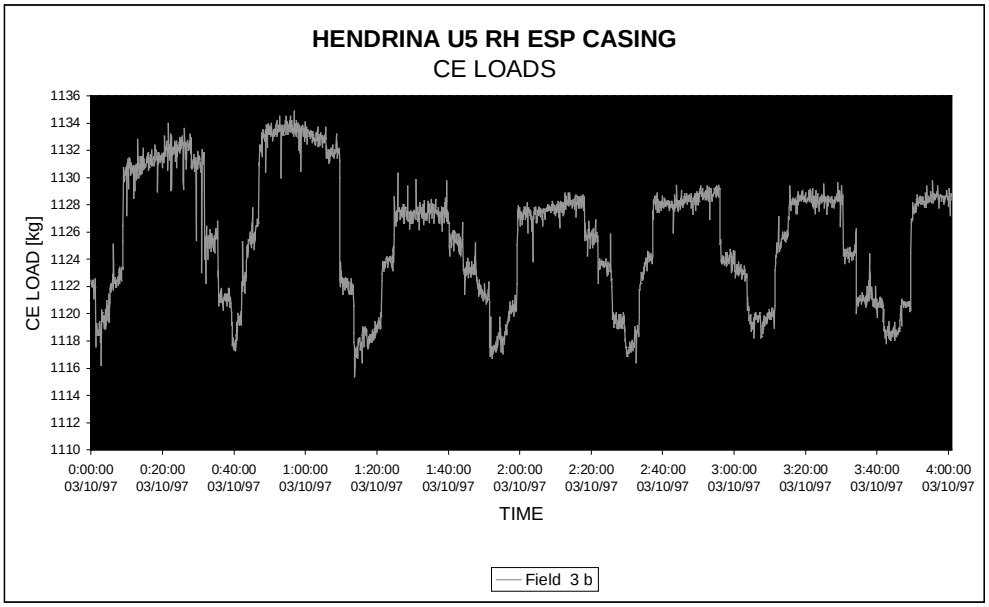

Figure 3 : Hendrina Power Station Field 3 "As found" collection trend.

From Figure 3, above we can see that the trend indicates a "flat top" form. This trend shows that field 3 is reaching saturation fairly quickly and then approximately twenty minutes passes, before the CE is emptied(rapped). This

results in a period of between 30 and 40 minutes or 50% in every hour when the field is inactive. An optimised rapping setting would be 10 minutes off : 3 minutes ON. However, the choice of field 3's times are a little difficult considering that it is the last field and rapping puffs will be problematic.

Previous loadcell data indicates that field 3 reaches a saturated collecting point after approximately ten minutes. If it was not the last field, these times would be recommended. Future tests will determine whether the shorter rapping times, with more rapping puffs are better than longer rapping-off times (without puffs but exceeding the CE saturation collection point). We can also see, from the "stepped" discharge of ash from the CE that rapping acceleration intensity is not as good as is required.

Lethabo Power Station Results

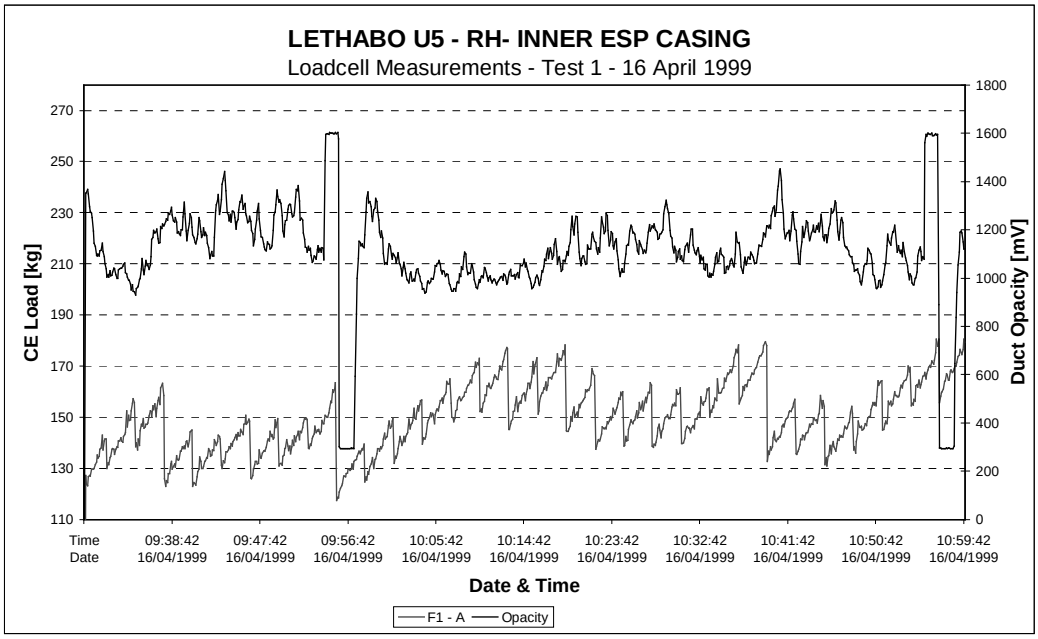

Figure 4 : Lethabo Power Station Field 1 "As found" collection trend.

Figure 4 above shows the collection trend, at full load(618 MW) for field 1. It can be seen that duct outlet opacity trends very closely with Field 1's rapping cycles, indicating re-entrainment. In the above trend, rapping was set to a continuous cycle (shaft speed - 1 revolution per 3 minutes).

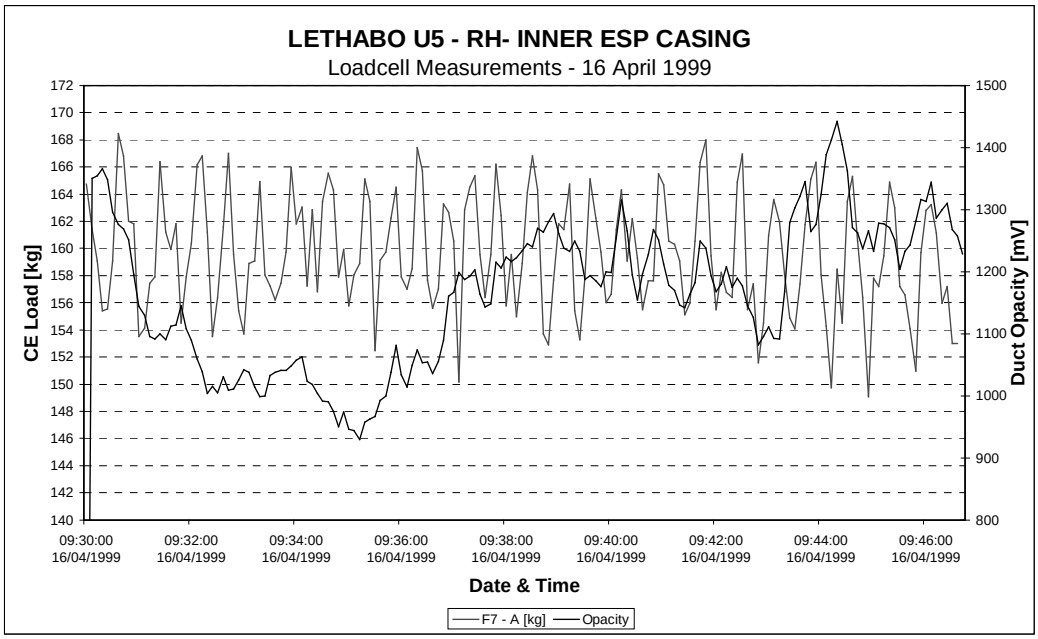

Figure 5 : Lethabo Power Station Field 7 “As found” collection trend.

Figure 5, above shows a trend for Field 7. A peculiar phenomena is occuring here. Usually , the last field in an ESP (especially in a 7 field casing) removes very little ash from the dust stream, considering that the dust stream has also been cleaned by the 6 previous fields. In this case it should be in the order of 2 to 5 kg per CE. However, trend indicates a very cyclic collection and discharge of 14 kg.

It can be concluded that the inlet dust stream to Field 7 is not high enough to provide this collection. Other sources of dust “input” to the system must then be investigated. The above can then be most probably attributed to a leaking hopper seal, combined with a high hopper ash level. Each time the slide gate opens to evacuate the hopper, (considering that the ESP casing is under vacuum), air is “sucked” into the system, re-entraining ash already collected in the hopper.

The above is a maintenance problem and the loadcell system indicates when and where it is occuring. This is very beneficial in the light of 336 hoppers at Lethabo Power Station. Hence the loadcells use as a “troubleshooting”, investigative tool is noted.

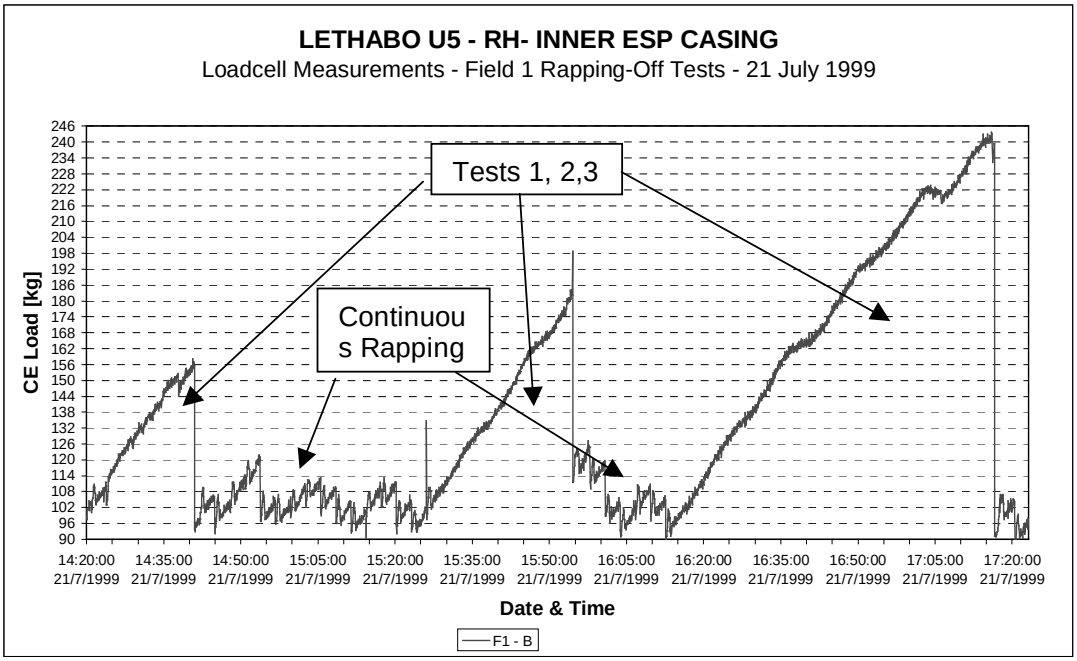

Figure 6 : Lethabo Power Station Field 3 “As found” collection trend.

Figure 6 above shows a “rapping-off” or field saturation test. Three tests were conducted to determine optimum rapping times. Original rapping times were on a continuous (each CE rapped once every 3 minutes) and this is shown above, in between the three test sessions. It is interesting to not that Field 1 did not reach saturation, even after the third test which

It can also be concluded that rapping acceleration forces are sufficient to dislodge a fairly large ash layer, without problems. This can be seen from the almost instantaneous reduction in CE ash load on commencement of rapping after each of the saturation tests.

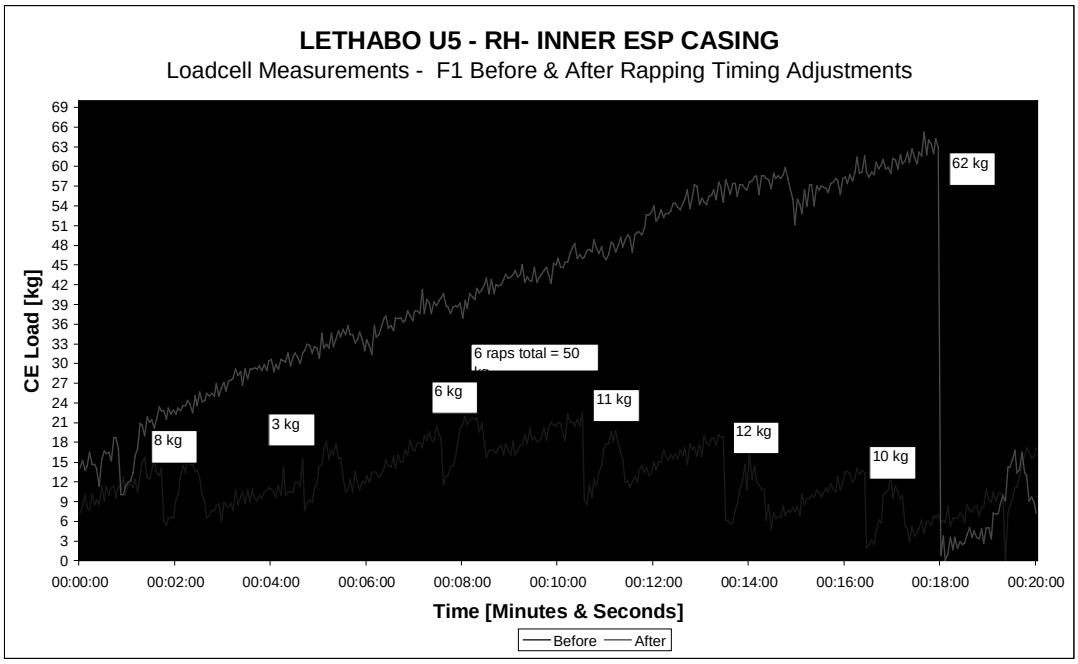

Figure 7 : Lethabo Power Station Field 3 “As found” collection trend.

In Figure 7, the data in Figure 6 was analysed on a common time axis to compare the original rapping (“before”) times with the recommended times (“after”). It was found that over a constant time period, the longer rapping “off” (collection) time promoted the collection of 62 kg compared to 50 kg for the continuous rapping. Hence a collection improvement of between 20 and 25% has been achieved by only optimising the first field. Improvements in the subsequent 6 fields are also achieved, though to a lesser degree.

Re-entrainment also is greatly reduced due firstly to the dislodgement of a larger ash cake, which when acted upon by the tangential forces of gravity and gas flow, falls more easily and quickly into the hopper. Secondly, re-entrainment is directly related to rapping frequencies, as shown in Figure 3. The less frequent the CE is rapped, the less re-entrainment occurs.

The longer “rapping-off” and hence collection times also have a secondary benefit in reduced wear and tear of the plant. Table 2 shows a summary of the presently optimised state and the rapping times used. It should be noted that in fields 2 to 7, where rapper shafts are installed at the bottom of both leading and trailing CE edges, the leading shafts were found to be not required. This can be very influential in affecting plant downtimes. If a failure occurs on any of the trailing edge shafts, repairs can be delayed until a suitable planned outage occurs by use of the leading edge shaft.

Table 2 : Rapping Analysis

Lethabo Power Station - Unit 5 RH Inner Casing **Rapping Analysis**

Time for full revolution (seconds) 180

As Found Conditions

	Front/Leading Edge Rapper Shaft						Back/Trailing Edge Rapper shaft					
FIELD	Off/Pause	On/Run	On/Off Cycles	1 Full Rev.	1 Full Rev.	1 Full Rev.	Off/Pause	On/Run	On/Off Cycles	1 Full Rev.	1 Full Rev.	1 Full Rev.
			[Rev]	[Seconds]	[Minutes]	[Hours]			[Rev]	[Seconds]	[Minutes]	[Hours]
1	No Shaft						6	21600	0.01	180.05	3.00	0.05
2	5	30	6.00	210.00	3.50	0.06	35	40	4.50	337.50	5.63	0.09
3	3	20	9.00	207.00	3.45	0.06	23	30	6.00	318.00	5.30	0.09
4	5400	20	9.00	48780.00	813.00	13.55	5420	30	6.00	32700.00	545.00	9.08
5	14400	20	9.00	129780.00	2163.00	36.05	14420	30	6.00	86700.00	1445.00	24.08
6	18000	20	9.00	162180.00	2703.00	45.05	18020	30	6.00	108300.00	1805.00	30.08
7	3600	4	45.00	162180.00	2703.00	45.05	3604	6	30.00	108300.00	1805.00	30.08

Optimised Times - 17 Novmber 1999

	Front/Leading Edge Rapper Shaft						Back/Trailing Edge Rapper shaft					
FIELD	Off/Pause	On/Run	On/Off Cycles	1 Full Rev.	1 Full Rev.	1 Full Rev.	Off/Pause	On/Run	On/Off Cycles	1 Full Rev.	1 Full Rev.	1 Full Rev.
			[Rev]	[Seconds]	[Minutes]	[Hours]			[Rev]	[Seconds]	[Minutes]	[Hours]
1	No Shaft						600	180	1.00	780.00	13.00	0.22
2							360	180	1.00	540.00	9.00	0.15
3							1800	360	0.50	1080.00	18.00	0.30
4				0			3600	360	0.50	1980.00	33.00	0.55
5							7200	360	0.50	3780.00	63.00	1.05
6							21600	540	0.33	7380.00	123.00	2.05
7							86400	720	0.25	21780.00	363.00	6.05

Table 3 : Summary of Impacts(per CE) and Rapper Shaft Rotation

IMPACT BLOWS

As Found		
Impacts per CE [over 24 hrs]		
Front shaf	Back shaft	Total
0.0	479.9	479.9
411.4	256.0	667.4
417.4	271.7	689.1
1.8	2.6	4.4
0.7	1.0	1.7
0.5	0.8	1.3
0.5	0.8	1.3
	Total	1845.1

Presently Optimised		
Impacts per CE [over 24 hrs]		
Front shaf	Back shaft	Total
	144	144.0
	240	240.0
	48	48.0
	24	24.0
	12	12.0
	4	4.0
0.0	1	1.0
	Total	473.0

SHAFT ROTATION

As Found		
Rotation per shaft [over 24 hrs]		
Front shaf	Back shaft	Total
0.0	24.0	24.0
20.6	12.8	33.4
20.9	13.6	34.5
0.089	0.132	0.221
0.033	0.050	0.083
0.027	0.040	0.067
0.027	0.040	0.067
	Total	92.3

Presently Optimised			
Rotation per shaft [over 24 hrs]			
Front shaf	Back shaft	Total	% Reduction
	5.5	5.5	76.92
	8.0	8.0	76.03
	4.0	4.0	88.39
	2.182	2.182	-888.72
	1.143	1.143	-1275.05
	0.585	0.585	-779.90
0.0	0.198	0.198	-198.15
	Total	21.6	76.54

The “as found” section reveals that the first three fields (Field 1, 2, and 3) were being rapped too frequently than was necessary. A comparison of the times shows this. Table 3 shows a summary of the “as found” and “optimised” rapping impacts to the CE (1 CE used for analysis) as well as shaft rotation as a function of time.

Impacts and shaft rotation were the two quantities used in the analysis as from a rapping point of view, they predominantly influence wear and tear rates. ESP components influenced by this are CE’s (7728 per 6 units), rapper hammers (14352), rapper shaft bearings (2184), anvils (14352), bushes, (78960) and rapper motors (312).

A reduction in shaft rotation also has an influence in auxilliary power saving considering Lethabo Power Station has a total of 312 rapper motors (3.7 kw each).

To summarise :

Emission Reduction (*estimated thus far-work still in progress*) = 20 %
Rapping induced Wear & Tear Reduction = 76 %

8. CONCLUSION

The use of the collecting electrode mass measurement method to optimise electrostatic precipitator operation has been shown to be successful.

9. REFERENCES

1. TASSICKER O J ; **Control of an electrostatic precipitator by continuous measurement of plate dust load** ; The Electric Power Research Institute.

2. BOSCH F J ; **Particulate Emission Control Technology Evaluation and Database** ; Eskom Technology Group ; Report No. TRR/P93/034.

3. YAMAMOTO T, et al ; **Studies of rapping re-entrainment from electrostatic precipitators** ; Sumitomo Heavy Industries Ltd ; Proceedings : ICESP 7 Conference ; September 1998 ; Kyongiu, Korea ; pp.163-166

4. LEE J, et al ; **Experimental study of electrostatic precipitator plate rapping and re-entrainment** ; Pusan National University, Korea ; Proceedings : ICESP 7 Conference ; September 1998 ; Kyongiu, Korea ; pp.155-162

5. WHITE H J ; **Removal And Re-entrainment** ; Chapter 6 ; pp105-117.

6. BOWMAN H ; ROBERTS R ; **Selecting and defining rapping schedules to prevent sodium depletion on hot side precipitators** ; Arkansas Power & Light Redfield, Arkansas.

7. McCULLOUGH M ; **Minor modifications and operating techniques to enhance precipitator performance** : **Experience report of Southwestern Public Service** ; Southwestern Public Service Co.

8. SAITO Y ; **The latest dust collecting technique** ; Technical Institute, Mitsubishi Heavy Industries Ltd Technical Review ; Vol. 13, No 3 ; October 1976.

9. SPROULL W T ; **Fundamentals of electrode rapping in industrial electrical precipitators** ; Journal of the Air pollution control association ; February 1965.

10. CRYNACK R R ; **Rigid frame and rigid discharge electrode electrostatic precipitator design comparison relating to upgrade technology** ; An Introduction to United States of America Electrostatic Precipitator Rebuild Technology, WPCA and Eskom.